TRACKING AND ANALYSIS OF EEG ACTIVATION ACROSS BRAIN LOBES IN AN ODDBALL TASK

LIM SENG HOOI

MASTER OF ENGINEERING SCIENCE

FACULTY OF ENGINEERING AND GREEN TECHNOLOGY
UNIVERSITI TUNKU ABDUL RAHMAN
JANUARY 2017

TRACKING AND ANALYSIS OF EEG ACTIVATION ACROSS BRAIN LOBES IN AN ODDBALL TASK

By

LIM SENG HOOI

A dissertation submitted to the Department of Electronic Engineering,
Faculty of Engineering and Green Technology,
Universiti Tunku Abdul Rahman,
in partial fulfilment of the requirements for the degree of
Master of Engineering Science
January 2017

DECLARATION

I hereby declare that the dissertation is based on my original work except for quotations and citations which have been duly acknowledged. I also declare that it has not been previously or concurrently submitted for any other degree at UTAR or other institutions.

Name ______________________________

Date ______________________________

ABSTRACT

TRACKING AND ANALYSIS OF EEG ACTIVATION ACROSS BRAIN LOBES IN AN ODDBALL TASK

LIM SENG HOOI

Brain is an important organ of nervous system that controls the body. It can be divided into four different lobes: occipital lobe, frontal lobe, temporal lobe, parietal lobe and the motor region. Every region has its specific functions. The signal that flows in the brain is generated by synchronised activity of thousands of neurons, it is called Electroencephalography (EEG).

In this dissertation, we have developed novel algorithms to track connectivity in brain by using Horn-Schunck (HS) optical flow and full search (FS) block matching motion estimation (ME) methods. First of all, we have acquired EEG data from twenty subjects using oddball paradigm to examine the flow of EEG signal across brain lobes for a specific activity. Next, the EEG data is converted into EEG topo-maps using EEGLAB. The motion vectors (MVs) between consecutive topo-maps is estimated by using HS optical flow and FS block matching ME methods. A tracking algorithm is developed to examine the flow of activation based on the overlapping of the MVs in the current frame and next frames. Different paths are tracked across various lobes for same activity. We have also used a classical method to find the functional connectivity of the brain. We have tracked the functional connectivity for different oddball cases by using cross-correlation method.

A comparison of HS and FS method shows that HS gives higher PNSR and uses less computational time as compared to FS method. In addition, the motion field of HS is more consistent than FS method. So, we conclude that HS is more suitable for tracking purposes. Finally we have come up with an average activation graph for different scenarios in the oddball paradigm. The behaviour of brain lobes for different oddball cases for individual subjects and average of all subjects has been observed on the average activation graph. For all subjects, the difference of the activation flow can be observed among different lobes for different oddball cases. Lobes for different cases also show different patterns for different activities. For frontal lobe, target response peak always come earlier or higher than target with no response at the end of the task. Besides, frontal lobes will have high amplitude of activation graph than other cases. For parietal lobe, the activation graph has very low amplitude. However, we are still able to observe a peak in the end of the task for target with response case. For occipital lobe, high peak occurs in the middle of the graph for all cases. However, the occipital lobe activation drop near the end of the task when the frontal lobe rises for target with response cases.

For individual subjects, different performances such as poor, average and good different patterns on the activation graph is observed for different activities. For poor performance, occipital or frontal lobe has inconsistent graph with many high peaks which cause poor performance for the subject. For average performance, the pattern of the activation graphs are more consistent than poor performance. For good performance, graph clearly shows the good performance of the subjects. For measuring functional connectivity using the cross correlation method; we have been able to conclude that different oddball cases show different connectivity in the correlation functional connectivity map. High connectivity can be observed in last segments when subjects give response to the target or non-target stimuli. In addition, we have also observed the connectivity in Fz, F3, F4, C3 or C4 electrodes which are used for motor planning or sensorimotor integrations in the last segment when subject responds to the target or non-target stimuli. In functional connectivity map, high connectivity can be observed in last segment when subject gives response to target on non-target stimuli which involves all lobes.

ACKNOWLEDGEMENTS

I would like to express my gratitude to my supervisor Dr. Humaira Nisar and co-supervisor Dr. Yap Vooi Voon for their constant guidance and valuable suggestions throughout the studies.

I would also like to thank my beloved parents and brother for supporting my decisions. Lastly I would like to thank UTAR for providing the opportunity and grant for my postgraduate study.

APPROVAL SHEET

This dissertation entitled "**TRACKING AND ANALYSIS OF EEG ACTIVATION ACROSS BRAIN LOBES IN AN ODDBALL TASK**" was prepared by LIM SENG HOOI and submitted as partial fulfilment of the requirements for the degree of Master of Engineering Science at Universiti Tunku Abdul Rahman.

Approved by:

____
(Assoc. Prof. Dr. HUMAIRA NISAR)
Date:…………………..
Professor/Supervisor
Department of Electronic Engineering
Faculty of Engineering and Green Technology
Universiti Tunku Abdul Rahman

____
(Assoc. Prof. Dr. YAP VOOI VOON)
Date:…………………..
Professor/Co-supervisor
Department of Electronic Engineering
Faculty of Engineering and Green Technology
Universiti Tunku Abdul Rahman

TABLE OF CONTENTS

LIST OF FIGURES

LIST OF TABLES

LIST OF ABBREVIATIONS

AR	Autoregressive
DTF	Directed Transfer Function
dDTF	Directed DTF
dMRI	Diffusion MRI
DTI	Diffusion Tensor Imaging
EEG	Electroencephalography
ERP	Event-Related Potential
F	Frontal
fMRI	Functional Magnetic Resonance Imaging
FS	Full Search
HS	Horn-Schunck
INT	Integration
L	Left Temporal
LFP	Local field potential
LUE	Left Upper Extremity
M	Motor
ME	Motion Estimation
MEG	Magnetoencephalographic
MEM	Memory
MID	Midline
MPEG	Motion Picture Experts Group
MV	Motion Vector
MVAR	Multivariate Autoregressive

NIRS	Near Infrared Spectroscopy
O	Occipital
P	Parietal
PDC	Partial Directed Coherence
PET	Positron Emission Tomography
PSNR	Peak Signal Noise Ratio
R	Right Temporal
RUE	Right Upper Extremity
UND	Understanding
VMF	Vector Median Filter

Chapter 1

Introduction

1.1 Background

In 1980s, the Institute of Medicine of the National Academy of Science, United States was commissioned to set up a panel to study the value of integrating neuroscientific info across various methods (Pechura & Martin, 1991).These methods include electroencephalography (EEG), magnetoencephalography (MEG), diffusion magnetic resonance imaging (dMRI), functional magnetic resonance imaging (fMRI), near infrared spectroscopy (NIRS) and other non-invasive methods to map anatomy, function, perfusion, phenotypes and physiology of the human brain. Human Brain Project was established to allow researchers for brain study in neuroscience field (Koslow & Huerta, 1997). Brain study can be divided into two types: normal brain study and diseased brain study. For normal brain study, researchers work on behavioural analysis, thinking, understanding, cognition, etc. For diseased brain study, researchers analyse the diseased brain. Diseased and healthy brains were mapped to understand, learning, memory, aging for normal brains, and drug effects in various brain diseases like patients with autism, clinical depression and schizophrenia. It is also critical to study the brain injuries and improve the treatment for brain injury (Van Horn, et al., 2012); (Irimia, et al., 2012).

1.2 Problem Statement

Brain mapping is the visual illustration of brain used by neuro-science to relate the connectivity and functionality of the brain through imaging. Connectivity helps to find functionally integrated relationship between spatially separated brain regions. Brain mapping is important as it may help to solve the mystery of human uniqueness. There are several methods for mapping brain connectivity but yet no specific way has been identified to find the functionality connectivity of the brain.

1.3 Aims and Objectives

The aim of this research it to develop a method to track the EEG activity across different brain lobes to map the neural connectivity for a particular activity. It may be very useful to help neuroscientists to examine the pattern of connectivity of a subject for different activities. Hence, the objective of the project is:

1. To develop an algorithm to track the brain EEG activation using motion estimation methods.

2. To investigate the behaviour of different brain lobes throughout a particular brain activity.
3. To investigate the connectivity of brain based on the brain functional connectivity estimators.

1.4 Overview of Dissertation

In this section, we will provide a brief overview of this dissertation. In chapter 1, we have discussed about the background, problem statement and objectives of this research. In chapter 2, we will go through the literature review for this research; which contains a brief introduction of brain and its functions, electroencephalogram, oddball experiment, brain connectivity and computer vision based motion estimation methods. In chapter 3, we will discuss the methodology of this research. In chapter 4, we will discuss the experimental results and their discussion. Lastly we will conclude our research and will provide future recommendations in chapter 5.

Chapter 2

Literature Review

2.1 Introduction

In this chapter, we will give a brief literature review. First, the different brain lobes and their functions are introduced. After that, we will talk about electroencephalogram (EEG), 10-20 international system of electrode placement for EEG acquisition and different EEG signal frequencies. Then we will discuss about the oddball experiment. Next, we will discuss about various brain connectivity methods which include a classical method that is used in this research by calculating the cross-correlation between signals. Finally, we will discuss the computer vision based algorithm for motion estimation which includes full search block matching and Horn-Schunck optical flow algorithm.

2.2 Different Brain Lobes and Their Functions

Brain is the centre organ in human nervous system that is protected by the skull and is located in the head. The main function of the brain is to generate signals to control the body. The brain can be divided into three main parts, brain stem, cerebellum and cerebrum. Cerebrum can be separated into four different lobes; occipital lobe, frontal lobe, temporal lobe, and parietal lobe. Each lobe has its specific function (Bermudez, 2010). Fig. 2.1 shows the different brain regions and their functions (Bermudez, 2010). For example, frontal lobe is located in the front of human brain that is used for planning and problem solving. Occipital lobe is used for visual processing, it is located at the back of the brain. Temporal lobes (left and right) are located on either side of the human brain are used for memory, understanding and language. Parietal lobe is located in the front of occipital lobe. It is used for sensing, perception, arithmetic and spelling. Lastly, motor and sensory cortex is located in between parietal lobe and frontal lobe. It is involved in controlling the movements and receive sensation of body.

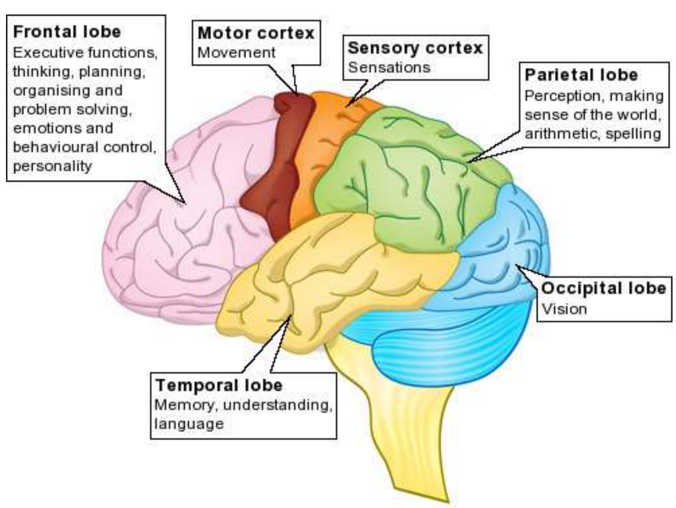

Fig. 2.1 Different brain regions and their functions (Bermudez, 2010)

2.3 Electroencephalogram (EEG)

Electroencephalography (EEG) is an electrical signal generated by the neurons in the brain. Our brain is full of neurons, these cells belong to the nervous system. The neurons are composed of a cell body. The individual nerve cells are interconnected with each other by axons and dendrites. The neurons are activated every time we think, feel, move and remember something. So, with more interconnection of neurons, the people will be smarter and clever. (Blackwell, et al., 2007). The brain cells or neurons talk to each other and produce tiny potential difference of the order of microvolts (μV). This potential difference is produced by the interchange of ions in the brain. EEG signal can be recorded by the help of electrodes placed on the scalp. EEG electrodes comprise of small metal discs of stainless steel, gold, tin, etc. The main advantage of EEG signal is very high time resolution; hence it is able to capture the cognitive processes in the same time frame as the cognition occurs. Cognition, emotional and motor processes are normally very fast. Most of the cognition processes occur within ten to hundreds of milliseconds. Brain mapping is the visual illustration of brain that is also known as topo-maps (Pechura & Martin, 1991); (Metwally, 2007). EEG topo-map displays can represent raw EEG data e.g. voltage amplitude, or derived parameters, like power or peak latency. Brain mapping is commonly used by neuroscientists to study the anatomical structure and the function of the brain.

2.3.1 10-20 International System of Electrode Placement

10-20 system is a standardized system for the placement of electrodes on the scalp for recording of EEG signals (Jurcak, et al., 2007). The system follows a standard method of electrode placement. In this method either 10% or 20% of the distance between fixed points from the Nasion (Nz) (the point between the forehead and the nose) to Inion (Iz) (lowest point of the skull) is used for electrode placement. These points are marked as occipital lobe (O), frontal (F), parietal (P), temporal (T) and central (C). Subscript z refers to electrode that is placed on midline. Each electrode in the 10-20 international system has their specific function. Fig. 2.2 shows the 10-20 international system of electrodes placement. Table 2.1 shows the list of electrodes (10-20 international system) and their functions (Walker, et al., 2007).

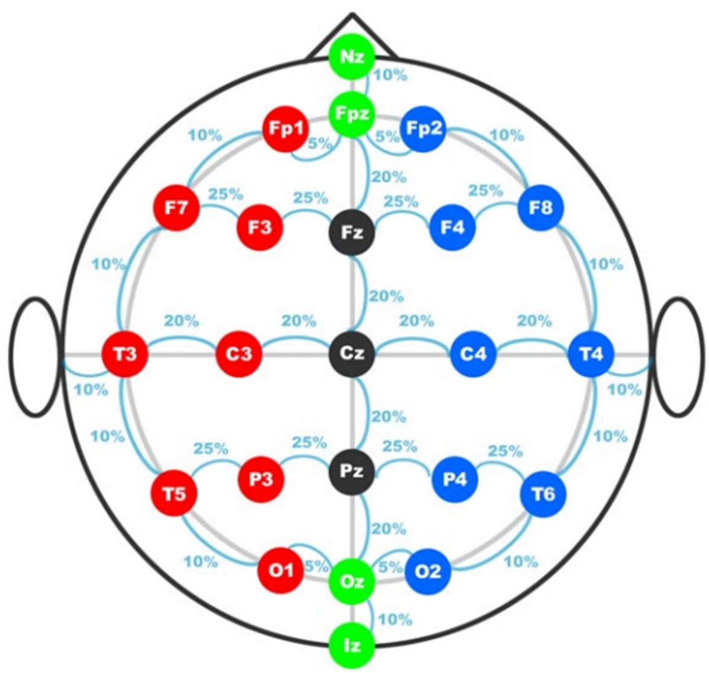

Fig. 2.2 10-20 international system of electrodes placement (Trans Cranial Technologies, 2012)

Table 2.1 List of electrodes (10-20 international system) and their functions (Walker, et al., 2007)

10-20 Electrodes	Functions
FP1	Logical Attention
FP2	Emotional Attention
CZ	Sensorimotor integration midline
FZ	Motor planning midline
F7	Logical (verbal) expression
F8	Emotional (non-verbal) expression
F3	Motor planning right upper extremity
F4	Motor planning left upper extremity
C3	Sensorimotor integration right upper extremity
C4	Sensorimotor integration left upper extremity
P3	Perception or cognitive processing (verbal)
P4	Perception or cognitive processing (non-verbal)
PZ	Perception and cognitive processing midline
O1	Visual processing
O2	Visual processing
T3 (T7)	Logical (verbal) memory
T4 (T8)	Emotional (non-verbal) memory
T5 (P9)	Logical (verbal) understanding
T6 (P10)	Emotional (non-verbal) understanding

Nowadays, higher number of electrodes are used in the data acquisition to obtain high resolution of EEG signal. 10-10 international system is the EEG electrode placement system where additional electrodes are added in 10% division, these are placed halfway between the points of 10–20 system. Fig. 2.3 shows the 10-10 international system of electrode placement.

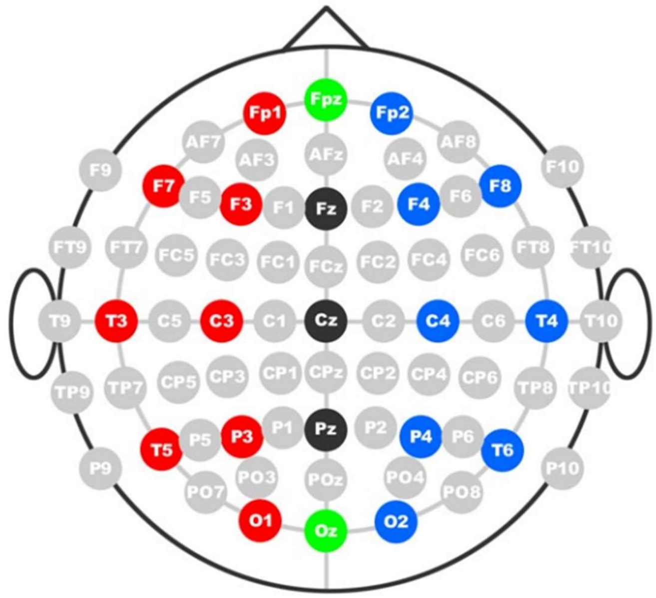

Fig. 2.3 10-10 international system of electrode placement (Trans Cranial Technologies, 2012)

2.3.2 EEG Signal Frequencies

There are five main frequencies of the EEG signals. These are delta (δ), theta (θ), alpha (α), beta (β) and gamma (γ). Firstly, Delta has the frequency range of 0 - 4 Hz. Delta is the slowest frequency and tends to have highest in amplitude. The signals are present during deep sleep. Secondly, Theta signals have a frequency between 4 - 8 Hz. It is classified as "slow" activity. The signals are present during light sleep and deep meditation. Thirdly, alpha signals lie within the frequency between 8 - 12 Hz. It is present when the eyes are closed and deep relaxation. Next, the beta has frequency range of 12 - 35 Hz. Beta activity is known as "fast" activity. The signals are present in our waking awareness and a heightened state of alertness, critical and logical reasoning. Last, gamma has frequency of 35 Hz and above, which are the fastest frequency.

The signals are involved in high processing task. Fig. 2.4 shows the main frequencies of the EEG signals.

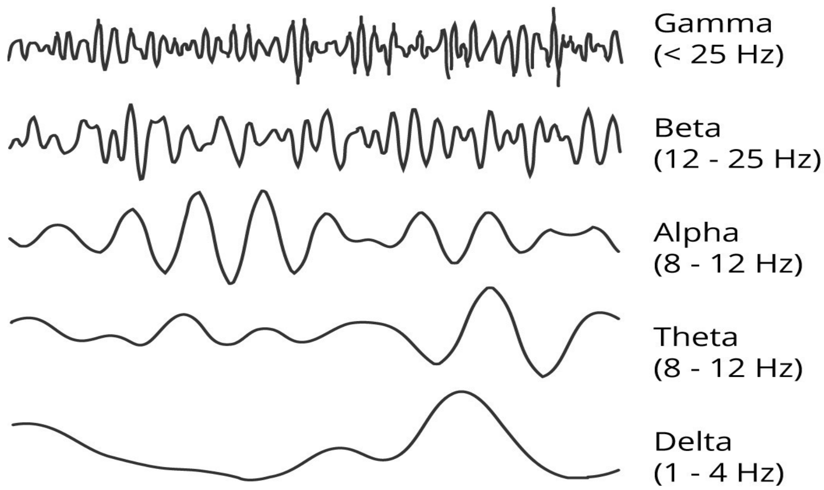

Fig. 2.4 Frequencies of the EEG signals

2.4 Oddball Experiment

Oddball paradigm is an experimental design used in neuroscience to study evoked neural activity; this is done by detecting the rare appearance of target stimulus (Nisar & Yeap, 2014); (Polich, 2007); (Höller, et al., 2013). In the oddball paradigm, subjects are commonly asked to identify rare appearance of target stimuli (e.g. circle) from a series of common standard or non-target stimuli (e.g. square). The subject is asked to press a button when the target stimuli appears. The oddball experiment has been used in more than thousand published articles in neuroscience for electrophysiological studies (Herrmann & Knight, 2001); (Picton, 1992). Fig. 2.5 shows an example of the visualization of oddball experiment.

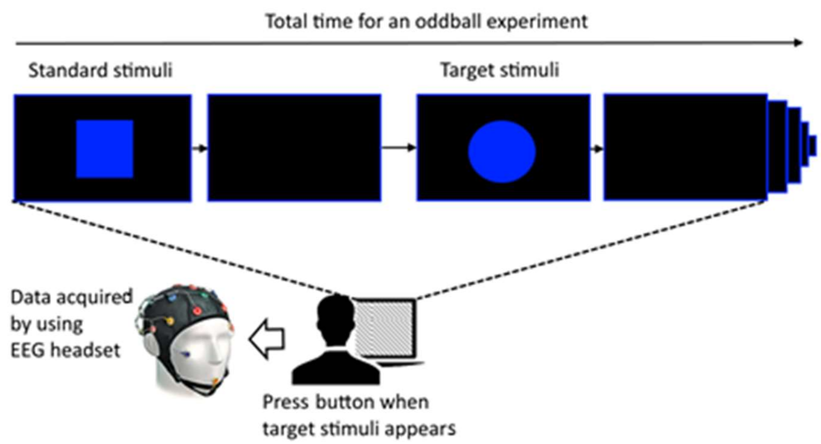

Fig. 2.5 Example of the visualization oddball experiment

P300 or p3 is a signal of event related potential component which is present during the decision making process. In EEG signal, there is a positive detection of the amplitude in the latency of around 300ms (commonly within 250-500ms) where an event is detected. It commonly occurs when a subject detects the target stimuli from high probability of standard stimulus (Picton, 1992). In oddball paradigm, the P300 signal will result in the activation of frontal, parietal and temporal cortical regions for target detection. Detection of target involves activity in the pre-frontal cortical region. The magnitude, timing, topography and the presence of this signal is normally used as metrics of cognitive function in process of decision making (Qassim, et al., 2013). Fig. 2.6 shows an example of P300 from one channel EEG signal (Amiri, et al., 2013).

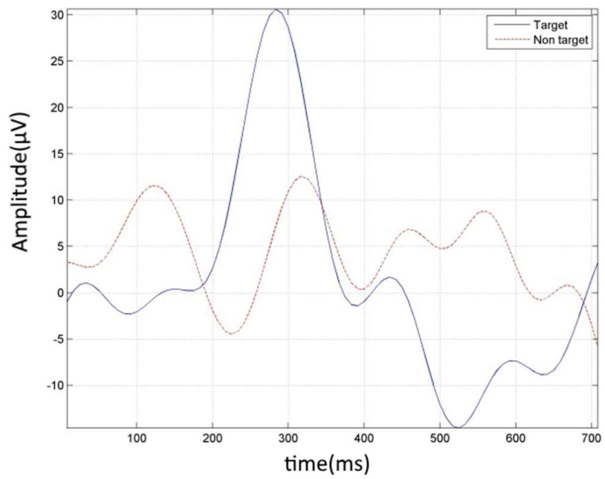

Fig. 2.6 Example of P300 from one channel EEG signal (Amiri, et al., 2013)

2.5 Brain Connectivity

Brain connectivity is a research area in neuroscience to study the brain networks. Brain connectivity can be classified into different types: structural or anatomical connectivity, functional connectivity and effective connectivity. Structural or anatomical connectivity represents the connectivity at the microscopic scale of neurons or synaptic connections. Diffusion tensor imaging (DTI) can be used to provide the anatomical information of the brain. Functional connectivity represents the temporal correlation between the neural systems as an outcome when different activities are carried out, whereas effective connectivity may be defined as the direct or indirect influence between the neural systems. Brain connectivity estimation is commonly used in neuroscience to evaluate functional or effective connectivity from different brain activities. The brain connectivity estimation can be divided into bivariate and multivariate measurement and analysis. Different brain connectivity estimation measurements provide different effectiveness of brain connectivity information. For example, multivariate method is able to provide the information of direct or indirect causality flow between the neural systems. However, bivariate method only provides the information of the directionality of interactions between two signals. The description and comparison between different methods are given in the reference (Kus, et al., 2004).

Bivariate measurement is one of the simplest brain connectivity estimation methods in which the relationship between pairwise signals is evaluated. It can be classified into linear and non-linear methods. Linear methods estimate functional connectivity by using classical coherence and correlation measurements. Both measurements provide information of the directionality of interactions between two signals in terms of phase or delay correlation. However they are not able to provide the causal interaction information. In neuroscience research, the cross correlation is normally use to observe the correlation coefficient between the electrodes at different time lags. In this research, we will track the functional connectivity of the brain by tracking the higher correlation coefficient at the zero lag from electrodes for every 20 samples per segment. By using this method, we will able to observe the changes of the functional connectivity at different time segments. Mutual information, generalized synchronization and phase synchronization, and transfer entropy; are the most common non-linear methods used in brain connectivity estimation. Among these methods, only transfer entropy is able to determine the directionality of the connectivity. Nonlinear measures are sensitive to noise and it requires long segments of stationary signals. Non-linear methods give poor performance than linear methods in the presence of noise (David, et al., 2004).

In statistical signal processing, an autoregressive (AR) model is used to represent time-varying processes; and it basically represents a random process. Specifically the output depends linearly on the previous values. In multivariate measurements, directed transfer function (DTF) was introduced by (Kaminski & Blinowska, 1991). DTF provides the direction and spectral properties of the relationship between brain signals by using multivariate autoregressive (MVAR) model. However, DTF will provide direct and indirect information. Directed DTF (dDTF) is enhancement of DTF introduced by (Korzeniewska, et al., 2003). It is able to distinguish direct from indirect flow. Partial Directed Coherence (PDC) is the most popular brain connectivity estimation proposed by (Baccalá & Sameshima, 2001); which transformed the MVAR coefficients into the frequency domain as a factorization of the Partial Coherence. PDC is able to distinguish direct and indirect causality flows of connectivity pattern likes dDTF method. The comparison between multivariate autoregressive and pairwise autoregressive approach had been demonstrated in (Kus, et al., 2004). Fig. 2.7 shows the example the pattern flow by using bivariate and multivariate methods (Kus, et al., 2004). In this research, we will use a simple method to track the functional connectivity of the brain by using cross-correlation method.

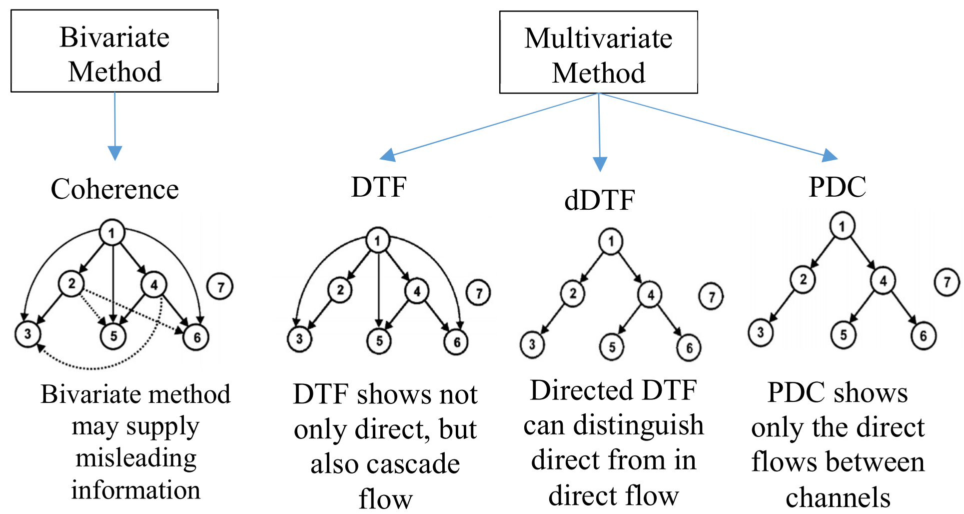

Fig. 2.7 Example of the pattern flow using bivariate and multivariate method (Kus, et al., 2004)

2.5.1 Cross Correlation Method

Functional connectivity captures deviations from statistical independence between neuronal units. In signal processing, cross-correlation is a linear method for measuring similarity of two series of variables and the lag (shifted) between these variables. The normalized cross correlation between different electrodes for a time interval can be calculated using Eq. 2.1.

$$NCOR[n] = \sum_{m=0}^{T} \frac{(f_m - \bar{f})(t_{m+n} - \bar{t})}{\sigma_f \sigma_t} \qquad \text{Eq. 2.1}$$

In Eq. 2.1, NCOR[n] stands for normalized cross-correlation in terms of time lag n. m is the sample number and T is the total number samples. σ_f and σ_t are the standard deviations of the signal f and t. The normalized cross-correlation value varies from -1 to +1. Higher correlation value means the two signals are strongly correlated with each other. For the cross-correlation function, if the highest correlation is at positive lag, it means that signal f is leading. If the highest correlation is at negative lag, it means that signal f is lagging. However, the functional connectivity analysis depend on the zero-lag correlation between two time series (Deshpande, et al., 2009). Zero-lag correlation measures the simultaneous linear coupling relationship between two time-series.

2.6 Motion Estimation Based Methods

Motion analysis is a very popular topic in computer vision, owing to its numerous applications. Motion estimation (ME) is a technique that determines the transformation between two consecutive images in a video. In motion estimation technique, the motion vector (MV) defines the motion or movement in vector form (magnitude and direction) between two consecutive frames. These motion vectors are frequently used in video compression. These motion vectors are also used for detecting or tracking the motion. Fig. 2.8 shows the example of different motion estimation techniques.

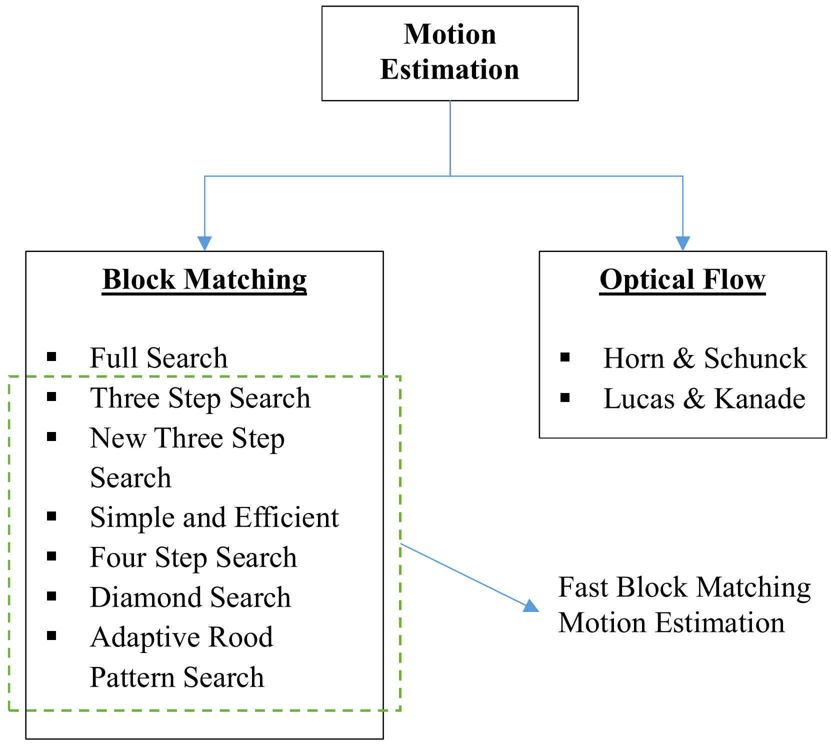

Fig. 2.8 Example of different motion estimation techniques

Motion estimation is classified into several techniques. Block matching and optical flow are the most common methods used for motion estimation. The most straight forward block matching method is full search or exhaustive search algorithm which searches all points within the search window. There are several types of fast block motion estimation algorithms proposed in literature (Nisar, et al., 2012). However their result in terms of PSNR is not as good as full search algorithm, but they are faster than full search (Barjatya, 2004).

Optical flow is the distribution of apparent velocities of movement based on the change of the brightness patterns in an image. Optical flow technique provides better estimation accuracy compared with other motion estimation algorithms (Philip, et al., 2014). Gradient method is one of the basic techniques in optical flow that was introduced by (Fleet & Weiss, 2006). However, gradient method cannot give a complete solution for optical flow fields because of the aperture problem. Aperture problem is the motion of an object (e.g. edge or bar) which cannot be determined in small aperture window. To solve the aperture problem, another mathematical constraint is needed. Horn-Schunck and Lucas-Kanade are the most common techniques used to solve the aperture problem by using differentiation method. Horn-Schunck method is a global method which introduces a constraint of smoothness (Horn & Schunck, 1981). The advantage of Horn-Schunck method is that it provides smooth flow, global information and also accurate time derivative. Although Horn-Schunck gives a solution for optical flow, but it takes high computational time due to the iterative problem (Zhariy, 2005). Hence, Lucas-Kanade method was introduced (Lucas & Kanade, 1981). Lucas-Kanade is a local method which assumes the motion between two consecutive frames is constant over a small neighbourhood. The advantage of Lucas-Kanade method is simple, low computation time and also accurate time derivative. Although Lucas-Kanade gives low computation time, but it causes errors on the boundaries (Zhariy, 2005).

2.6.1 Full Search Block Matching Method

Block matching algorithm is the most popular technique used for ME in which current frame is divided into non-overlapping macro blocks of size N x N. Full search (FS) algorithm calculates the motion vectors by using sum of absolute difference (SAD) at every possible location in the search window of range p in the reference frame. SAD can be calculated by using Eq. 2.2.

$$SAD(x+i, y+j) = \sum_{x=0}^{N-1}\sum_{y=0}^{N-1}\left|c(x,y) - s(x+i, y+j)\right| - p \leq i, j \leq p \qquad \text{Eq. 2.2}$$

In Eq. 2.2, (x, y) is the position of the current block and N is the size of the block. Current block is represent by c(x, y), whereas the reference block for possible locations in the search window range of p is represented by s(x+i, y+j), and (i, j) represents the motion vector (MV). The MV shows the displacement of the current block with respect to the reference frame which has the lowest SAD value in the search window. Fig. 2.9 gives an overview of full search block matching motion estimation algorithm.

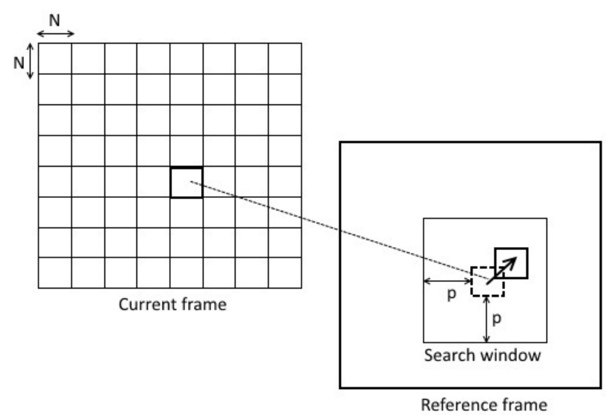

Fig. 2.9 Overview of full search block matching motion estimation algorithm

2.6.2 Horn-Schunck Optical Flow Method

Optical flow is apparent of movement based on the brightness patterns of an image. Horn-Schunck (HS) algorithm estimates the optical flow by introducing a global constraint of smoothness. It is able to minimize the distortion of the flow by assuming smoothness in the flow over whole image

(Horn & Schunck, 1981). The optical flow is computed by using the Eq. 2.3 and Eq.2.4

$$u^{k+1} = \bar{u}^{k} - \frac{f_x\left(f_x\bar{u}^{k} + f_y v^{k} + f_t\right)}{\alpha^2 + f_x^{\,2} + f_y^{\,2}} \qquad \text{Eq. 2.3}$$

$$v^{k+1} = \bar{v}^{k} - \frac{f_x\left(f_x\bar{u}^{k} + f_y v^{k} + f_t\right)}{\alpha^2 + f_x^{\,2} + f_y^{\,2}} \qquad \text{Eq.2.4}$$

In the equation, f_x, f_y and f_t are the derivatives of the image intensity along the x, y and t (time) dimension and the parameter α is the regularization constant. Larger value of α leads to smoother flow. $\bar{u}$ and $\bar{v}$ is the weighted average of u and v calculated in a neighbourhood around the pixel at location (x, y). k is the iteration number for computing the flow vectors. The higher the iteration, the vectors is supposed to be more accurate.

2.7 Vector Median Filter

Vector median filter (VMF) is used to smooth the motion field. MVs are often distorted or are noisy at the boundaries/edges in an image, which may result in wrong ME. VMF is used avoid this problem (Liu, 2013). The basic idea of the median filter is that the current pixel value is replaced by the median of the pixels contained in a window around it. The median value is defined as (n/2)th element in the order of a set of n elements. Fig. 2.10 shows the illustration of the concept of median filter for a 3x3 window.

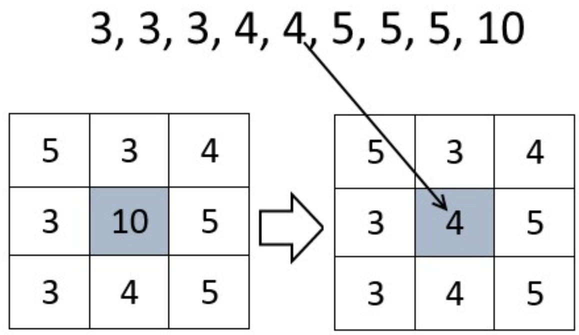

Fig. 2.10 Illustration of the concept of median filter for a 3x3 window

The VMF is introduced for a vector signal. The vector median operator is obtained from the element of a set of vectors which have lowest sum of distances from all other elements. The distances can be calculated by using L2-norm (Weisstein, n.d.). The distance between two vectors, $[u_x, u_y]$ and $[v_x, v_y]$ is given in Eq. 2.5:

$$\|u, v\|_2 = \sqrt{(u_x - v_x)^2 + (u_y - v_y)^2} \qquad \text{Eq. 2.5}$$

In Eq. 2.5, u_x and u_y are the horizontal and vertical components of the vector u; v_x and v_y are the horizontal and vertical components of vector v. The mathematical representation of VMF is given below in Eq. 2.6:

$$v_{m_i} = \arg\min_{v_m \in S_i} \sum_{k=1}^{K} \|v_m - v_k\|_2 \qquad \text{Eq.2.6}$$

In Eq. 2.6, v_m is the median vector in the VMF window. Given a set of vector $S_i = \{v_k, v_{k+1} \ldots v_K\}$, K is the total number of members in the window. The motion field is clean after applying VMF.

Chapter 3

Methodology

In this chapter, we will discuss the research methodology. In this research, the EEG data is acquired using the oddball experiment and converted into EEG topo-maps that are used in our computer vision based algorithms. Different brain lobes are marked on the EEG topo-map. Next, we will track the EEG activity on EEG topo-maps by using full search (FS) block matching and Horn-Schunck (HS) optical flow motion estimation (ME) method. As a result, we will be able to observe the path of the EEG activation flow and the lobes involved for individual and all subjects for a complete activity (from the start to the end of the experiment). Lastly, we will compare these results with the classical method of computing the functional connectivity. In this work, we have developed correlation based tracking algorithm to measure the functional connectivity. Fig. 3.1 shows the flow chart of the research.

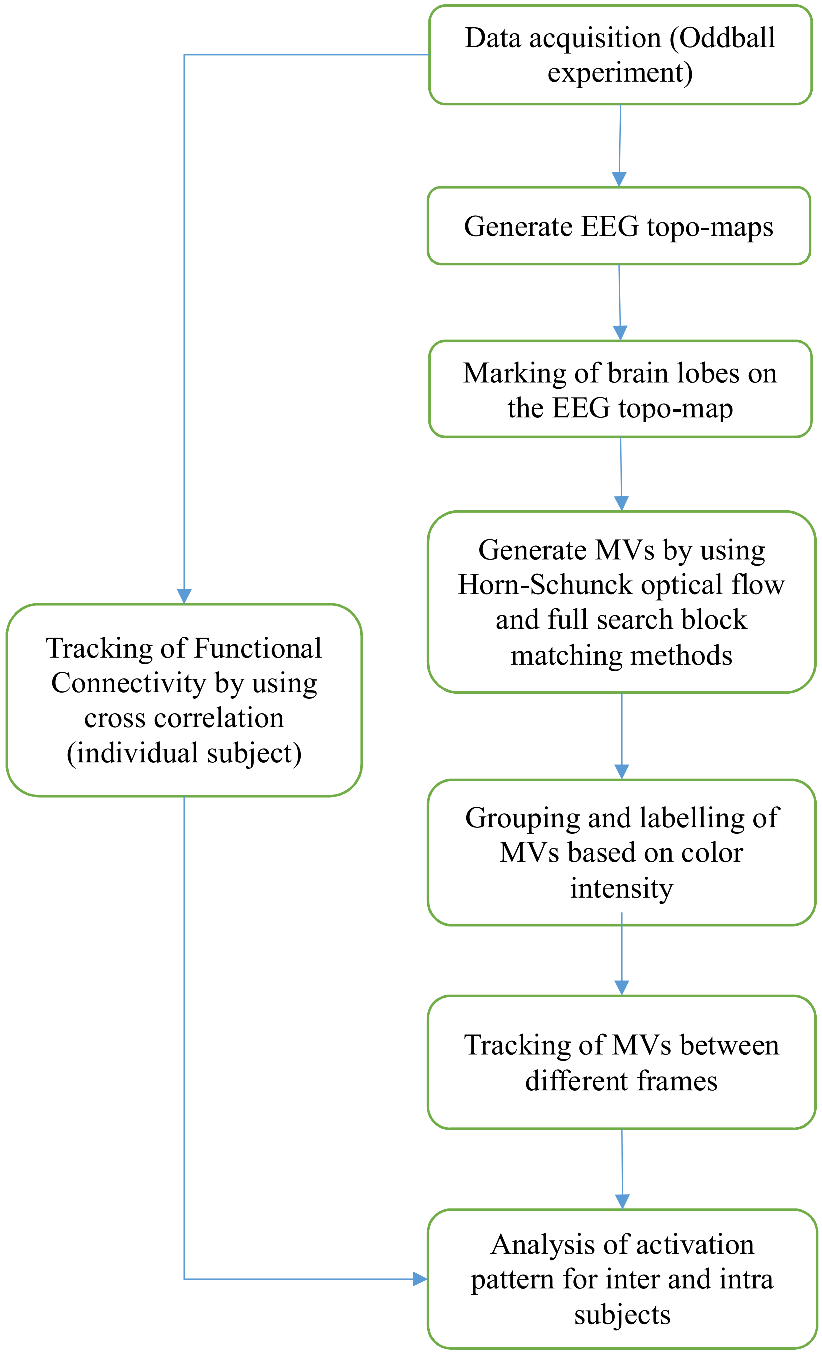

Fig. 3.1 Flow chart of the research

3.1 Experiment Setup and Data Acquisition

The EEG data is acquired using oddball experiment to study the functional brain connectivity. In the oddball experiment, the data was acquired from 20 healthy subjects with an age of around 19-23 years with normal or corrected-to-normal vision. The EEG data is acquired by using EGI 128-channel EEG machine with the sampling rate of 250 Hz. Subjects were asked to focus on the computer screen; when the target stimuli appears, they are required to respond to it by pressing a button. In this experiment, target (circle) and non-target (square) stimuli appears randomly on the computer screen for a duration of 500ms. Target stimuli appears 40 times whereas the non-target stimuli appears 95 times in random order. In between stimuli, a blank screen will appear for a duration of 1000ms for fixation time. Fig. 3.2 shows the visualization of the oddball experiment for the data acquisition.

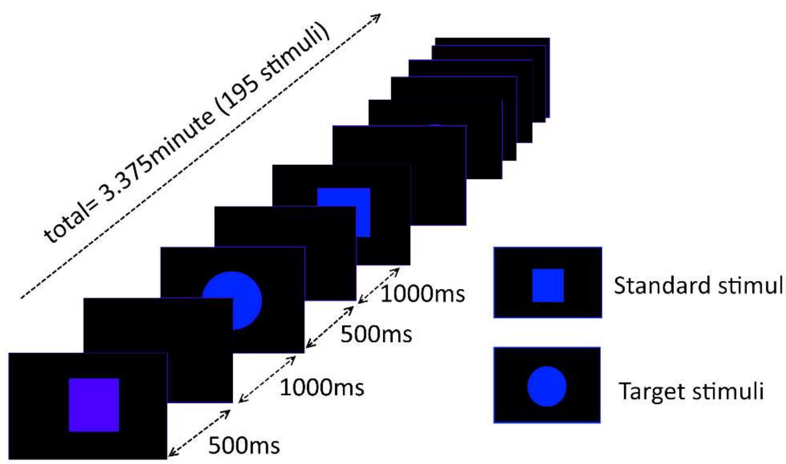

Fig. 3.2 Visualization of the oddball experiment for the data acquisition

The results for oddball experiment can be divided into four different cases, i.e.: target with response, target with no response, non-target with response and non-target with no response. Target stimuli with response means that target stimuli appears and the subject responded correctly. Target stimuli with no response means the subject does not give any response when the target stimuli appeared. Non-target stimuli with response means the subject responded wrongly when the non-target stimuli appeared. Non-target with no response means the non-target stimuli appeared and the subject did not respond which is correct response. Table 3.1 shows the oddball experiment results for all subjects. From the table, we can see that subject 9 gives the best response for the oddball experiment. Subject 9 responded the target-stimuli 37 out of 40 times and did not give response to non-target stimuli.

Table 3.1 Oddball experiment result for all subjects

Subject	**Target**		**Non-target**	
	Response	**No response**	**Response**	**No response**
1	28	12	0	95
2	13	27	1	94
3	28	12	0	95
4	34	6	2	93
5	13	27	2	93
6	35	5	1	94
7	24	16	0	95
8	25	15	0	95
9	37	3	0	95
10	37	3	3	92
11	17	23	1	94
12	34	6	7	88
13	12	28	1	94
14	27	13	2	93
15	28	12	1	94
16	23	17	0	95
17	36	4	0	95
18	30	10	1	94
19	31	9	2	93
20	24	16	1	94

The EEG data can be converted into visual form; EEG topo-maps by using the function “topoplot()” in EEGLAB (Delorme & Makeig, 2004). Fig. 3.3 shows the example of EEG topo-map generated by EEGLAB from EEG signal at a particular frame. In this research, 35 out of 128 of the outermost electrodes are removed because the outermost electrodes may have some noise; as some subjects may have small head size and the outermost electrodes may not touch the scalp well. Table 3.2 shows the list of electrodes in the EGI system used for data acquisition and their corresponding names in the 10-10 electrodes placement system (Luu & Ferree, 2005).

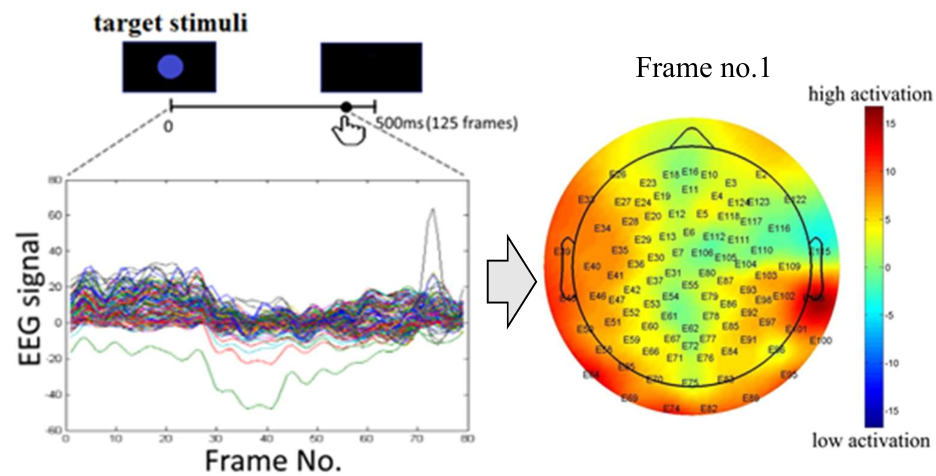

Fig. 3.3 Example of EEG topo-map generated by EEGLAB from EEG signal at a particular frame.

Table 3.2 List of electrodes in the EGI system used for data acquisition and their corresponding names in the 10-10 electrodes placement system (Luu & Ferree, 2005)

No.	Electrode	No.	Electrode	No.	Electrode	No.	Electrode
1	E2/AF8	**25**	E35	**49**	E67/PO3	**73**	E97
2	E3/AF4	**26**	E36/C3	**50**	E69	**74**	E98/CP6
3	E4/F2	**27**	E37/CP1	**51**	E70/O1	**75**	E100/TP10
4	E5	**28**	E39	**52**	E71	**76**	E101
5	E6/FCZ	**29**	E40/T7	**53**	E72/POZ	**77**	E102/TP8
6	E7	**30**	E41/C5	**54**	E74	**78**	E103/C6
7	E10	**31**	E42/CP3	**55**	E75/OZ	**79**	E104/C4
8	E11/FZ	**32**	E45	**56**	E76	**80**	E105/C2
9	E12	**33**	E46/TP7	**57**	E77/PO4	**81**	E106
10	13/FC1	**34**	E47/CP5	**58**	E78/P2	**82**	E108
11	E16/AFZ	**35**	E50	**59**	E79	**83**	E109/T8
12	E18	**36**	E51	**60**	E80	**84**	E110
13	E19/F1	**37**	E52/P5	**61**	E82	**85**	E111/FC4
14	E20	**38**	E53	**62**	E83/O2	**86**	E112/CF2
15	E23/AF3	**39**	E54	**63**	E84	**87**	E115
16	E24/F3	**40**	E55/CPZ	**64**	E85/P4	**88**	E116/FT8
17	E26/AF7	**41**	E58/P9	**65**	E86	**89**	E117/FC6
18	E27/F5	**42**	E59/P7	**66**	E87/CP2	**90**	E118
19	E28/FC5	**43**	E60/P3	**67**	E89	**91**	E122/F8
20	E29/FC3	**44**	E61/P1	**68**	E91/P8	**92**	E123/F6
21	E30/C1	**45**	E62/PZ	**69**	E92/P6	**93**	E124/F4
22	E31	**46**	E64	**70**	E93/CP4		
23	E33/F7	**47**	E65/PO7	**71**	E95		
24	E34/FT7	**48**	E66	**72**	E96/P10		

3.2 Marking of Brain Regions on the EEG Topo-map

After EEG topo-maps are generated, we need to mark the different brain lobes on EEG topo-maps so that we can track the brain activation across different lobes. The EEG topo-maps are divided into six different regions: frontal (F), occipital (O), right temporal (R), left temporal (L), parietal (P) and center or motor region (M). This division is based on the 10-10 international electrode placement system. Fig. 3.4 shows the layout illustrating the 10 – 10 equivalent on the 128-channel HydroCel GSN (Luu & Ferree, 2005).

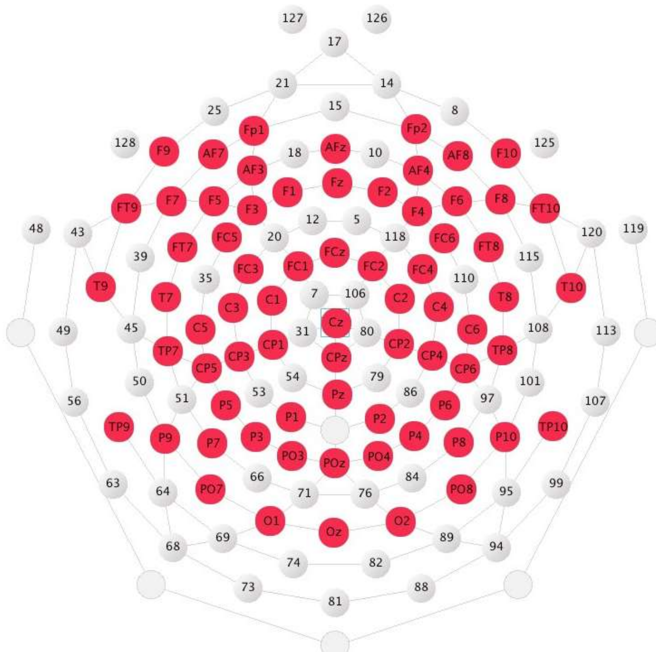

Fig. 3.4 Layout illustrating the 10 – 10 equivalent on the 128-channel HydroCel GSN (Luu & Ferree, 2005)

10-10 international system contains electrodes in between two different lobes e.g. Frontal-Parietal (FP), Frontal-Center (FC), Center-Parietal (CP), Parietal-Occipital (PO) and Temporal-Parietal (TP). Based on this electrode information, we were able to divide the EEG topo-map into six different lobes. Fig. 3.5 shows the marking of different lobes based on the electrodes information from the 10-10 system. The red color circles are the electrodes of 10-20 international system. In 10-10 system, the electrode T7, T8, P9, and P10 are equivalent to T3, T4, T5, and T6 in 10-20 system. Based on the electrodes in the 10-20 system, the function of electrodes C3 and C4 are used for sensorimotor integration (Walker, et al., 2007). So, we assume that the lobes between C electrodes belong to the motor region (M).

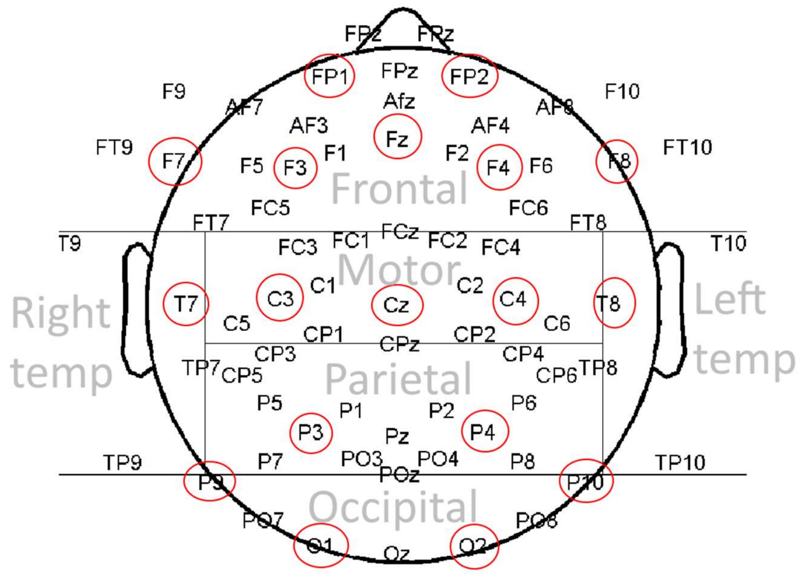

Fig. 3.5 Marking of different lobes based on the electrodes information of 10-10 system

3.3 Motion Field Generation

3.3.1 FS Block Matching algorithm

In FS block matching algorithm, there are some parameters that are very critical for good ME and tracking. These are the search window range (p), and the macro block size (N). Smaller the macro block size, more computation time is required but better result in terms of matching is achieved; on the other hand if macro block size is big, computation time decreases and so the accuracy of the result. Search window range (p) also has a significant effect on the ME results. The computation time increases by increase in the search window range. A bigger search window is useful if the range of motion is high. The peak signal to noise ratio (PSNR) is a quality measurement metric between the original image and the compensated image. Higher PSNR means better quality of compensated image. The comparison of different macro block sizes and the search window range for FS block matching motion estimation is discussed in Chapter 4.

3.3.1.1 Vector Median Filter

For FS block matching algorithm, it has been observed that MVs are often distorted or are noisy at the boundaries/edges of topo-map, which may result in wrong ME. Since the noisy vector field may result in distortion in direction calculation especially for tracking. Vector median filter (VMF) is used to reduce the distortion in motion vector calculations. The displacement vector is replaced by the median vector in the 3x3 window size. The motion field is clean after applying VMF. The noisy MVs in the edges of topo-map are removed. The results for PSNR and the motion field after applying VMF are discussed in chapter 4.

3.3.2 HS Optical Flow algorithm

In HS optical flow algorithm, k is the iteration number for computing the flow vectors. The higher the iteration, the vector is more accurate. The motion field generated by using HS method is more detailed and noiseless compared with the block matching method, in addition it does not use vector median filter.

After we generate the MVs, we extract the MVs at every 8, 16 and 32 pixels in horizontal and vertical direction of topo-map to reduce the computation time. Fig. 3.6 shows the example of MVs extracted at different pixel ranges for HS method (topo-map size of 351 x 351 pixels).

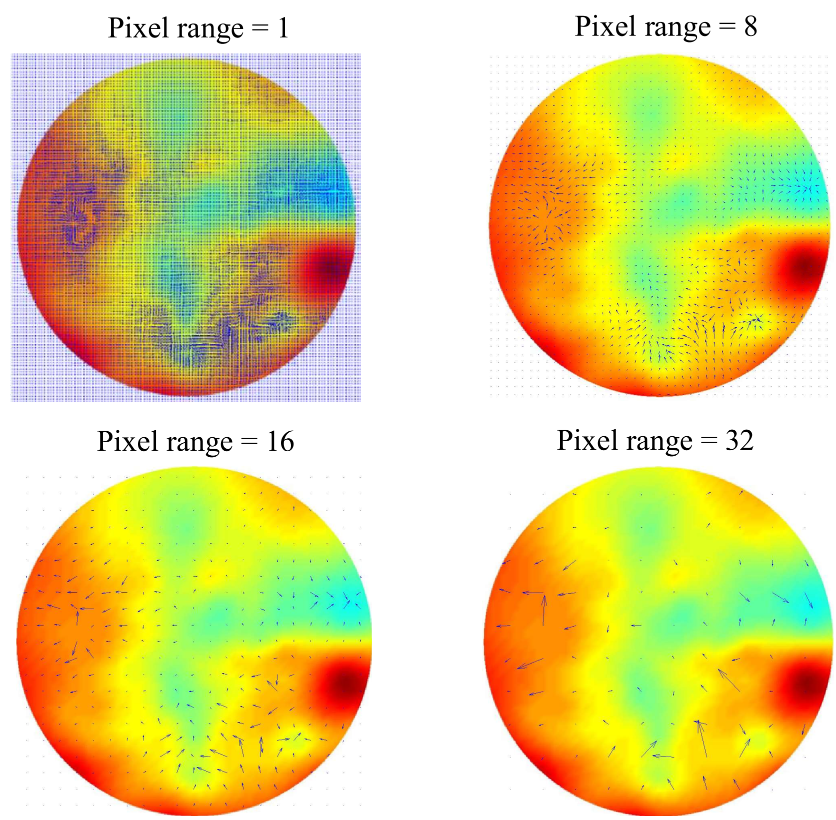

Fig. 3.6 Example of MVs extracted at different pixel ranges for HS method (topo-map size of 351x351 pixels)

3.4 Grouping and Labelling of Motion Vectors (MVs)

In this research, we have focused only on the high activation region on the topo-map. Red color on the EEG topo-maps corresponds to high activation and blue color corresponds to low activation. The MVs with low activation on the topo-maps are removed and not used for tracking. The activation can be classified into high activation when the grayscale intensity of the pixel is lower than 150 and the B-channel intensity in the RGB color model is lower than 10. We grouped the MVs based on the color intensity of topo-map. Fig. 3.7 shows the steps of grouping and labelling of motion vector clusters based on the color intensity of topo-maps. We have set the threshold of the grayscale intensity level from 0 to 150 by increasing threshold in steps of 5 intensity levels per step. Note that the grayscale intensity level varies from 0-255. So we considered the values from 151-255 as low activation region and do not track the motion vectors in this range. The grayscale values from 0-150 are considered as high activation region. For every threshold step, we group and label the MVs that are linked together in 8-connected neighborhood. Then we compare the grouped MVs of current threshold step with the grouped MVs of previous threshold to obtain more accurate but separate groups for MVs for every label. This will result in separate groups instead of combined groups. The final selected grouped MVs at current threshold will be compared with next threshold (+5) and the same step will be repeated till a threshold of 150. The advantage of this method is that we can separate MVs and provide more precise groups instead of setting one threshold only. Fig. 3.8 shows the example of grouped and labelled MVs for grayscale threshold of 70 and 75. It can be seen from the figure that at the grayscale threshold of 70, two MV clusters (label 1 and label 2) are observed whereas at grayscale threshold of 75 only one cluster (label 1) is present. Hence, the grouped MVs of label 1 and label 2 with grayscale threshold of 70 will be selected instead of grouped MVs of label 1 of grayscale threshold of 75.

Step 1:
Read EEG TOPO-MAP

↓

Step 2:
Set grayscale threshold = 0 ; B_{rgb}<10 (fixed)

↓

Step 3:
Remove all MVs lower than grayscale threshold and label all motion fields (e.g. 1, 2 …) as group A.

↓

Step 4:
Increase grayscale threshold (+5)

↓

Step 5:
Remove all MVs lower than grayscale threshold and label all motion fields (e.g. 1, 2 …) as group B.

↓

Step 6:
Choose the motion field in group A or B which has more clusters and put in group A

↓

Step 7:
Repeat step 4 to step 6 until the grayscale threshold= 150 and choose group A as final group

Fig. 3.7 Steps of grouping and labelling motion vector clusters based on the color intensity of topo-maps

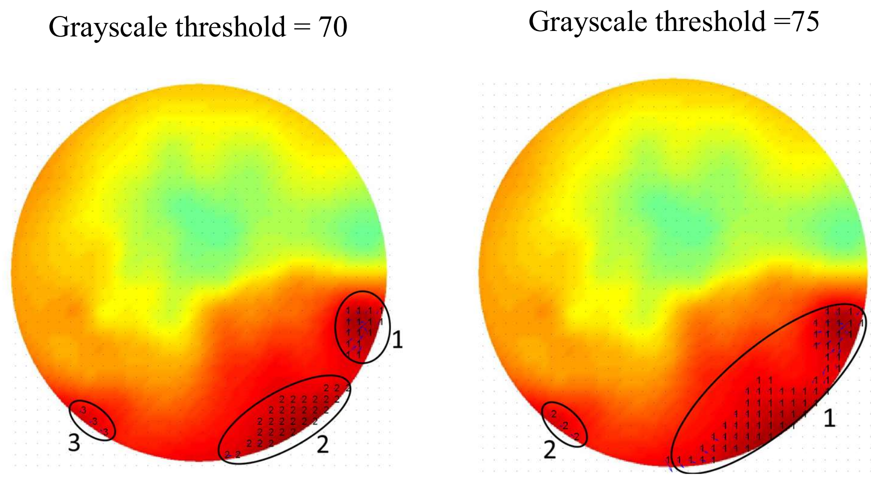

Fig. 3.8 Example of grouped and labelled MVs for grayscale threshold of 70 and 75

3.5 Tracking of MV Clusters

After all the MVs are grouped and labelled, the movement will be tracked by the overlapping of the grouped motion field (cluster) in the current frame and the motion field in the next frames. If a group motion field overlaps with another motion field in the next frame, it means that the activation is moving from the current frame to next frame at this particular area. If there is no overlapping between consecutive frames, we will skip that frame and continue search in the next frame; however we will mark/hold the previous location. If a motion field overlaps then the tracking will be started again. Fig. 3.9 shows an example of tracking of the MVs based on the overlapping of motion field in the next frame. The arrow shows the direction of the activation flow.

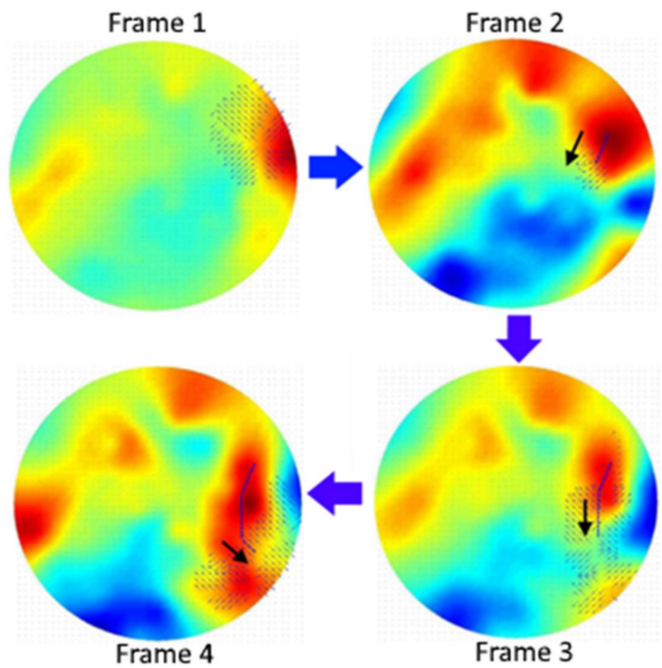

Fig. 3.9 Example of tracking of the MVs based on the overlapping of motion field in the next frame

3.6 Plotting of Activation Graph for Analysis

After tracking all the possible paths, we need to analyze the inter subject and intra subject activation behavior in different brain lobes for different oddball. We have converted all the possible tracked paths into a graph for each lobe for average activation of all subjects. Fig. 3.10 shows the procedure for plotting of average graph for each lobe for all subjects. First, we mark the lobe for every MV in every frame. After that, we count and record how many MVs are involved in activation in each lobe; e.g. if there are a total of 4 MVs in a particular frame in frontal lobe, the value under frontal lobe at that frame in the table is recorded as 4. Here the trial no. represents the number of trials for one case (e.g. target stimuli with response). The total no. represents the total number of frames for which the subject response to the stimuli is observed. For different trials, subject responds with different timings for the case Target with response, as for different trials the subject response depends on when he observes the target. So the timing of response for different trials may be different. In order to average out the result of different trials we have considered three cases, i.e. the fastest the slowest and middle time trial. However, this results in different total no. of frames for every trial. Therefore, we have shifted the response of recorded lobes involving all the tracked paths to the right, so all of the tracked paths are aligned with the timing when button is pressed. After that, we calculate the average activation of each lobe for all subjects. However for the case target with no response and no target with non-response, there is not any timing issue as all the sequences end at the same time. Lastly, we plot the average activation graph. The graph is smoothed by using a 5-point moving average filter; this is plotted on the original graph to observe the pattern of flow of activation.

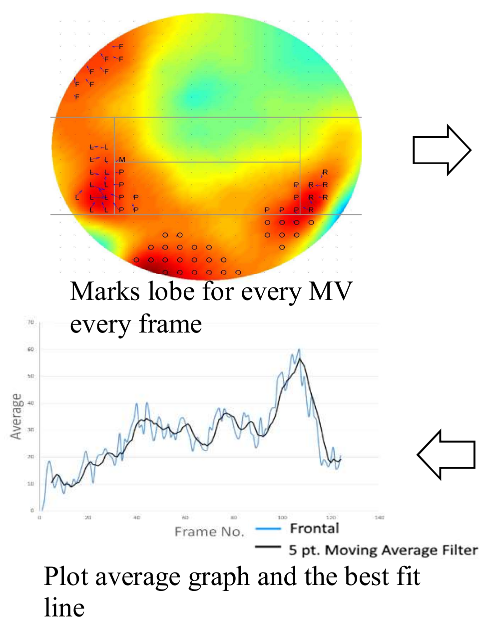

Frontal						
Trial No.	Total Frame	Frame No. 1	2	3	4	5
1	5	8	4	5	2	0
2	3	0	5	2		
3	2	2	3			
4	3	4	1	1		

Frontal						
Trial No.	Total Frame	Frame No. 1	2	3	4	5
1	5	8	4	5	2	0
2	3	0	0	0	5	2
3	2	Shift 0	0	0	2	3
4	3	0	0	4	1	1
Average		2	1	2.25	2.5	1.5

Fig. 3.10 Procedure for plotting of average graph for each lobe for all subjects.

3.7 Tracking of Functional Connectivity by using Cross-Correlation Method

In this research, cross-correlation is used to track the functional connectivity between different electrodes. Next, we compare the functional connectivity with the average activation graph using motion estimation method at different segment for different cases. Fig. 3.11 shows the flow chart of tracking functional connectivity by using cross- correlation method. First of all, we extract the EEG data from for each stimuli segment (from appearance of stimuli to the event when button is pressed in response to stimuli appearance). After that, we separate the data into samples of 20 segment each (e.g.: 1-20, 21-40 …). We have chosen 20 samples based on trial and error; as if the number of samples is too small, the correlation value will approximate to 1 or -1 (perfect correlation). On the other hand, if the average number of samples is too large, we may not be able to find a good correlation value. Hence, we have found that 20 samples give good correlation results. Then, we calculate the cross-correlation between different electrodes. We only calculate the cross-correlation for the electrodes that have high EEG signal (EEG amplitude higher than 20µV. The maximum amplitude of EEG signal is 700µV. Next, we will plot the connection between the electrodes that have correlation value higher than the specified threshold value at zero lag. We have set the threshold value at 0.9. However, if there is no connectivity in the segment, we will reduce the threshold value in steps of 0.1 until a value of 0.7. Fig. 3.12 shows the pseudo code for tracking the functional connectivity by using cross- correlation method. Fig.

3.13 shows the tracking of functional connectivity by using cross-correlation (2^{nd} subject target with response trial no.4).

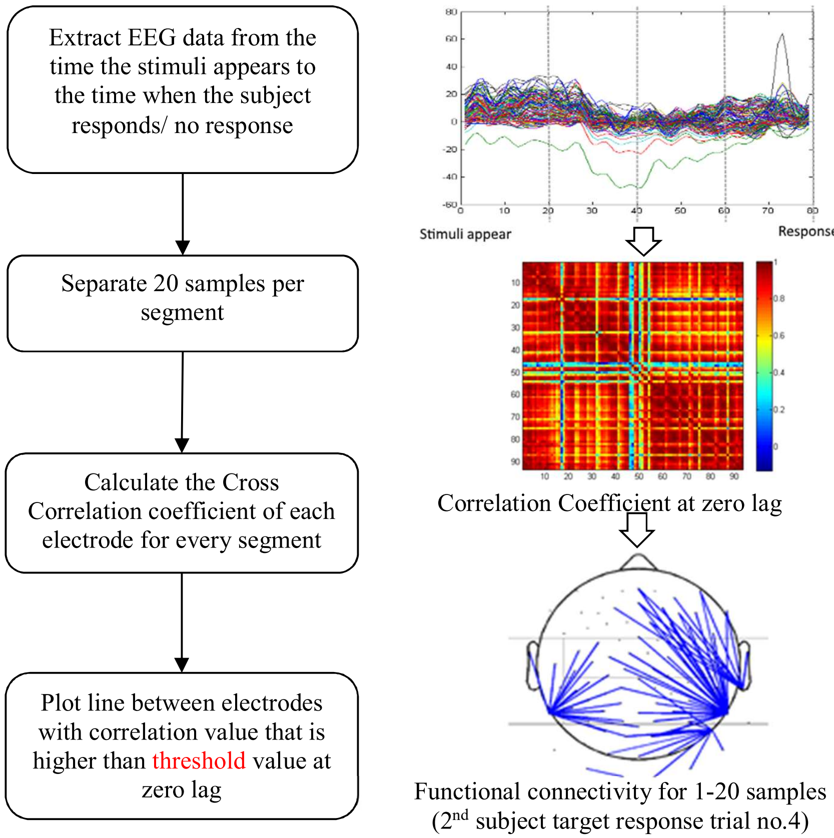

Fig. 3.11 Flow chart of tracking functional connectivity by using cross-correlation method

```
threshold = 0.9
count = 0
while(count == 0 && threshold>=0.7)
   for electrode A=1: total electrode
      if (maximum amplitude of electrode A <20)
         continue to next electrode;
      end
      for electrode B=1: total electrode
         Calculate cross correlation between electrode A and B
         if (max correlation > threshold && max correlation lag==0)
            plot connectivity between electrode A and B
            count = count+1
         end
      end
    end
    threshold = threshold-0.1
end
```

Fig. 3.12 Pseudo code for tracking the functional connectivity by using cross-correlation method

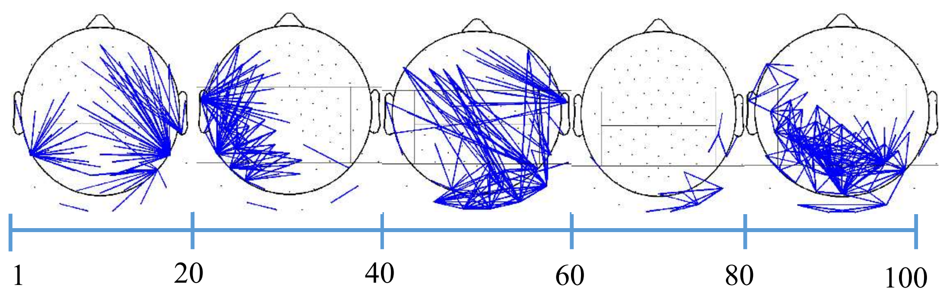

Fig. 3.13 Tracking of functional connectivity by using cross-correlation (2^{nd} subject target with response trial no.4)

Chapter 4

Result and Discussions

In this chapter, we will discuss the experimental results. The experiment results are divided into seven parts. First of all, the parameter selection for motion estimation will be discussed. Secondly, we will make comparison between FS block matching and HS optical flow motion estimation. Thirdly, we will discuss the activation path involved for all subjects for different oddball cases for each brain lobe by using FS and HS method. Fourthly, we will make an analysis on the lobes involved for activation for all subjects at different oddball cases by using FS method. Fifthly, we will analyse the lobes involved for activation for all subjects at different oddball cases by using HS method. Sixthly, we will perform an analysis for activation for individual subjects for different oddball cases by using HS method. Lastly, we will observe the pattern of functional connectivity of brain by tracking cross-correlation method for single trial of each oddball case for each segment of 2^{nd} and 9^{th} subject.

4.1 Parameters Selection for Motion Estimation

In this section, we will discuss about the parameters selection for motion estimation for this research. Firstly, we will discuss about the comparison of different topo-map sizes. After that, we discuss the macro block size and the search window range used in FS block matching method. Next, we discuss the motion field after applying VMF for FS method. Next, we discuss the iteration number and pixel range used in HS method. Lastly, we will discuss about comparison between FS and HS motion estimation techniques for this research.

4.1.1 Comparison of Different Topo-map Sizes

In this section, we will compare different topo-map sizes for proposed method to get optimized results. Fig. 4.1 shows tracked paths by using different topo-map sizes for HS method. The original topo-map size is 702x702 pixels. We have performed tracking on a single oddball trial (1^{st} subject target response trial no.1) for topo-map size of 0.2, 0.5, 0.8 and 1.0 of the original size. Subjective assessment of tracked path shows that the change in topo-map size does not have much influence on the tracking results. Hence we will use a topo-map size of 0.5 of the original size (351 x 351 pixels) in the rest of the paper. This will help to reduce the computation time taken by the proposed algorithms.

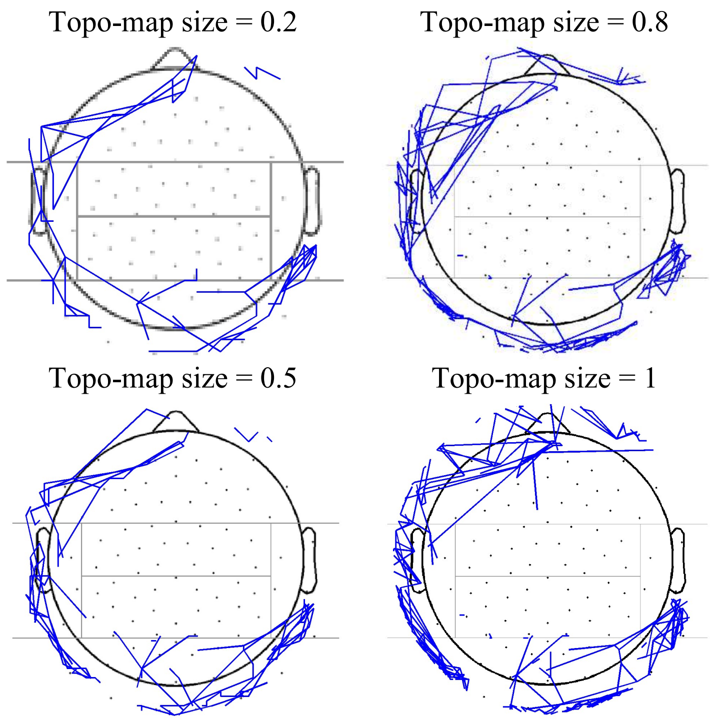

Fig. 4.1 Tracked paths by using different topo-map sizes for HS method

4.1.2 Macro block Size and Search Window Range for FS Method

Fig 4.2 shows a comparison of different macro block sizes and search ranges (p) for FS method (topo-map size of 351 x 351 pixels). From the figure, we have used three different macro-block sizes, 8, 16 and 32; and the search window ranges of 4, 8, 16 and 32 with the topo-map size of 351 x 351 pixels. The table also includes example of motion field, average PSNR and computation time for a single oddball trial (1st subject target response trial no.1). From the table, it is seen that when we increase the macro-block size, it produces less MVs and have lower PSNR value. It means that smaller the macro-block size, better the compressed image and motion field but it needs longer computation time as the total number of blocks in a frame will be increased. Change in the search window range does not have much influence on the motion field for EEG topo-maps but the computation time is different. Larger the search window range, longer the computation time and PSNR is also decreased. For the proposed algorithm, we are focusing on the motion field and not on PSNR value and computation time. More MVs are needed to track the overlapping motion field between current and reference frames. Hence, we are using macro-block size of 8 and the search window range of 4 for the FS block matching algorithm; it also gives better results in terms of PSNR. PSNR is a metric used to calculate the picture quality. A higher value of PSNR corresponds to an image of good subjective quality. Hence higher PSNR value may also mean that the image quality is good for tracking.

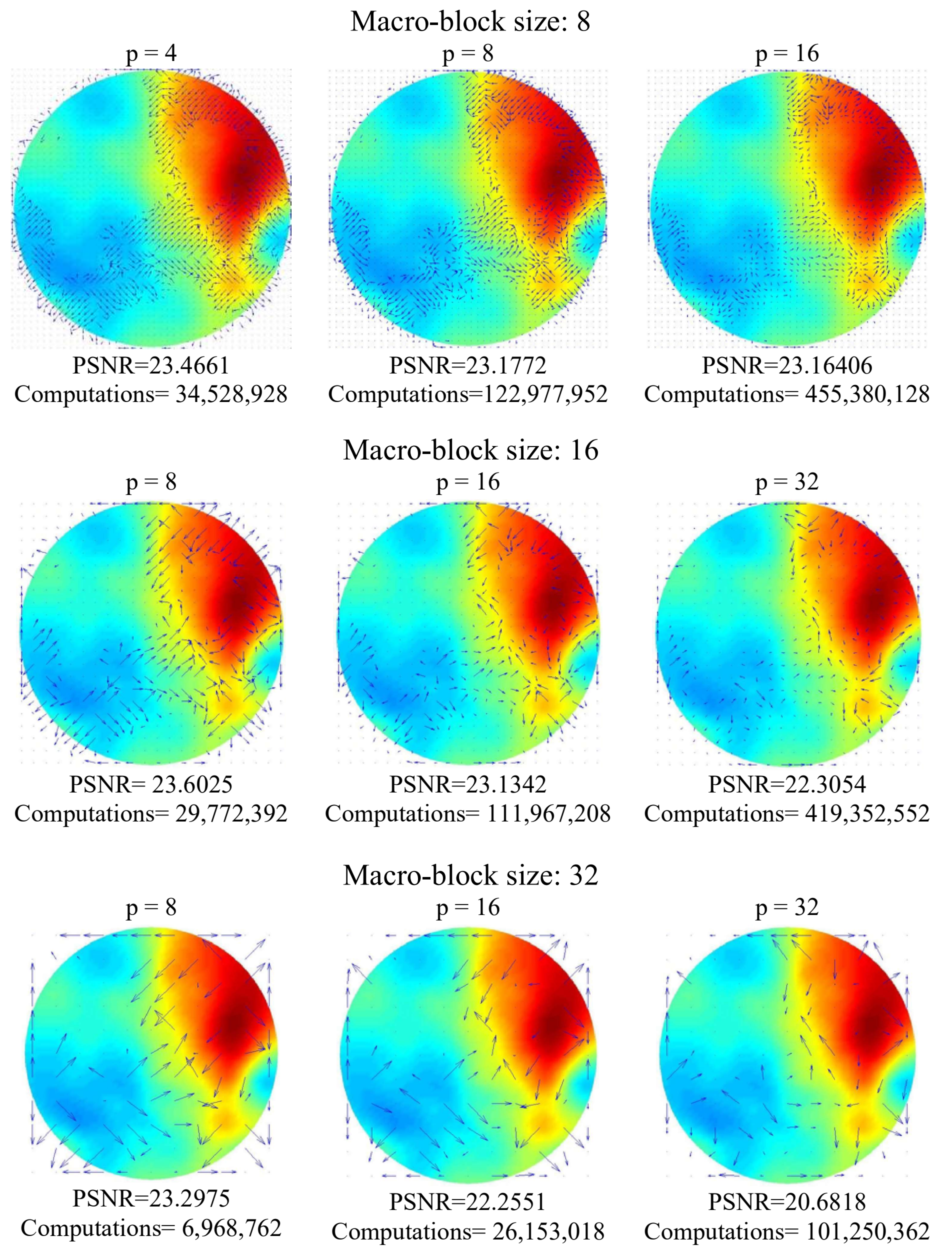

Fig. 4.2 Comparison of macro-block size and the search window range (p) for FS method (topo-map size of 351 x 351 pixels)

4.1.3 Motion Field After Applying VMF for FS Method

For FS method, vector median filter (VMF) is used to reduce the distortion in motion vector calculations. Fig. 4.3 shows the example of motion field before and after applying VMF and the respective PSNR values for FS method (topo-map size of 351 x 351 pixels). The motion field is clean after applying VMF. Besides, the noisy MVs in the edges of topo-map are removed. Moreover, it is observed that the value of PNSR is higher after applying VMF. The higher PSNR means better quality of image.

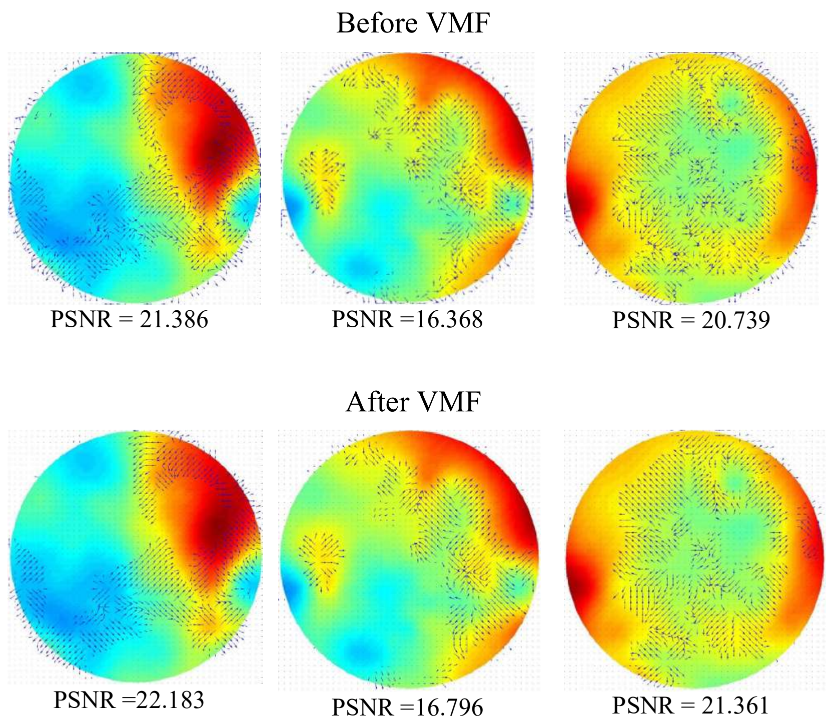

Fig. 4.3 Example of motion field before and after applying VMF for FS method (topo-map size of 351x351 pixels)

4.1.4 Iteration Number and Pixel Range for HS method

In HS optical flow algorithm, k is the iteration number for computing the flow vectors. The higher the iteration, the vectors are more accurate. Fig 4.4 shows the example of motion field generated with different iteration numbers for HS method (topo-map size of 351 x 351 pixels). The increase in the iteration does not influence the motion field as observed subjectively but it takes more computational time. So we will use the iteration k=1 for our experiments.

Iteration: 1

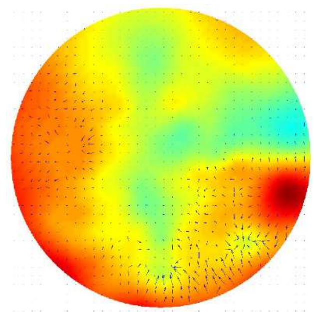

Computation time is 0.418120 seconds.

Iteration: 10

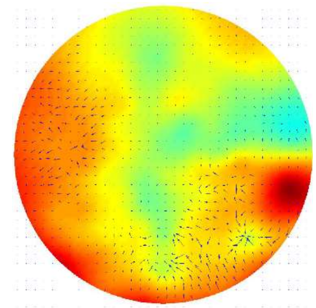

Computation time is 0.747896 seconds.

Iteration: 50

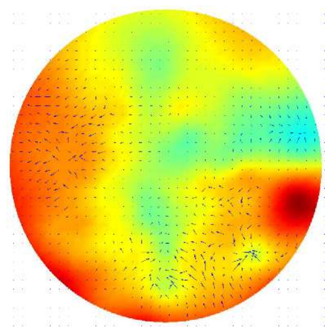

Computation time is 2.212394 seconds.

Iteration: 100

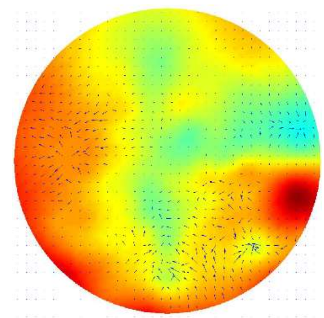

Computation time is 4.009570 seconds.

Fig. 4.4 Example of motion field generated with different iteration numbers for HS method (topo-map size of 351x351 pixels)

4.1.5 Comparison between FS and HS Motion Estimation Techniques

In this section, we have compared FS block matching and HS optical flow motion estimation techniques. Fig. 4.5 shows the comparison of the motion field between FS and HS motion estimation techniques (original topo-map size). The figure shows the comparison of PSNR, computation time, compensation time between FS and HS. The PSNR and computation time is calculated by using EEG topo-map between two consecutive frames with the original topo-map size (704 x 704 pixel). PSNR of HS is higher than FS. The higher PSNR means better quality of compensated image. As observed subjectively, the motion field of HS method is smoother and less chaotic than FS. The computation time to generate MVs of HS is faster than FS but HS need more compensation time. However the total time for HS is still less than FS.

FS	**HS**
Search window range of 8	Iteration of 1
Macroblock size = 16	Pixel range = 16

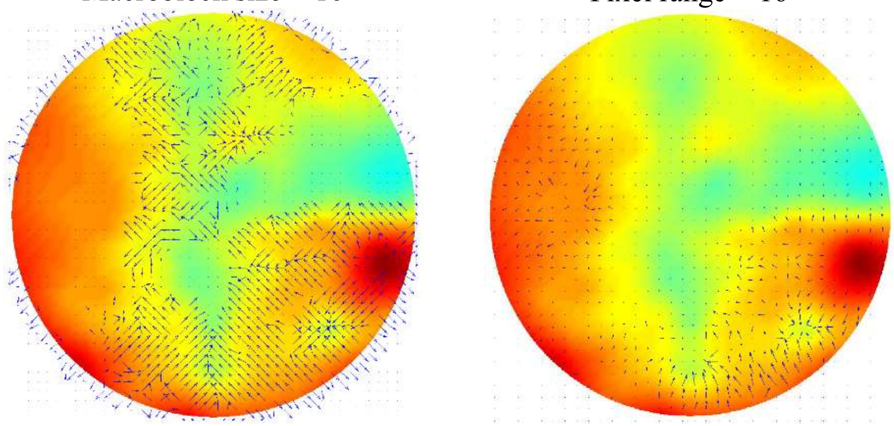

Computation time = 8.87 s	Computation time = 1.33 s
Compensation time = 0.011 s	Compensation time = 0.31 s
PSNR = 20.89	PSNR = 24.96

Fig. 4.5 Comparison of motion field between FS and HS motion estimation techniques (original topo-map size)

Fig 4.6 shows the tracking path for FS and HS method (topo-map size of 351 x 351 pixels). The FS and HS tracking methods give different tracking results for different pixel ranges and block sizes. By increasing the pixel range and block size, we track less number of possible paths. We observed that block size (FS) or pixel range (HS) of 8 gives the maximum number of possible paths. So, we will use the HS method with the pixel range of 8 in the rest of the paper.

FS **HS**

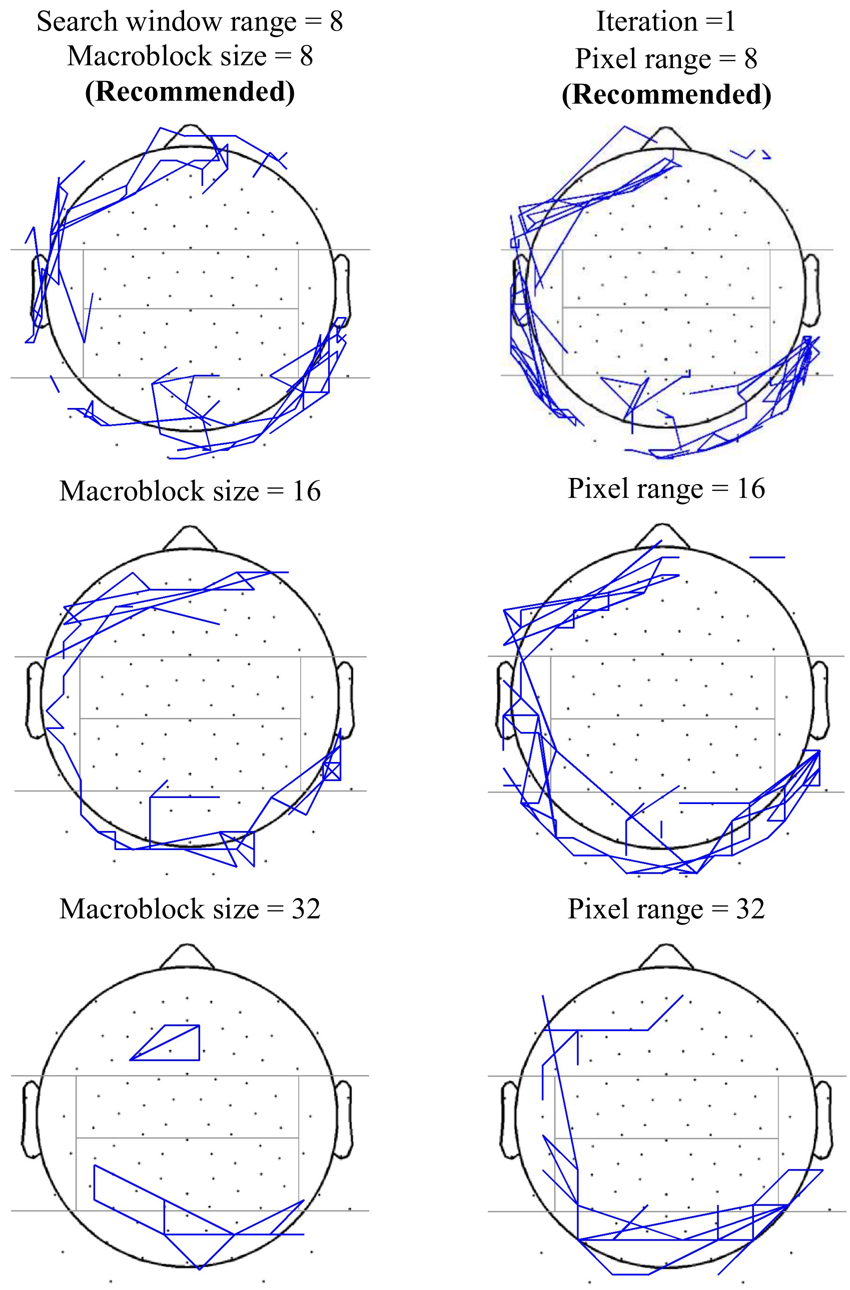

Fig. 4.6 Tracking path for FS and HS method (topo-map size of 351 x 351 pixels)

4.2 Activation Analysis

In this section, we will discuss about the activation analysis in this research. Firstly, we do analysis on average activation for different oddball cases by using both HS and FS method to identify which method is better. Later we will do analysis using the chosen method. For activation analysis, first we analyze all subjects together and then we will perform inter and intra subject analysis. We will also identify the pattern of activation for different oddball tasks. Lastly we will identify the pattern of activation across different brain lobes.

4.2.1 Average Activation Paths for Different Oddball Cases for Each Brain Lobe

In this section, we will discuss about the average activation path tracked for all subjects for different oddball cases for each brain lobe by using FS and HS method. Fig. 4.7 shows average activation graph of different brain lobes. In the figure, we compare the pattern of the graph for all brain lobes for different oddball cases. This figure shows the average result for all subjects except subjects 4 and 8 for which data is inconsistent. For target with response case, we have used three trials (fastest, slowest and medium) for each subject. Hence a total of 54 trials are used to plot the graph. For target with no response and non-target with no response, we have used 3 trials for each subject, which means 54 trials for each case. In the figure, FS and HS method show almost similar pattern of average activation graph. However, HS shows higher amplitude when compared with FS method. The pattern of average graph for every lobe is different for different cases. From the figure, we conclude that the pattern for different types of oddball responses is different for different brain lobes. This difference in pattern correlates with the overall process encountered in the Oddball paradigm.

(a) Frontal

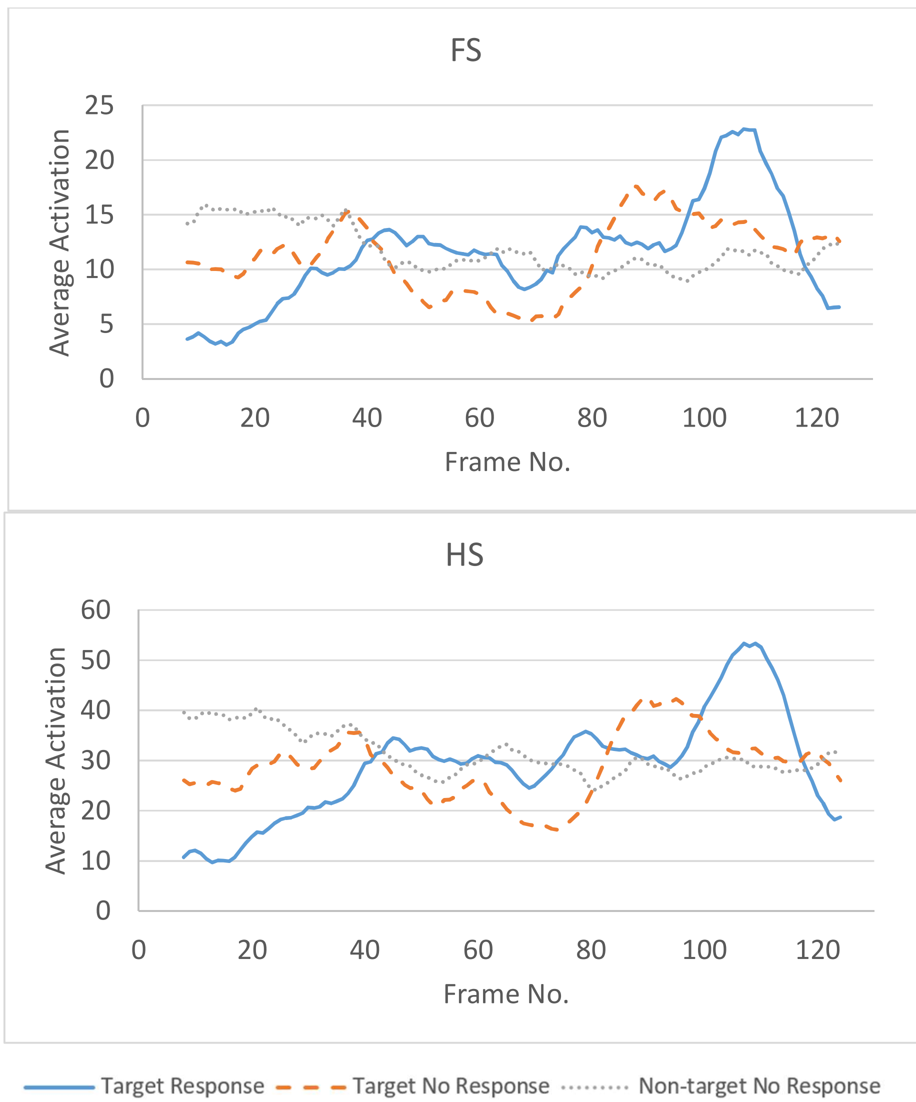

Target with response starts rising earlier than Target with no response. Hence there is a delay in rise in the target with no response, based on which we can conclude that because of this delay the subject was unable to make a decision. Target response also displays a very high peak at the end of the task (frame no.110). Non-target with no response graph does not show lots of variation.

(b) Parietal

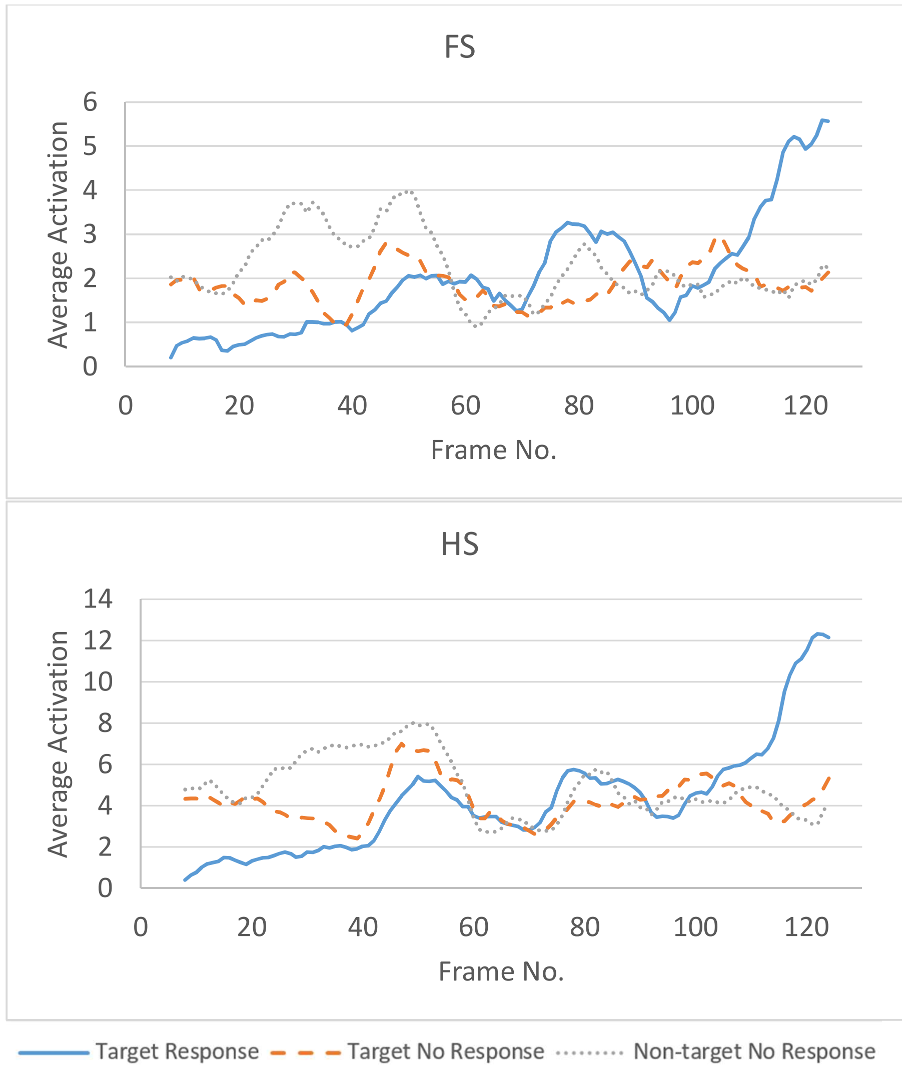

For event related task, higher activity is observed in frontal-parietal region so the graph for target response has highest peak around the end of the task (frame no. 120).

(c) Occipital

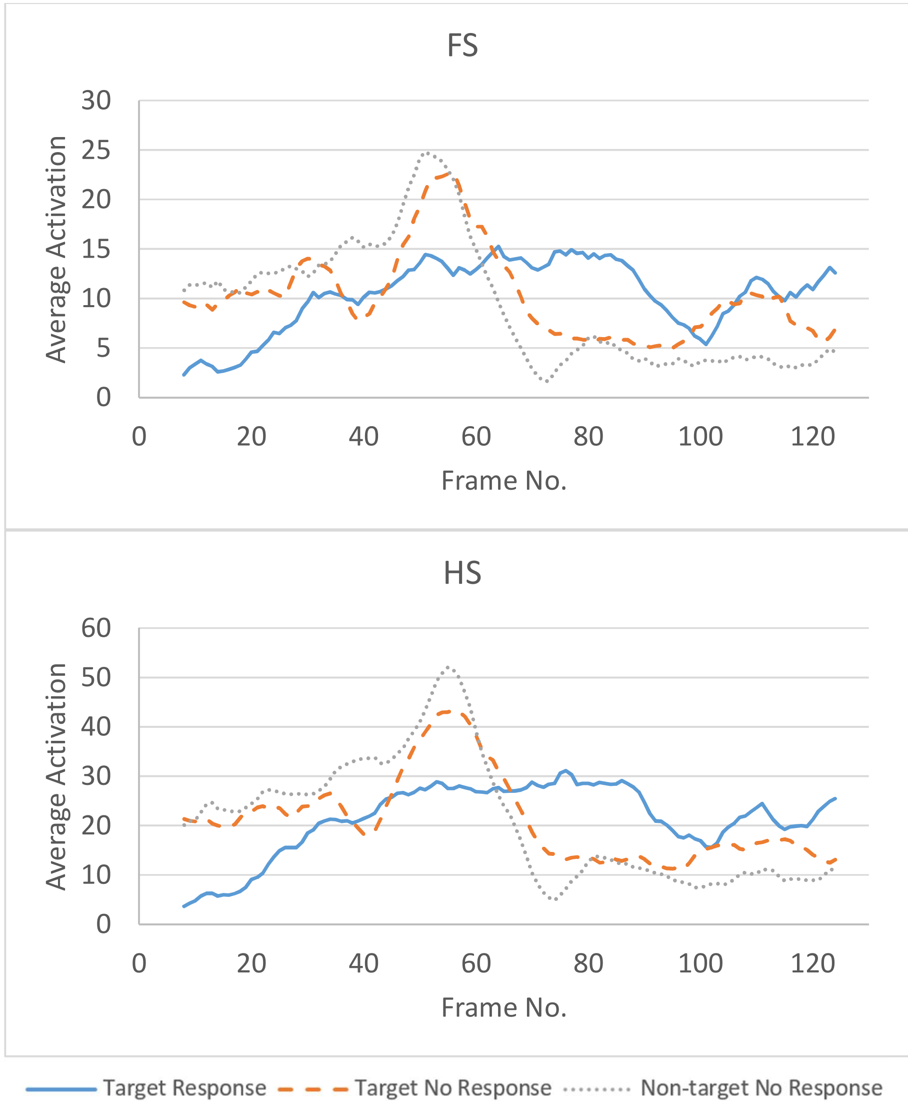

Target response has almost constant graph but it slightly drops near the end of the task (when frontal graph rises). Target with no response and non-target no response have highest peaks around frame no.50 and drop to very low.

(d) Right Temporal

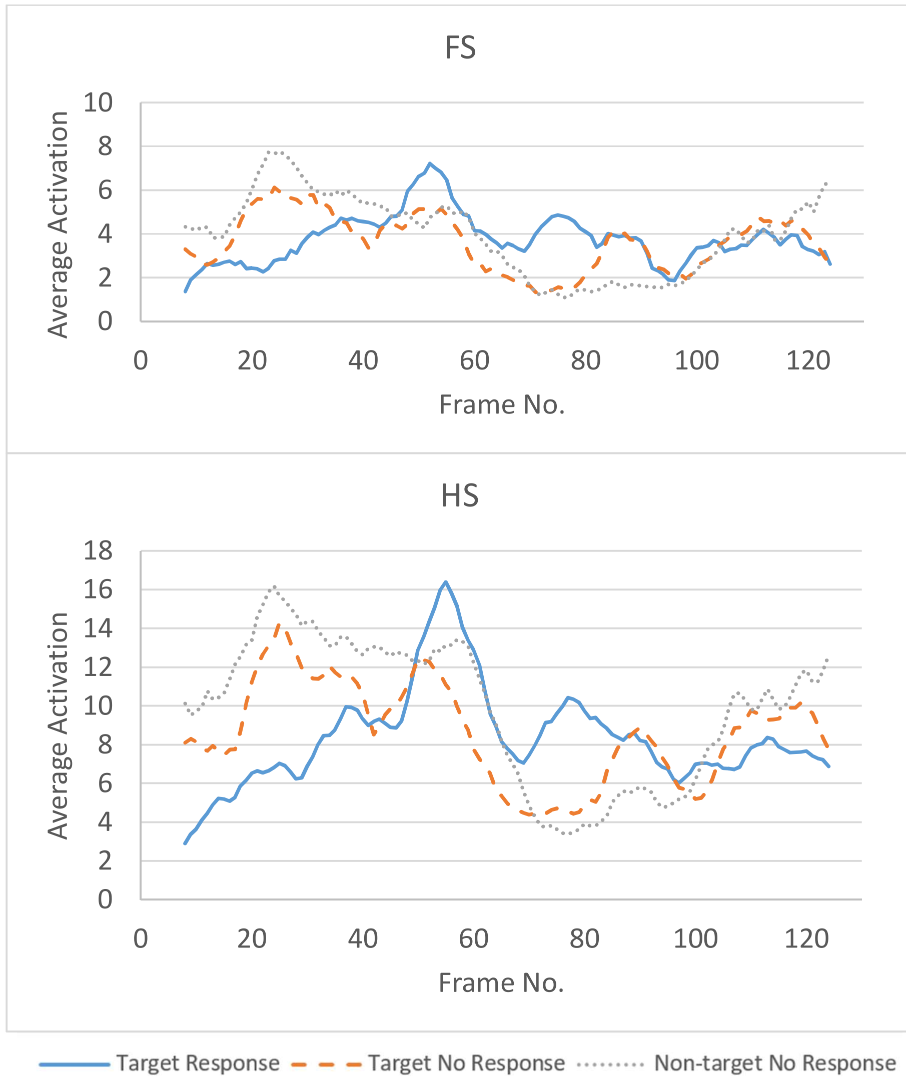

Activation will pass through temporal lobes when the signal in transferred from the occipital lobe to frontal lobe for memory matching. The target response activation rises till it reaches the peak value around frame no.60 and has higher amplitude (average) than other two cases till frame no.90.

(e) Left Temporal

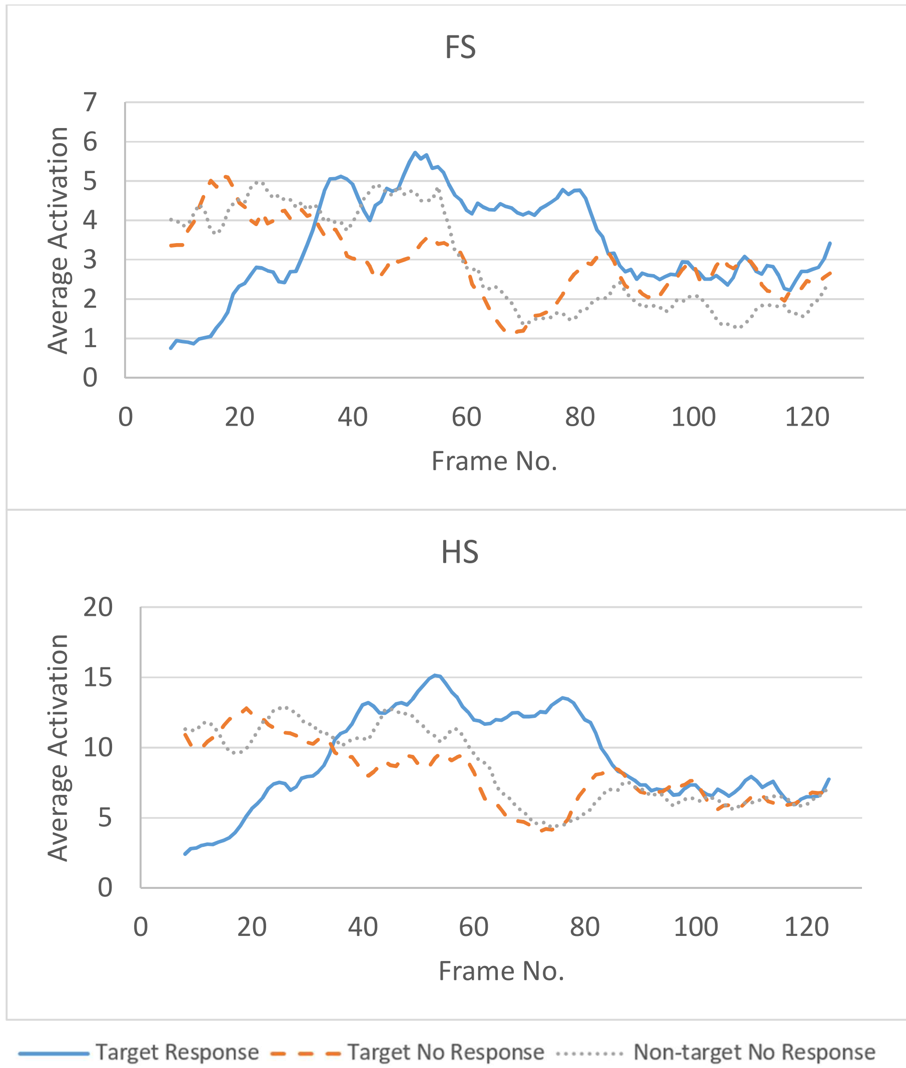

Activation will pass through temporal lobes when transfer the signal from occipital lobe to frontal lobe for memory matching. The target response activation rises till it reaches higher than the other two cases at frame no.40 and has the peak value around frame no. 60 and has higher amplitude (activation) than other two cases till frame no.90.

(f) Motor/ Center

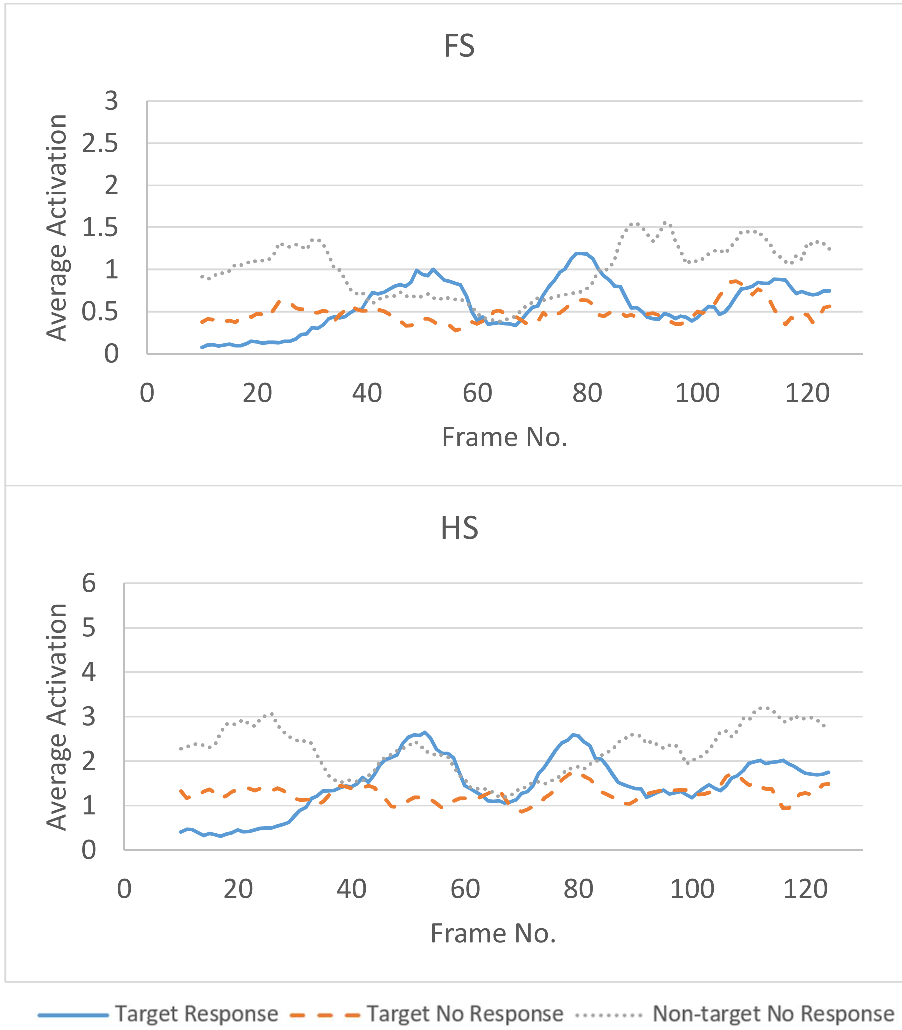

The motor region is less active. So the amplitude is very low. However we see two peaks for the motor region at around frame no.50 and no.80 for the target response which are not present for the other two cases within this time range.

Fig. 4.7 Average activation graph of different lobe.

From the above figure we may conclude that although the pattern of graphs for both FS and HS method are same however HS method shows higher activation as compared to FS method. Hence in the rest of the results we will concentrate on HS method for analysis.

4.2.2 Average Activation Paths for Different Oddball Cases (FS Method)

In this section, we have done an analysis of the brain lobes involved for activation path for all subjects at different oddball cases by using FS method. Fig. 4.8 shows the average activation path graph for brain lobes involved for average of all subjects for different oddball cases using FS method. It is observed that the behaviour of different lobes for target response, target no response and non-target no response are different. The discussion and explanation of different patterns of the graph for each lobe is provided in the figure. From Fig. 4.8, we conclude that the pattern for different types of responses is different for different brain lobes. This difference in pattern correlates with the overall process encountered in the Oddball paradigm.

(a) Target Response

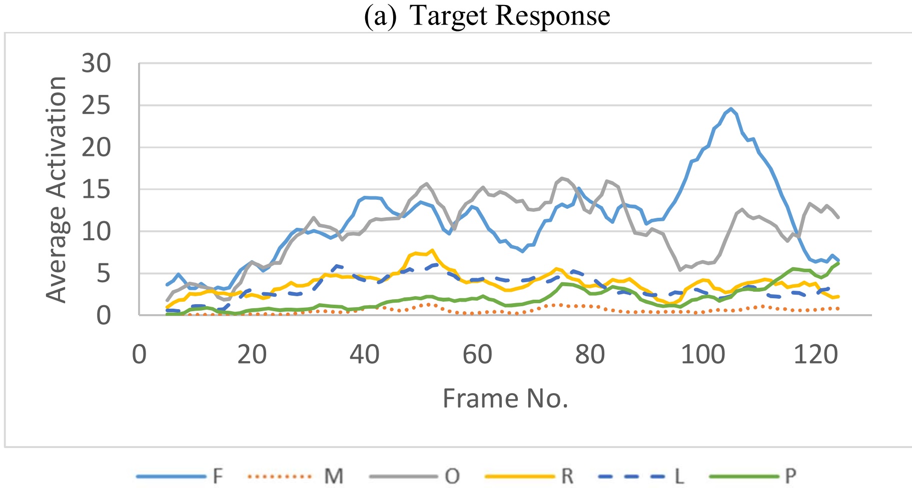

For frontal lobe, peak around frame no.80 (320ms) and no.110 (440ms) exists. Here subjects made decision to respond to the stimuli. For occipital lobe, peak appear around frame no. 80 (320ms) and drops till the end of the task. A very small increase in parietal activation is observed towards the end of the task around frame no.110

(b) Target No Response

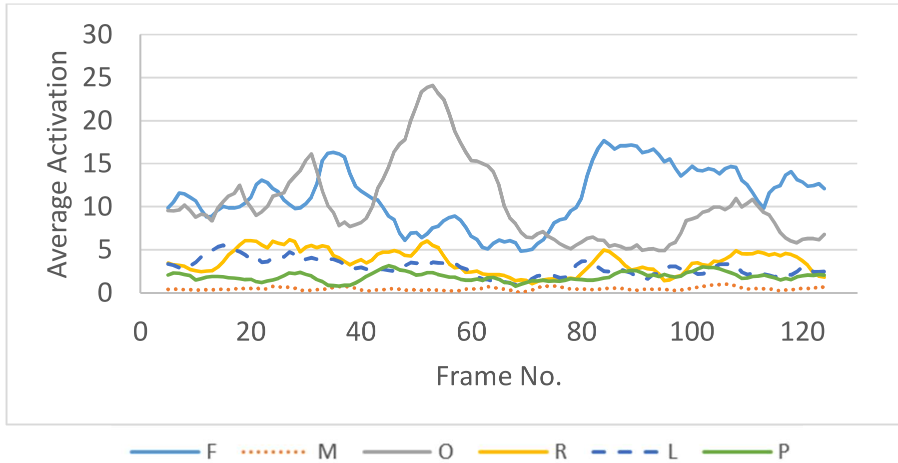

For frontal lobe, peak occurs around frame no. 85(340ms) but it occurs with a delay of 20ms than the case of target with response. Hence subject is not able to respond on the stimuli. For Occipital lobe, high peak around frame no.50 (200ms) and drops to a very low value towards the end.

(c) Non-target No Response

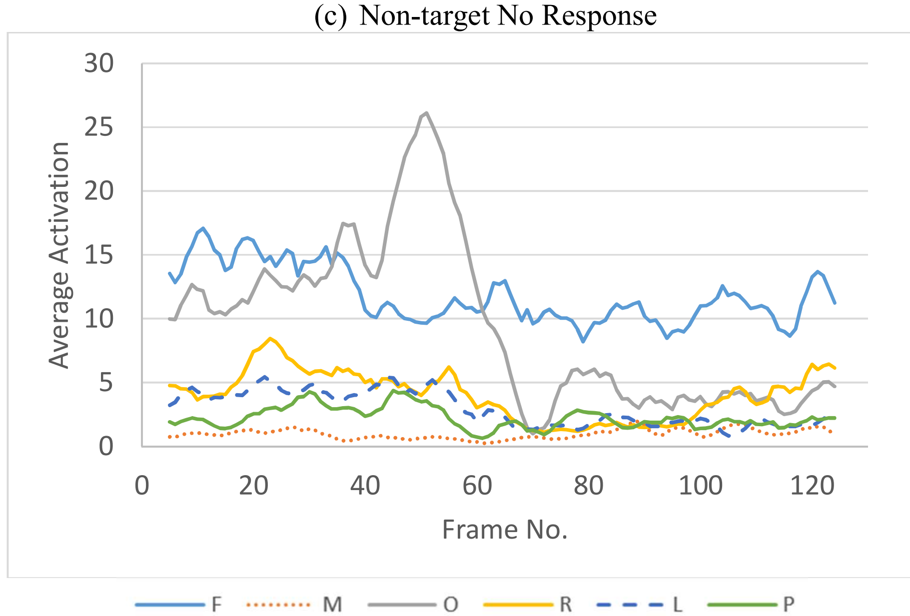

Smooth signal for frontal lobe. Because this is a non-target stimuli. For Occipital lobe, high peak around frame no.50 (200ms) just like previous case and drop to very low value. Subject has no need to respond. No ERP is generated here as it is a non-target case, so no frontal peak observed here.

Fig. 4.8 Average activation path graph for average of all subjects for different oddball cases using FS method.

4.2.3 Average activation Paths for Different Oddball Cases (HS Method)

In this section, we have done an analysis of the brain lobes involved for tracking activation path for all subjects at different oddball cases by using HS method. Fig. 4.9 shows the average activation path graph for average of all subjects for different oddball cases using HS method. It is observed that the behaviour of different lobes for three cases are different. The discussion and explanation of different patterns of the graph for each lobe is provided in the figure. Furthermore, we observed that the average activation path graph of HS method show almost similar result with the average activation path graph of FS method in the Fig. 4.8. However, HS method has higher amplitude compare with FS method.

(a) Target Response

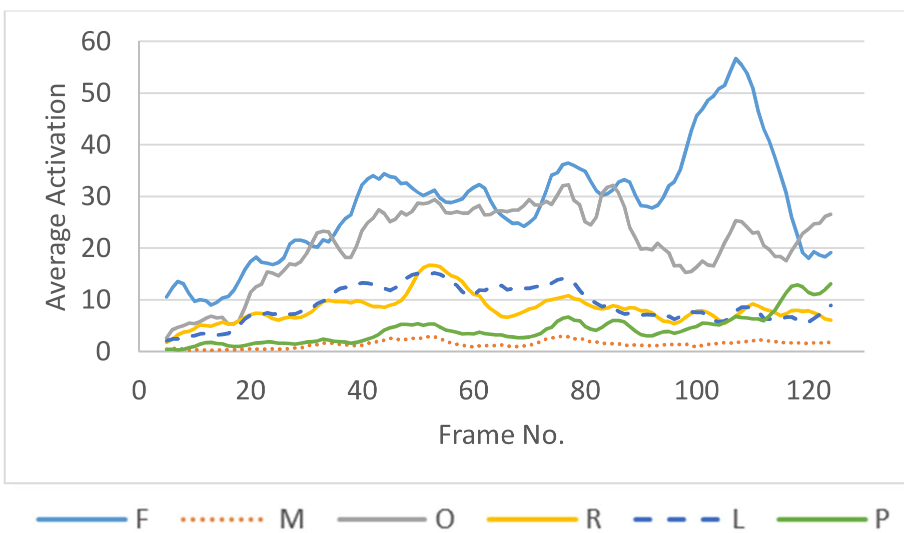

For frontal lobe, peak around frame no.80 (320ms) and no.110 (440ms) exists. Here subjects made decision to respond to the stimuli. For occipital lobe, peak exits around frame no. 80(320ms) and drops till the end of the task. A very small increase in parietal activation is observed towards the end of the task around frame no.110.

(b) Target No Response

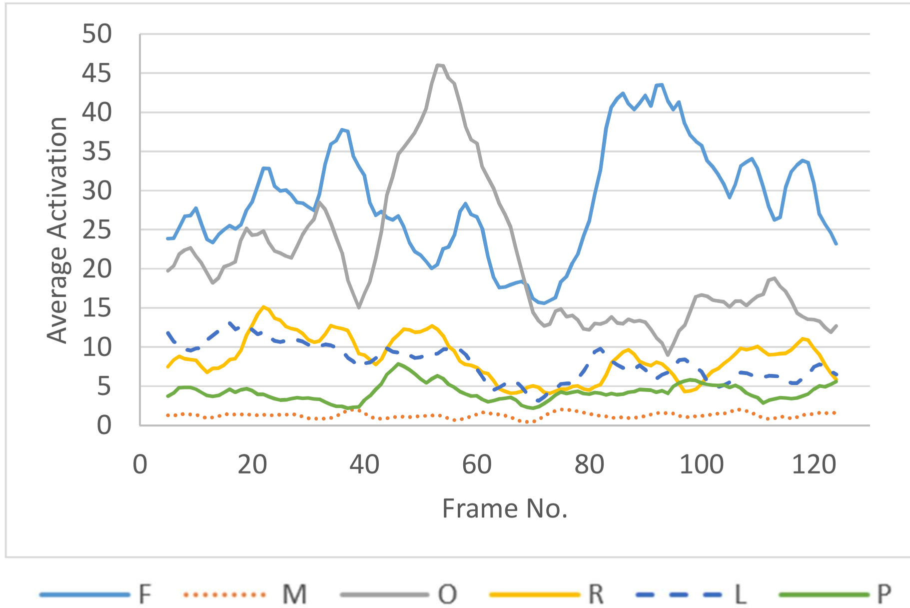

For frontal lobe, peak occurs around frame no. 90 (360ms) but it occurs with a delay of 10ms than the case of target with response. Hence subject is not able to respond on the stimuli. For Occipital lobe, high peak around frame no.50 (200ms) and drops to a very low value towards the end.

(c) Non-target No Response

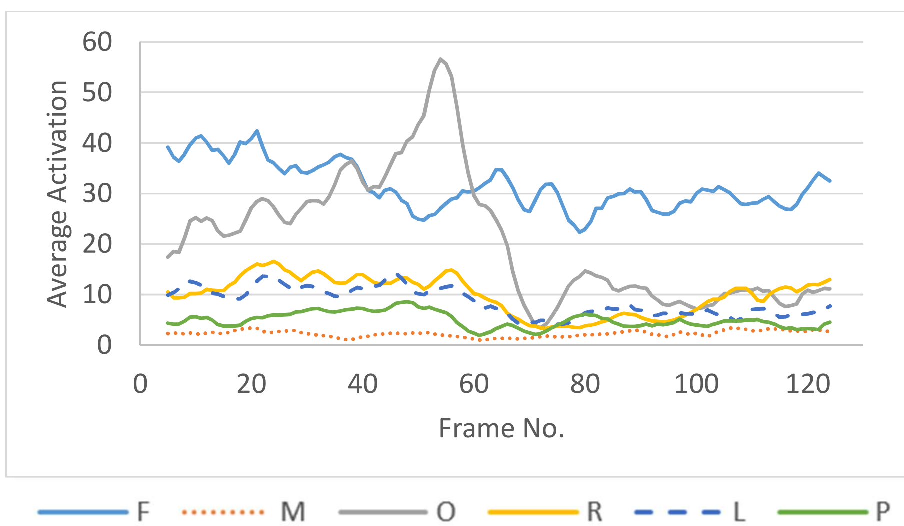

Smooth signal for frontal lobe. Because this is a non-target stimuli. For Occipital lobe, high peak around frame no.50 (200ms) just like previous case and drop to very low value. Subject has no need to respond. No ERP is generated here as it is a non-target case, so no frontal peak observed here.

Fig. 4.9 Average activation path graph for average of all subjects for different oddball cases using HS method.

4.2.4 Analysis of Activation Pattern for Different Oddball Cases for Individual Subjects (HS Method)

In this section, we will discuss the average activation pattern for brain lobes involved for different oddball cases for individual subjects by using HS method. Seven different subjects were chosen based on good, average and poor performance in the oddball experiment. For example, subject 13 had responded on target stimuli only 12 times out of 40, subject 2 and 5 had responded on target stimuli for only 13 times out of 40, subject 7 and 20 had responded on target stimuli for 24 times, and subject 9 and 10 give very good response on target stimuli that is 37 times. The number of trials used to calculate the average of all cases is based on the minimum number of trials that can be used for these cases with different performances. For poor performance, subject 2 and 5 had responded 13 times out of 40 times on target stimuli. So, we calculated the average for 13 trials for each case. However, subject 13 responded 12 times only on target stimuli. So, we calculated the average for 12 trials for each case. For average performance, subject did not respond to target stimuli for 16 times out of 40 times. So, we calculated the average for 16 trials for each case. For good performance, subject had responded to target stimuli for 37 times out of 40 times. So, we calculated the average for 37 trials for each case. Therefore, we ignored the target with no response case which had only 3 trials. Table 4.1 shows the response of individual subjects with different performances.

Table 4.1 Response of individual subjects with different performance

Performance	Subject	Target Response	Target No response	Non-target Response	Non-target No response
poor	2	13	27	1	94
	5	13	27	2	93
	13	12	28	1	94
average	7	24	16	0	95
	20	24	16	1	94
good	9	37	3	0	95
	10	37	3	3	92

Fig. 4.10 4.11 and 4.12 shows the average activation graph for different oddball cases for 2nd, 5th and 13th subject who gave poor response. From Fig. 4.10, we observed that occipital lobe has inconsistent graph with many high peaks which may result in poor performance of the subject. From Fig. 4.11, we observed that frontal lobe has inconsistent graph with many high peaks which cause poor performance of the subject. From Fig. 4.12, we observed that frontal lobe has inconsistent graph as same with 5th subject with many high peaks which cause poor performance of the subject. Based on the Fig. 4.10, 4.11 and 4.12, subjects were unable to concentrate or focus on the screen that leads to the inconsistent graph for occipital or frontal lobe hence resulting in poor performance. However, we still are able to observe a peak that occurred in end of the stimuli for frontal and parietal lobe for target with response cases.

(a) S2 Target Response

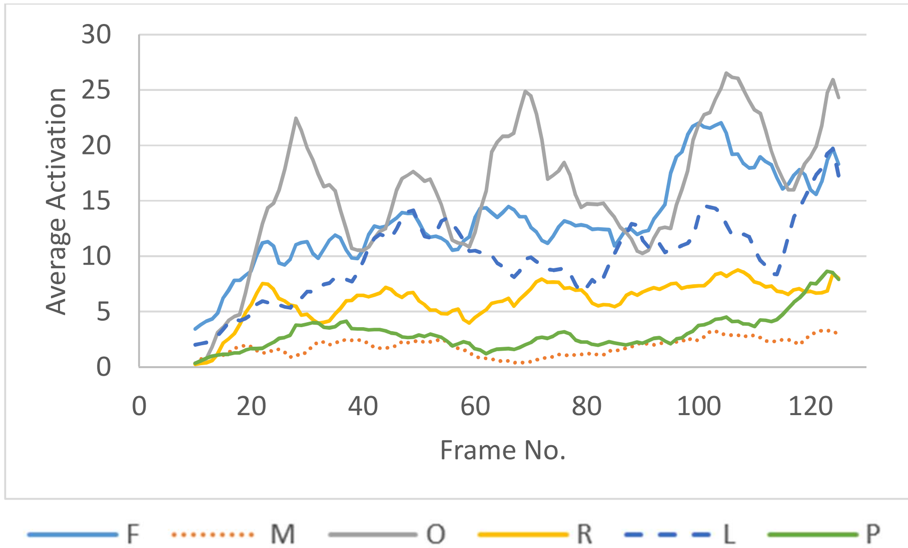

For frontal lobe, high peak around frame no.100(400ms) that is consistent with the appearance of the stimuli. Hence the subject makes decision to respond to the stimuli. Occipital lobe has inconsistent graph with many high peaks. For parietal lobe, a very small increase is observed towards the end of the task around frame no.120.

(b) S2 Target No Response

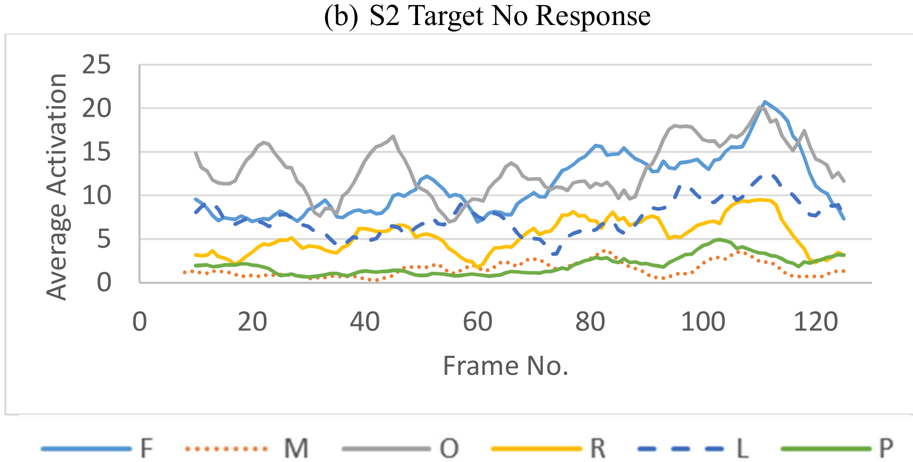

For frontal lobe, peak occur around frame no.110 with an amplitude of 20. Hence, we may say that due to this delay the subject was not nable to make a decision. Occipital lobe has inconsistent graph with many peaks.

(c) S2 Non-target No Response

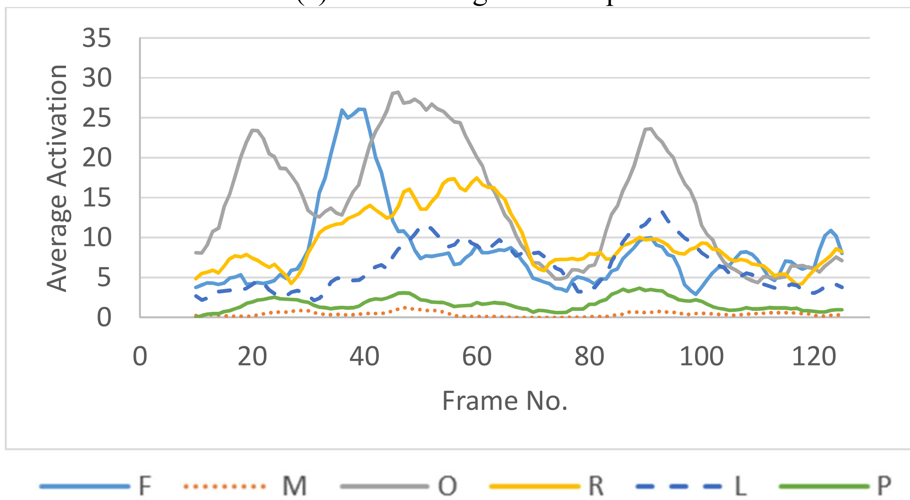

Frontal peak appeared very early around frame no.40 and drop until very low as it's a non-target case. Occipital lobe has inconsistent graph with many peaks.

Fig. 4.10 Average activation graph for different oddball cases for 2nd subject (S2)

(a) S5 Target Response

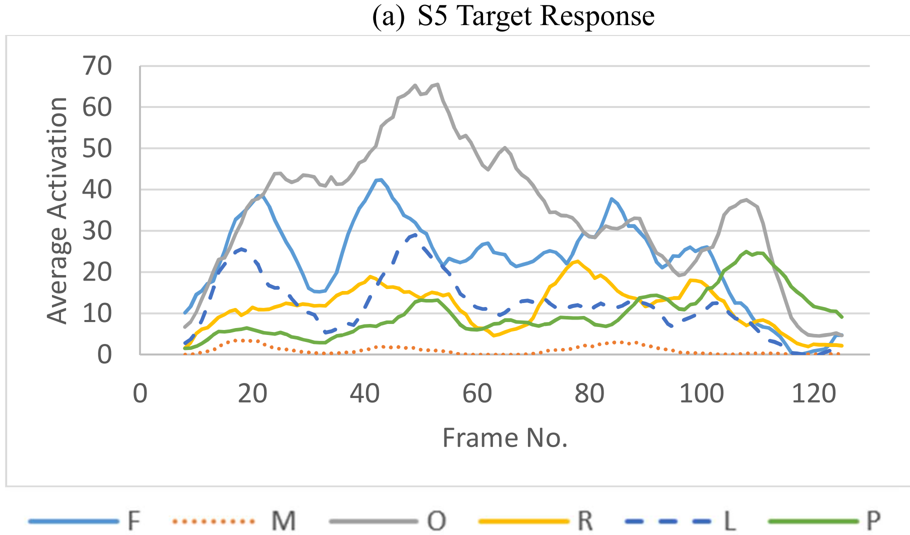

Frontal lobe has inconsistent graph with many high peaks. However, we can observe that the peak that occurs arround frame no.80 with an amplitude of around 40 may be responsible for response to the target stimuli. Another peak can be seen at around frame no.100(400ms). For occipital lobe, peak occurs arround frame no. 50 and no.110. Parietal lobe also shows a peak around frame no. 110.

(b) S5 Target No Response

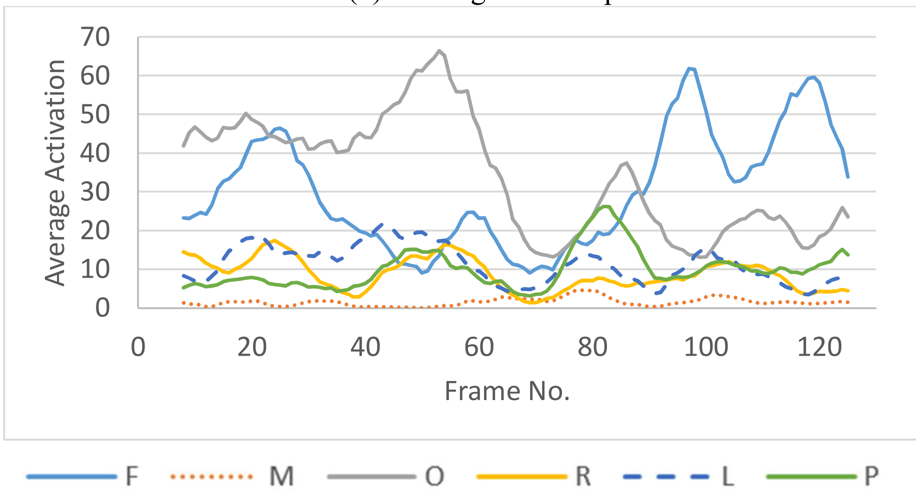

For frontal lobe, peak occurs arround frame no.100 and no.120. Hence there is a delay of peak for target no response, based on which we can conclude that because of this delay the subject was unable to make a decision. For occipital lobe, peak occurs arround frame no. 50 and frame no.80.

(c) S5 Non-target No Response

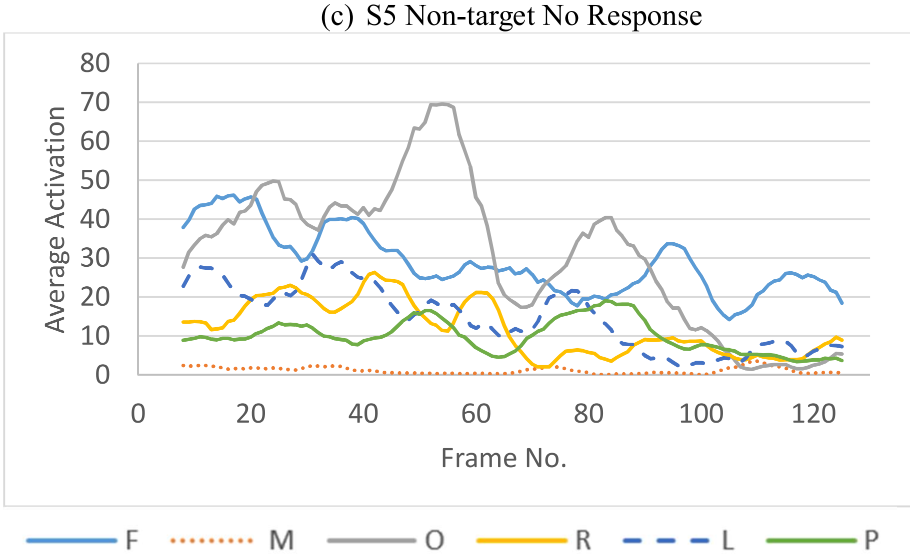

Frontal lobe has inconsistent response here. However, subject has no need to respond to stimuli. For occipital lobe, peak occurs around frame no. 50 and no.80 as with target with no response case.

Fig. 4.11 Average activation graph for different oddball cases for 5th subject (S5)

(a) S13 Target Response

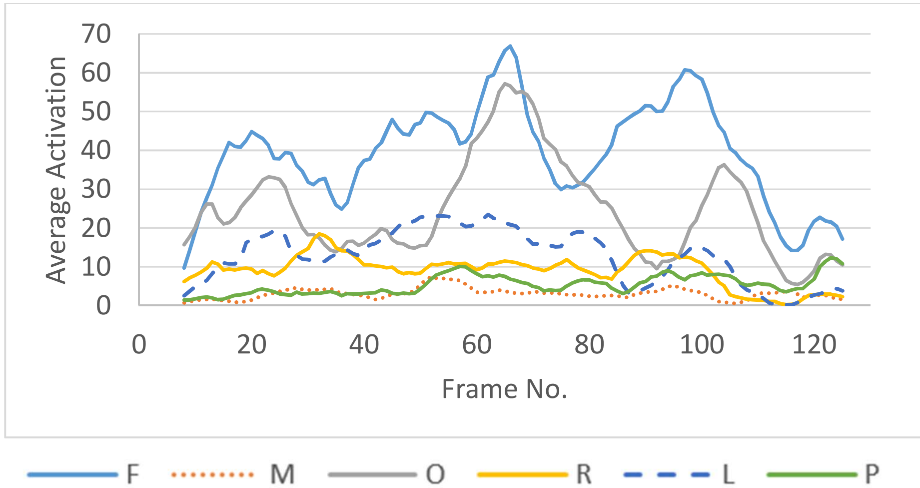

Frontal lobe has inconsistent graph with many high peaks. However, we can observe that the peak that occurs arround frame no.60 with an amplitude of around 70 may be responsible for response to target stimuli. Another peak can be seen at around frame no.100(400ms) with amplitude of 60. For occipital lobe, peak occurs arround frame no. 60 and no.110. Parietal lobe also shows a peak around frame no. 120.

(a) S13 Target No Response

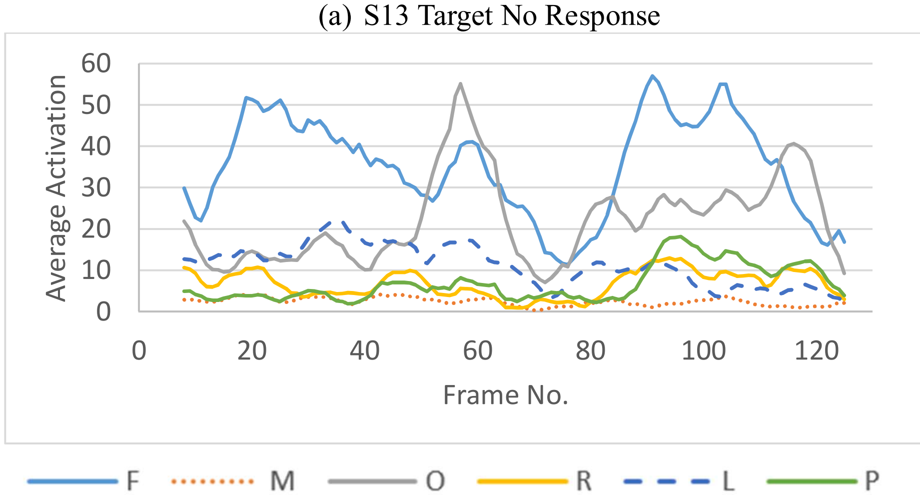

Frontal lobe has inconsistent graph with many high peaks. However, we can observe that the peak that occurs arround frame no.60 with an amplitude of 40 and arround frame no.100 with amplitude of below than 60 which amplitude is lower than target with response. For occipital lobe, peak occur arround frame no. 60 and no.120.

(b) S13 Non-target No Response

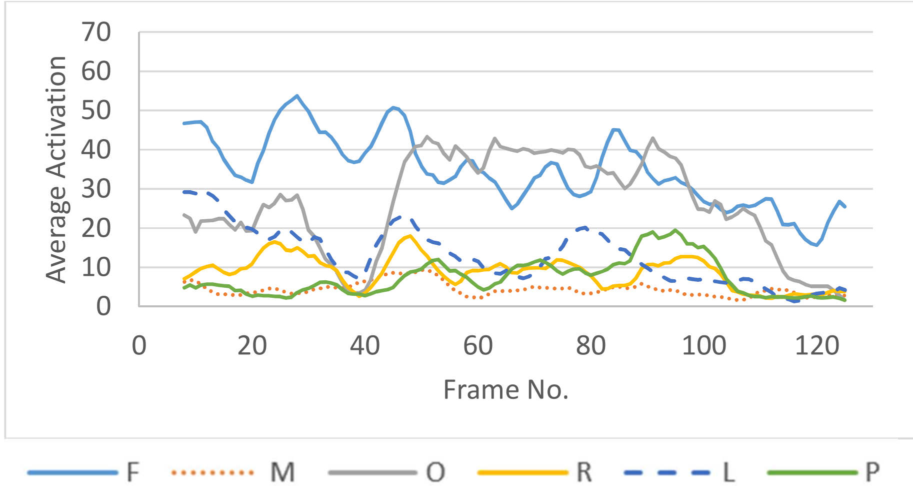

Frontal lobe has inconsistent response here. However, subject has no need to respond on stimuli. For occipital lobe, graph raise after frame no.40 and remain constant. Graph start dropping after frame no.90.

Fig. 4.12 Average activation graph for different oddball cases for 13th subject (S13)

Fig. 4.13 and 4.14 shows the average activation graph for 7th and 20th subject who gave average response. From Fig. 4.13 and 4.14, we can conclude that the pattern of the graph clearly follows the same trend for target with response and no response cases in terms of frontal and occipital activation. However here the activation graphs are clearer than the case for poor performance. For target response, high peak occurs in the frontal lobe in the end of the task after peak of occipital lobe. For non-target with no response, frontal and occipital lobe graphs are almost constant towards the end of the task.

(a) S7 Target Response

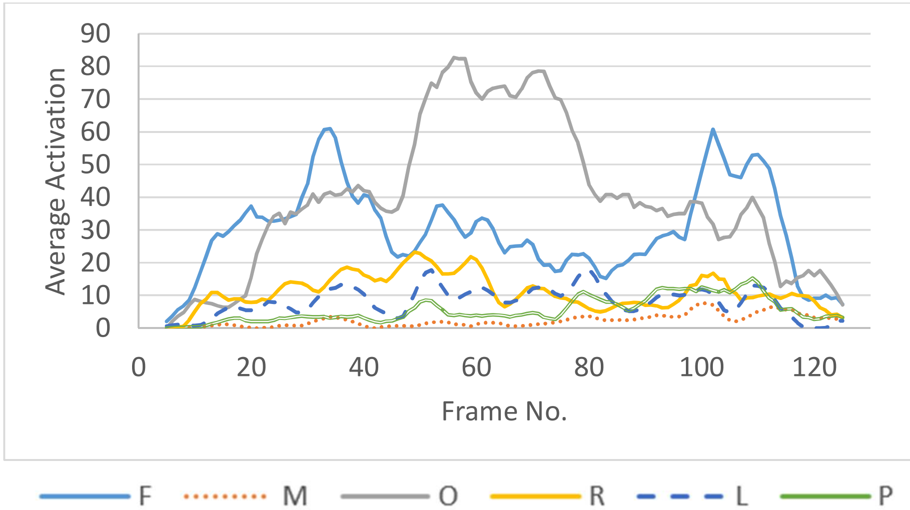

For frontal lobe, peak occur arround frame no.100 (400ms). Hence subject able to response on target stimuli. For occipital lobe, peak occurs arround frame no.60.

(b) S7 Target No Response

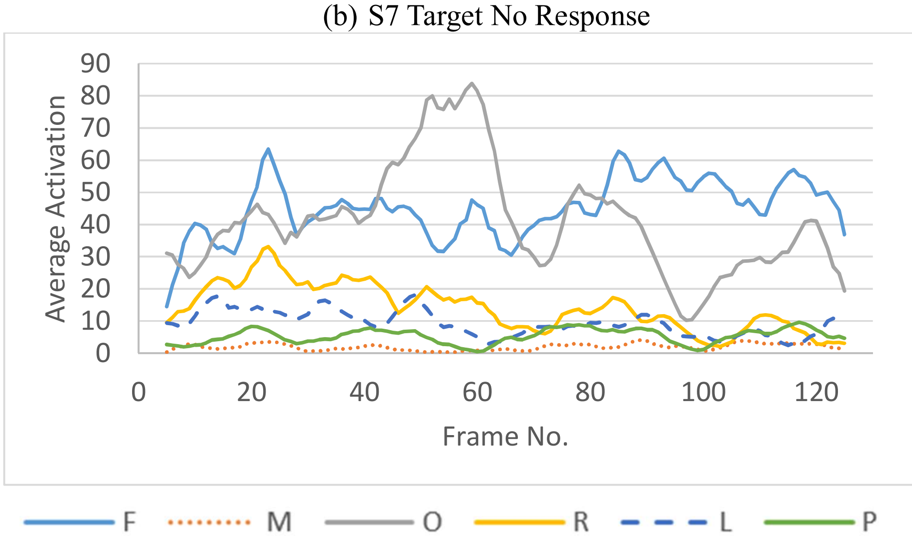

For frontal lobe, graph is almost constant as subject does not respond on target stimuli. For occipital lobe, peak occurs arround frame no.60, no.80 and no.120. With so many peaks in the occipital lobe, it seens the subject in unable to concentrate on screen.

(c) S7 Non-target No Respose

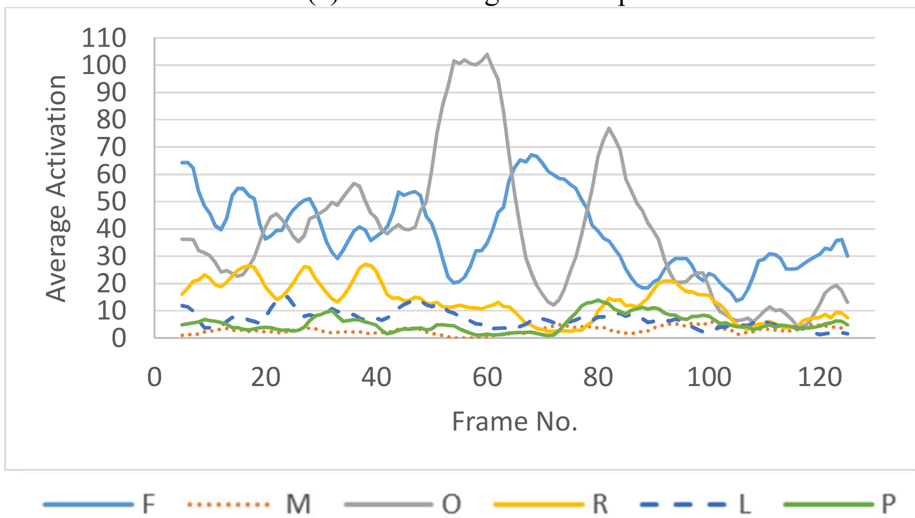

For frontal lobe, peak occurs around frame no.70 and drop to very low since it is non-target stimuli. For occipital lobe, peak occurs around frame no.60 and no.80 and drops till the end of the task.

Fig. 4.13 Average activation graph for different oddball cases for 7th subject (S7)

(a) S20 Target Response

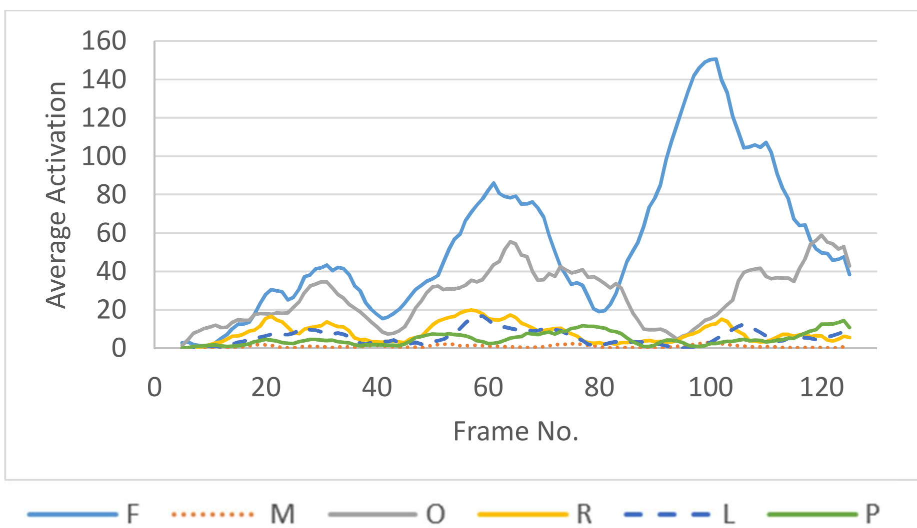

For frontal lobe, peak occurs arround frame no.60 (amplitude 80) and no.100 (amplitude 150). Hence subject is able to respond to the target stimuli. For occipital lobe, peak occurs arround frame no.60 and then shows an increasing trend from frame no 100.

(b) S20 Target No Response

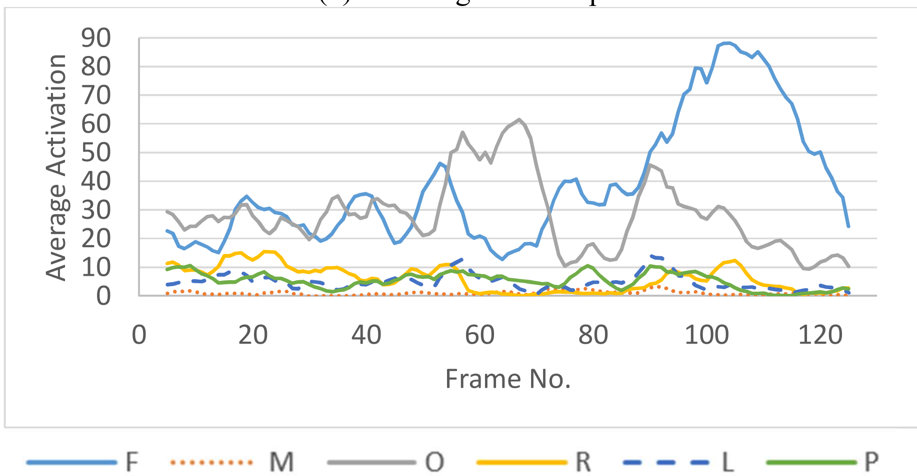

For frontal lobe, peak occurs arround frame no.60 (amplitude 40) and no.100 (amplitude 90). In both cases the amplitude is less than target with response case. Subject does not respond to the stimuli. For occipital lobe, peak occurs arround frame no.60 and no.90.

(c) S20 Non-target No Response

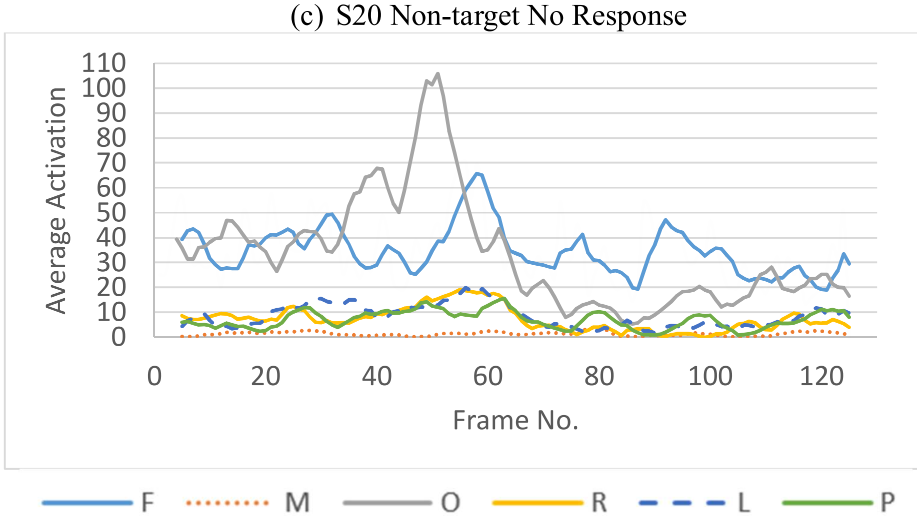

For frontal lobe, a peak occurs around frame no.60 only. The subject has no need to respond as it is non-target stimuli, so the amplitude is lower than other cases in the end of the task. For occipital lobe, peak occurs arround frame no.50 and drops till the end of the task.

Fig. 4.14 Average activation graph for different oddball cases for 20th subject (S20)

Fig. 4.15 and 4.16 shows the average activation graph for brain lobes involved for different cases for 9th and 10th subject who gave good response. For the case “Target with no response” these subjects responded only for 3 times, therefore we will ignore the target with no response cases. From Fig. 4.15 and 4.16, we can conclude that the pattern of the graph clearly shows the good performance of the subjects. For target with response, a clear high frontal activation is observed; this activation rises sharply to a high amplitude in both cases at around frame no. 40 and then decreases slowly till the end. For non-target no response, the frontal activation is sort of constant from the start and drops faster than the case of target with response.

(a) S9 Target Response

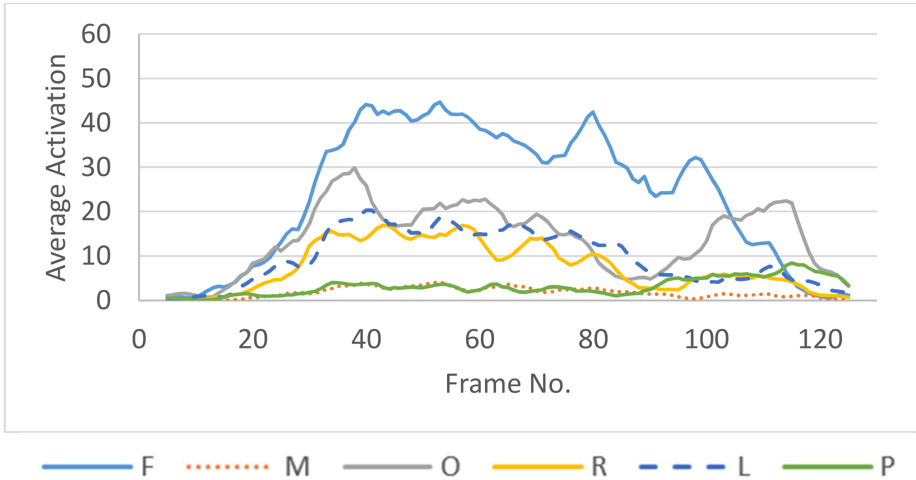

For frontal lobe, highest peak occurs around frame no. 80 and and another peak around frame no.100 (400ms). For occipital lobe, peak is around frame no.40 and no.110.

(b) S9 Non-target No Response

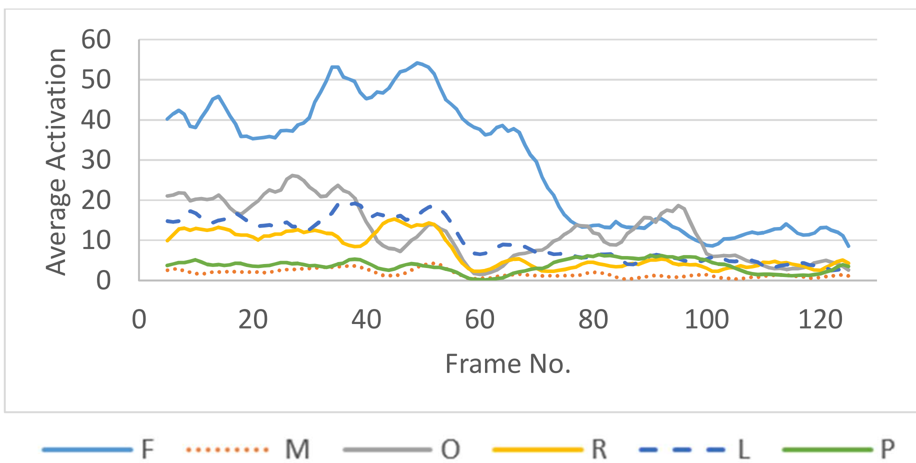

For frontal lobe, graph drops after peak arround frame no.50. For occipital lobe , the peak occur arround frame no.30 and no.90 and drops until the end of the task for non-target stimuli.

Fig. 4.15 Average activation graph for different oddball cases for 9th subject (S9)

(a) S10 Target Response

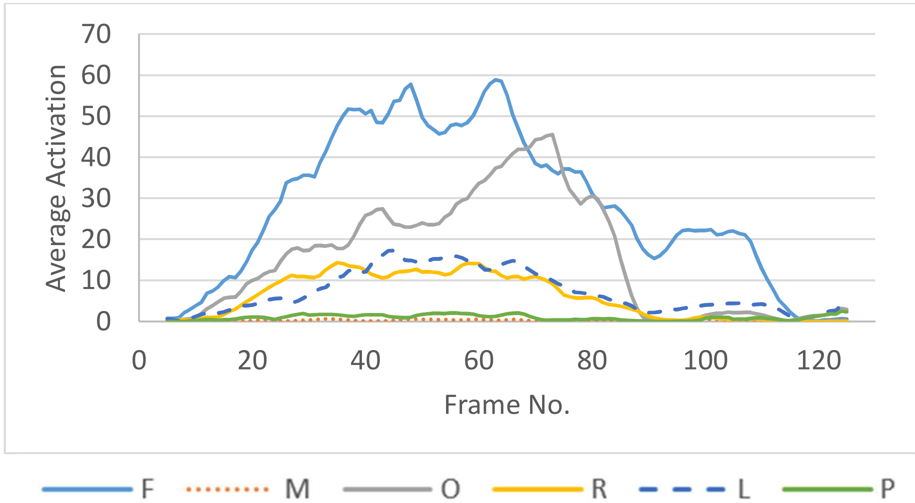

In frontal lobe, peak occur around frame no. 60 later around frame no.100 (400ms). In Occipital lobe, peak occur around frame no.70 for visual processing.

(b) S10 Non-target No Response

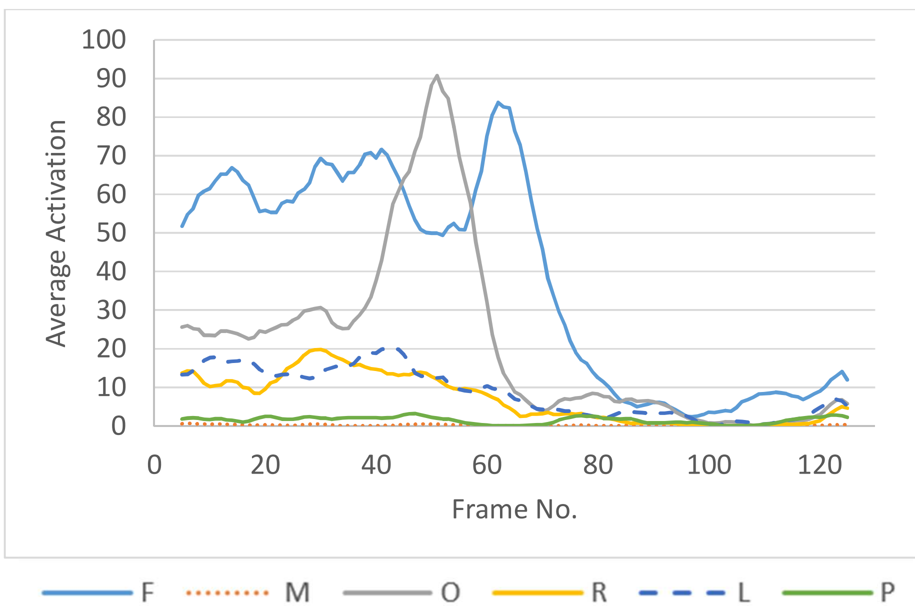

For frontal lobe, graph is drops after peak arround frame no.70. For occipital lobe, the peak occur arround frame no.50 and drops until the end of the task for non-target stimuli.

Fig. 4.16 Average activation graph for different oddball cases for 10th subject (S10)

Table 4.2 shows the summary of analysis for different performance of the subjects. From the table, we are able to conclude that different patterns of graphs can be observed for different performances. For Poor performance, the frontal or occipital lobe will have inconsistent graph. This can prove that the subject is not focussing or concentrating on the experiment. For average performance, the pattern of the graph is more consistent than poor performance. For good performance, the graph are clearly shows the frontal activation. The details of the summary of analysis are given in the table.

Table 4.2 Summary of Analysis for different performance of subject

Performance	Subject	Summary
Poor	**2** **5** **13**	• Occipital or frontal lobe has inconsistent graph with many high peaks which cause poor performance for the subject. • However, we are still able to observe a peak that occurs in the end of the stimuli for frontal and parietal lobe for target with response cases.
Average	**7** **20**	• The pattern of the activation graphs are more consistent than poor performance. • For target response, high peak occurs in the frontal lobe in the end of the task after peak of occipital lobe. • For non-target with no response, frontal and occipital lobe graphs are almost constant towards the end of the task.
Good	**9** **10**	• Graph clearly shows the good performance of the subjects. For target with response, a clear high frontal activation is observed; this activation rises sharply to a high amplitude in both cases at around frame no. 40 and then decreases slowly till the end. A second frontal peak is also observed at the end of the task. • For non-target no response, the frontal activation is sort of constant from the start and drops faster than the case of target with response.

4.3 Tracking of Functional Connectivity by using Cross Correlation Method

In this section, we will observe the pattern of the functional connectivity of brain by using cross-correlation method for single trial of each case for every segment. Firstly, we will discuss the functional connectivity for 2^{nd} subject who had poor performance. Second, we will discuss the functional connectivity for 9^{th} subject who had good performance.

4.3.1 Functional Connectivity of 2^{nd} subject

Fig. 4.17 shows the functional connectivity of 10-20 electrode for target stimuli with response (fastest) for 2^{nd} subject. In the figure, there are connectivity between 10-20 electrodes for every segment except only sample 61-80. Besides, we can see that these are connectivity for O1, O2, P3, P4, Pz, T6 and C3 in the last segment. These are involved in visual processing, perception, emotional understanding and sensorimotor integration in the last segment (when button pressed).

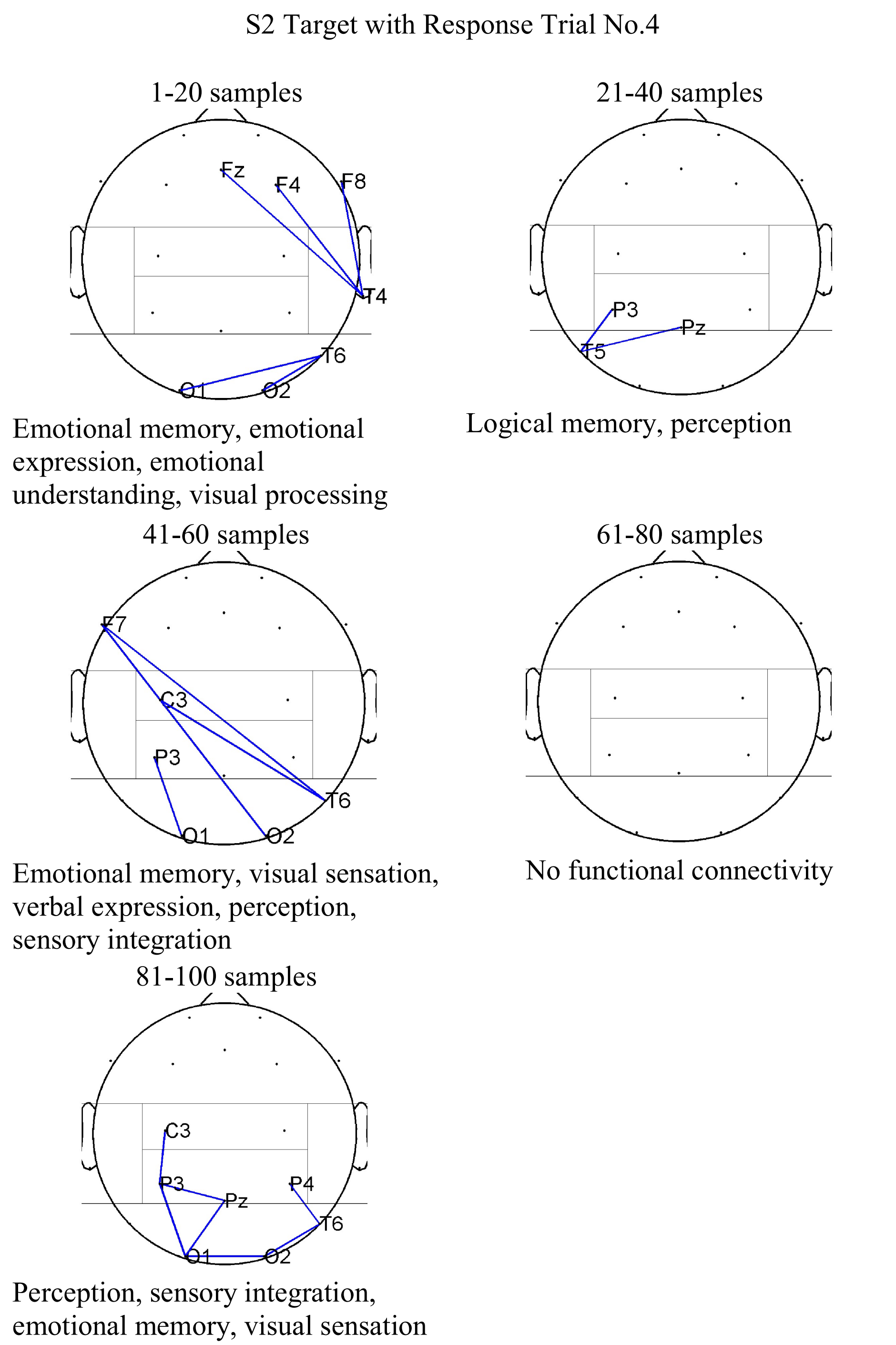

Fig. 4.17 Functional connectivity of 10-20 electrodes for target stimuli with response (fastest) for 2nd subject

Fig. 4.18 shows the functional connectivity of 10-20 electrodes for target with no response for 2nd subject. Less connectivity is observed for target with no response. However, we still can observe that, there are connectivity for T4 and O2 in the beginning of the appearance of stimuli appear. This involves visual processing and emotional memory. However, no connectivity is present in the last segment as subject did not respond on the target stimuli.

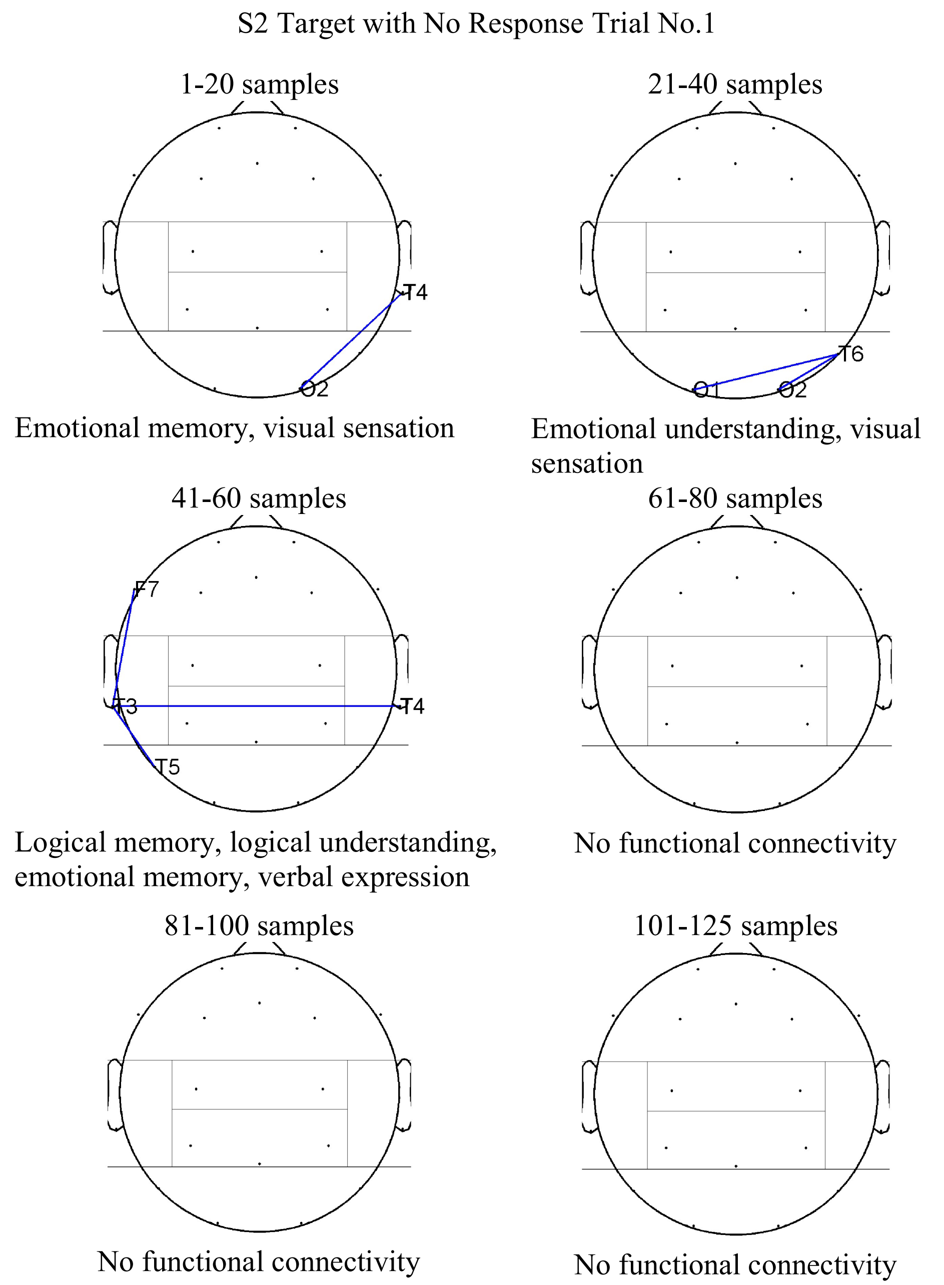

Fig. 4.18 Functional connectivity of 10-20 electrodes for target with no response for 2nd subject

Fig. 4.19 shows the 10-20 functional connectivity for non-target with response for 2nd subject. In the figure, here are connectivity for O1, O2, P3, P4, PZ, T5, T6, C3, and C4 in last segment. This involves visual processing, perception, logical and emotional understanding and sensorimotor integration.

S2 Non-target with Response Trial No.1

1-20 samples

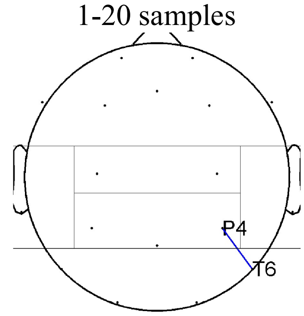

Emotional understanding, perception

21-40 samples

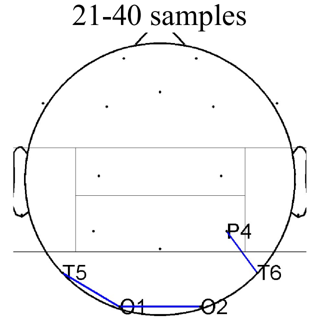

Logical understanding, emotional understanding, visual sensation, perception

41-60 samples

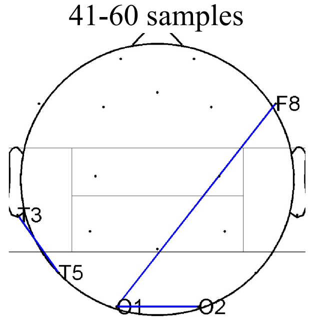

Logical memory, logical understanding, visual sensation, emotional expression

61-80 samples

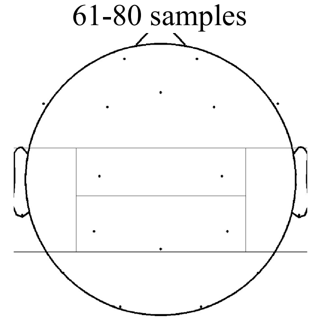

No functional connectivity

81-108 samples

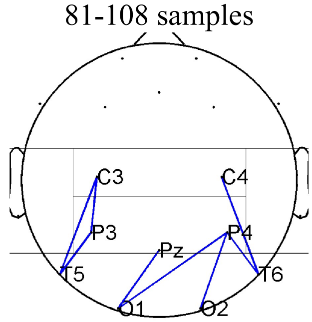

Perception, sensorimotor integration, logical understanding, emotional understanding, visual sensation

Fig. 4.19 Functional connectivity of 10-20 electrodes for non-target with response for 2^{nd} subject

Fig. 4.20 shows the functional connectivity of 10-20 electrodes for non-target with no response for 2nd subject. In the figure, here are connectivity for O1, T4 and T6 in the beginning of stimuli appear. These involve the visual processing, emotional memory and understanding. However, no connectivity involved in the last segment as subject does not need to respond to the non-target stimuli.

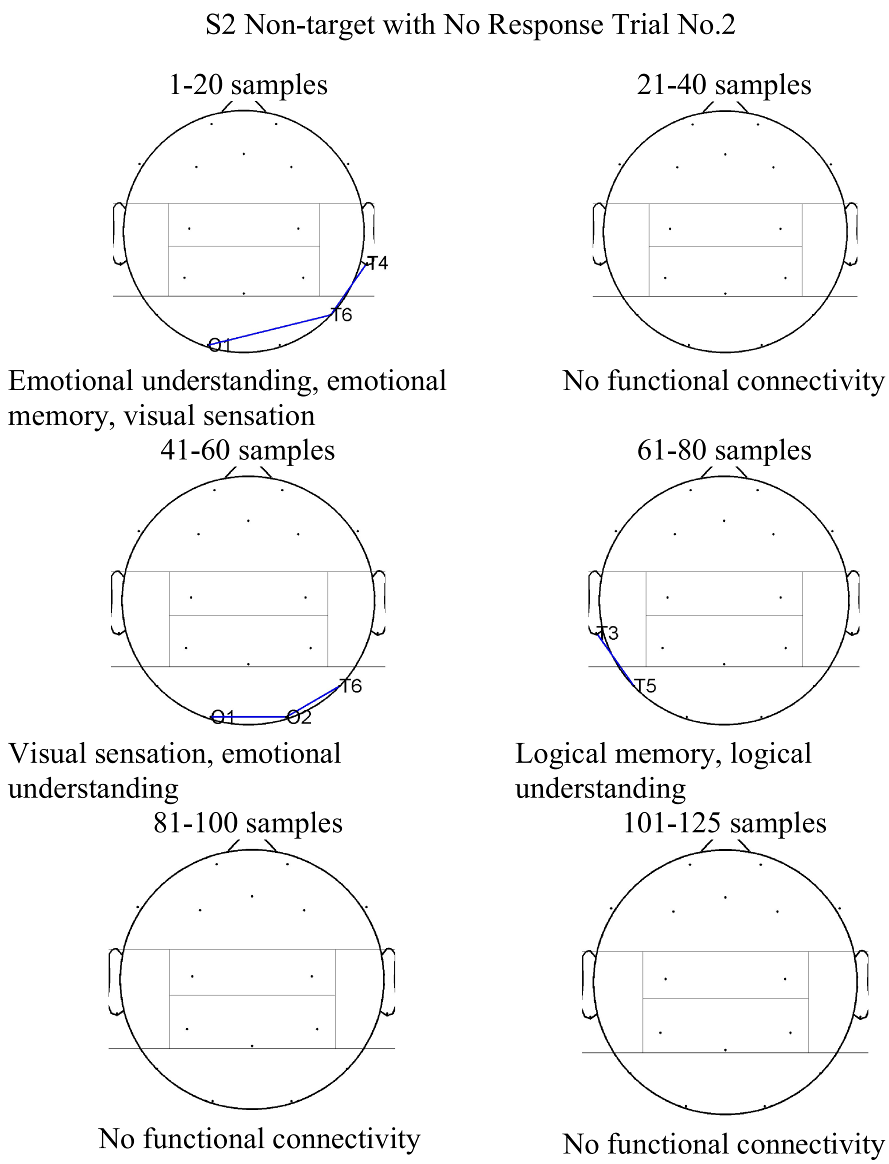

Fig. 4.20 Functional connectivity of 10-20 electrodes for non-target with no response for 2nd subject

Fig. 4.21 shows the functional connectivity of all electrodes for target with response for 2nd subject for three different trials (fastest, medium and slowest). For target with response, trial 4, 6 and 8 are the fastest, medium and slowest responses from the subject to the target stimuli. In the figure, high connectivity is observed for all cases in general for all segments compared with target with no response and non-target no response in Fig. 4.22 and 4.23. High connectivity can be observed in occipital lobe for every segment except for first segment of trial no.8 (slowest) only. In last segment, it shows high connectivity between occipital, temporal, parietal, frontal, and center region as response is given. We are able to observe connectivity in the frontal and center region for last segment, which is used for movement to press the button.

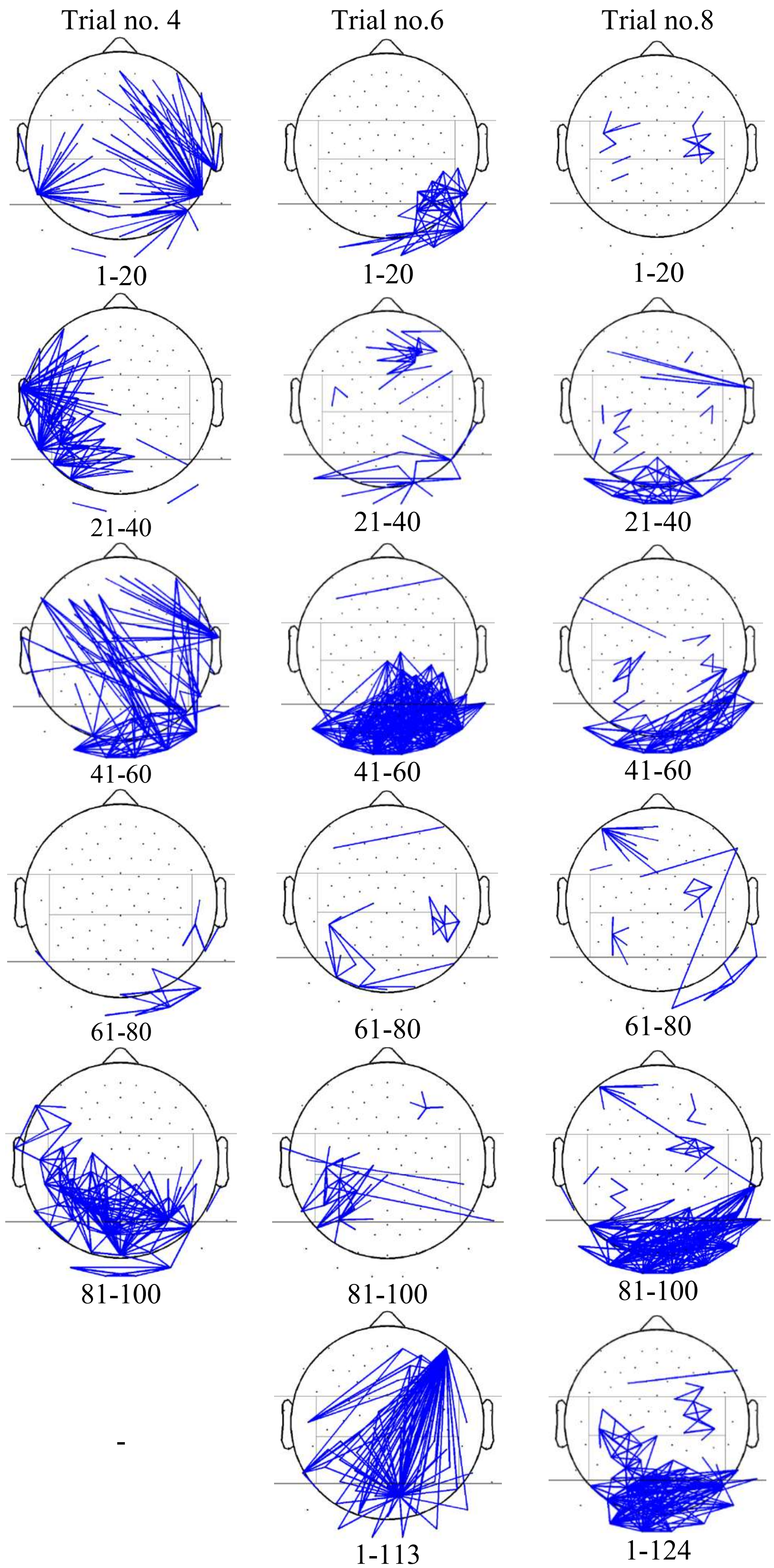

Fig. 4.21 Functional connectivity of all electrodes for target with response for 2nd subject

Fig. 4.22 shows the functional connectivity of all electrodes for target with no response of 2nd subject for three different trials. For target with no response, three trials were selected from the subject that has consistent EEG data. In the figure, target with no response shows less connectivity than target with response cases in Fig. 4.21. Since subject is not able to make response on the target stimuli. In trial no.1, segment 61-80 and 81-100 does not have any connectivity. Subject is not able to respond to this trial. In trial no.2, low connectivity for all segments. However, there is only a little connectivity in the frontal lobe at segment 21-40. Subject is not able to make decision to respond to this trial. Trial no.3 has higher connectivity compared to trial no.1 and no.2 but the connectivity is still lower than target with response cases in Fig. 4.21.

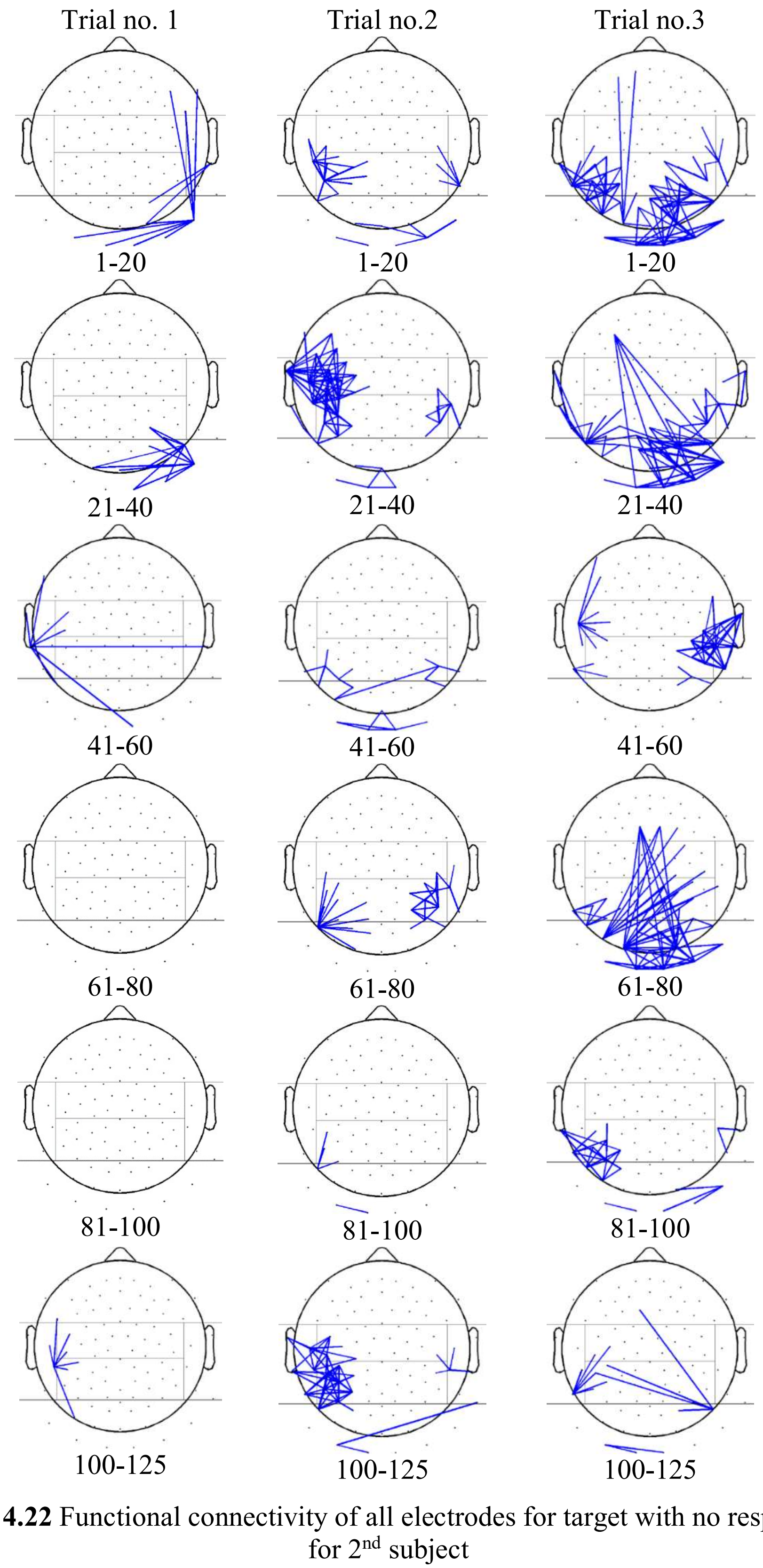

Fig. 4.22 Functional connectivity of all electrodes for target with no response for 2nd subject

Fig. 4.23 shows the functional connectivity of all electrodes for non-target with no response for 2nd subject for three different trials. For non-target with no response, three trials were selected from the subject which have consistent EEG data. In the figure, non-target with no response shows less connectivity than target with response cases in Fig. 4.21 except the first segment of trial no.2 and trial no.4. High connectivity is observed only in the first segment where all lobes are involved for trial no.2 and no.4. Since subject does not need to respond to the non-target stimuli. In trial no.3, we are only able to observe the connectivity in segment 81-100 which is in occipital lobe.

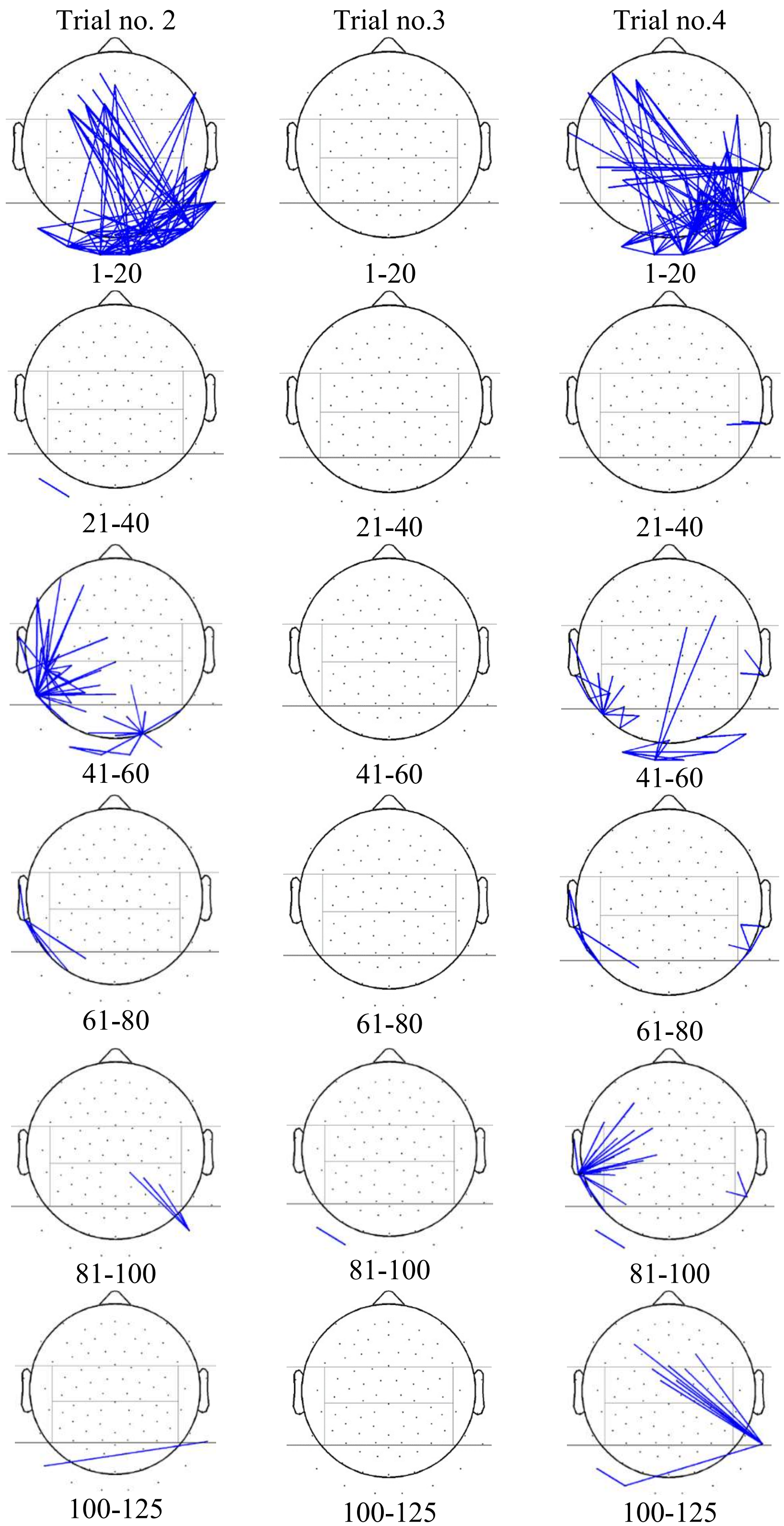

Fig. 4.23 Functional connectivity of all electrodes for non-target with no response for 2nd subject

By summary, the target with response cases have high connectivity for every segment compared with target with no response and non-target with no response cases. Moreover, target response has high connectivity in the last segment. Fig. 4.24 shows the comparison of the average activation graph and the functional connectivity for last segment of target with response cases for 2^{nd} subject. From the figure, the average activation graph is shifted to the timing when the button is pressed. So the functional connectivity of the segment 81-100 will be around frame no.105-125 in the activation graph. From the figure, we can observe the activation graph and the functional connectivity of last segment shows high average activation and high connectivity for frontal, occipital and parietal lobes, which shows that the average activation graph gives same result with the functional connectivity.

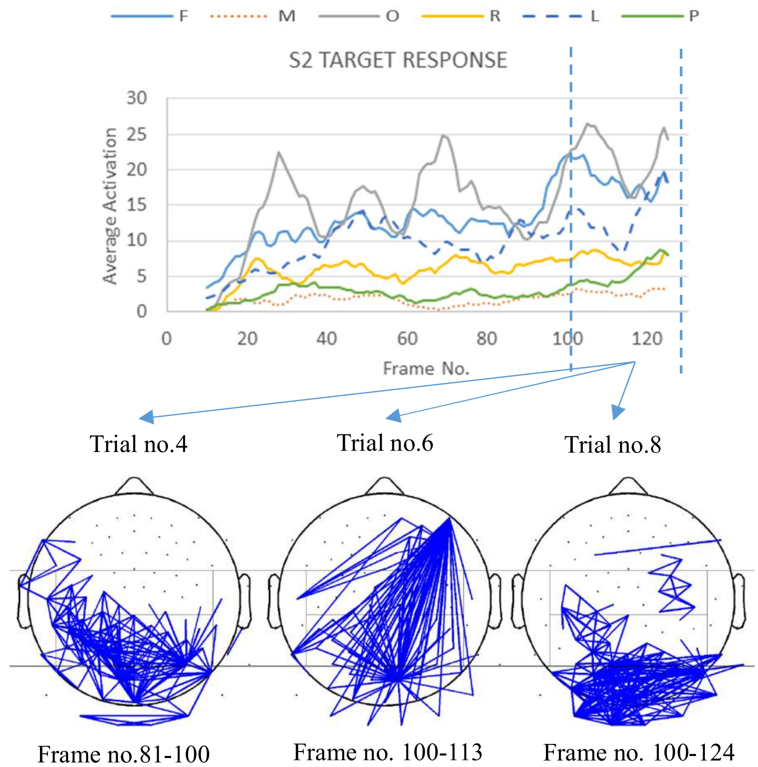

Fig. 4.24 Comparison of the average activation graph and the functional connectivity at last segment of target with response cases for 2nd subject

For target with no response cases, the connectivity is less than target with response cases for every segment. However, we are still able to observe some connectivity in the occipital lobe. Fig. 4.25 shows the comparison of the average activation graph and the functional connectivity for last segment of target with no response cases for 2nd subject. From the figure, a little peak is observed in the average activation graph for all lobes, but the amplitude is lower than target with response case. In addition, the connectivity is also lesser than target with response case. Since subject doesn't respond to stimuli.

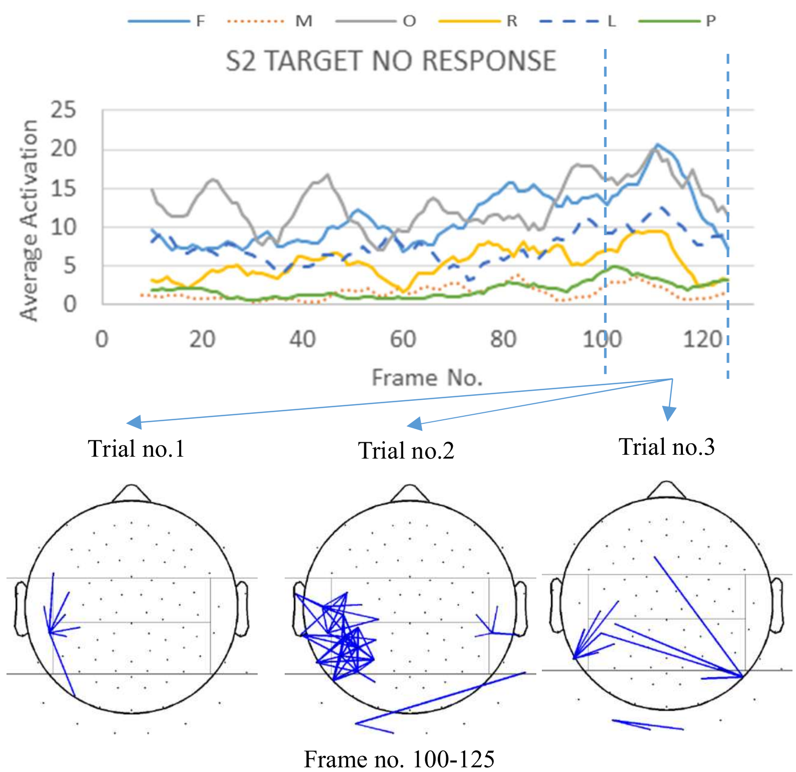

Fig. 4.25 Comparison of the average activation graph and the functional connectivity for last segment of target with no response cases for 2nd subject

For non-target no response cases, high connectivity is observed for frame no.1-20 only and there is very less connectivity from frame no. 100 -125 as subject has no need to respond to the stimuli. Fig 4.26 shows the comparison of the average activation graph and functional connectivity of the last segment of non-target with no response cases for 2nd subject. From the figure, we are able to conclude that non-target with no response shows lower amplitude and lesser connectivity in last segment.

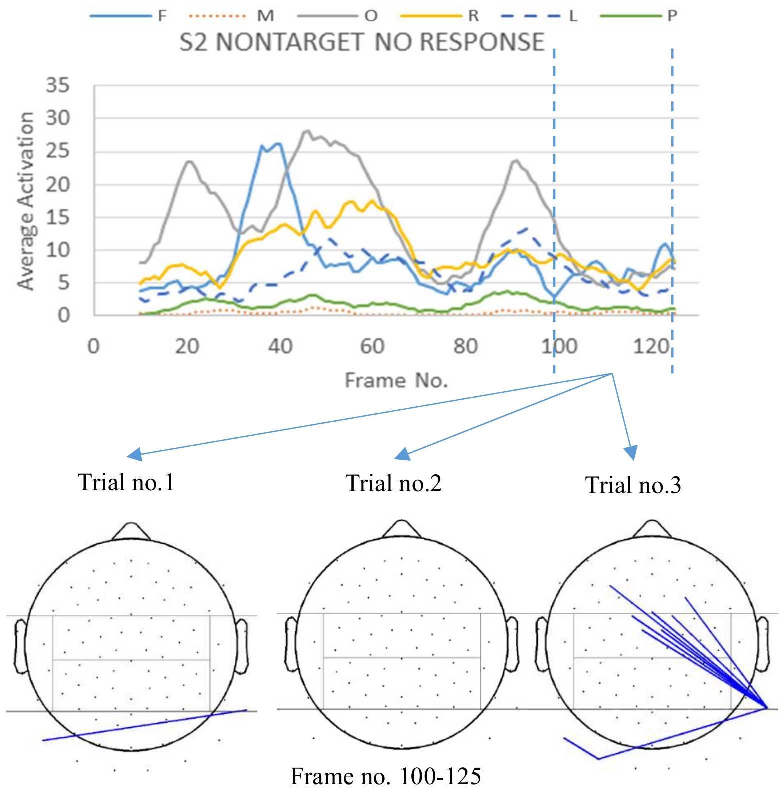

Fig. 4.26 Comparison of the average activation graph and functional connectivity for last segment of non-target with no response cases for 2nd subject

4.3.2 Functional Connectivity of 9th subject

Fig. 4.27 shows the functional connectivity of 10-20 electrodes for target stimuli with response (fastest) for 9th subject. In the figure, there are connectivity between 10-20 electrodes for all segments. Besides, we can see that these are connectivity for O1, O2, Pz, F3, F4, Fz and T6 in the last segment. These are involved in motor planning, emotional understanding, visual processing and perception in the last segment (when button pressed).

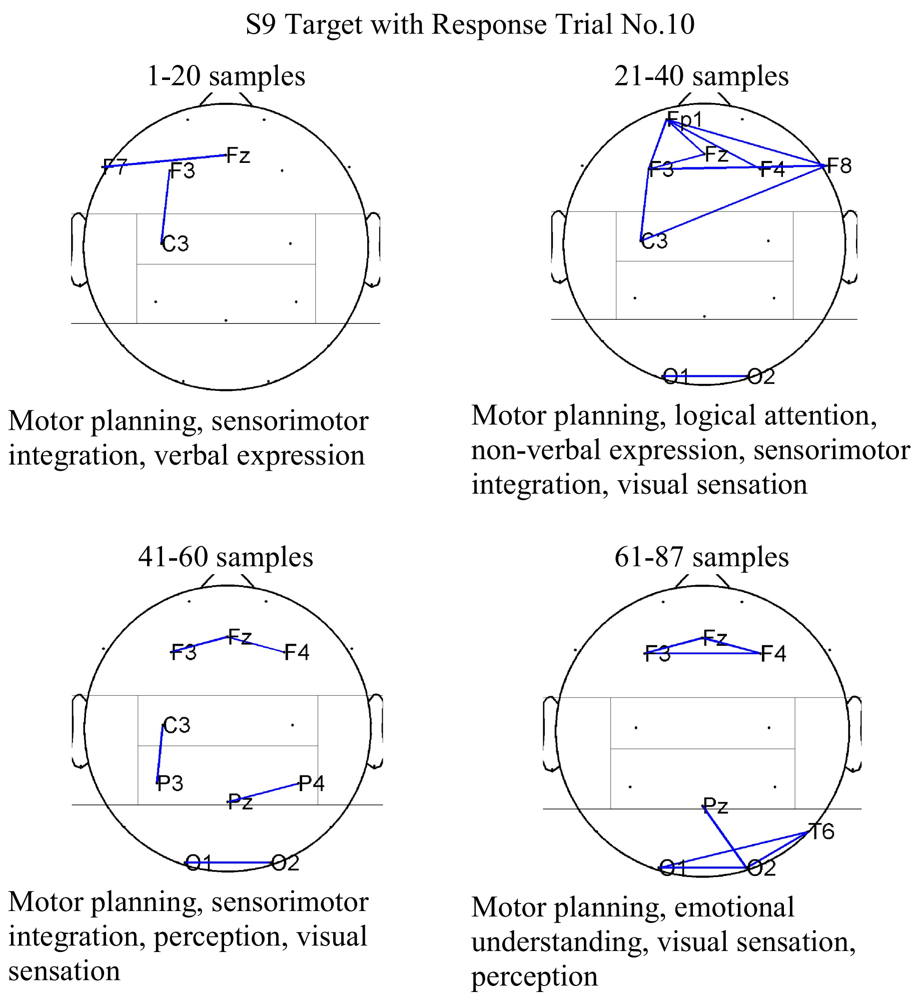

Fig. 4.27 Functional connectivity of 10-20 electrodes for target stimuli with response (fastest) for 9th subject.

Fig. 4.28 shows the functional connectivity of 10-20 electrodes for target stimuli with no response for 9th subject. Target with no response have less connectivity compare with target with response cases. However, we still able to observe the connectivity for O1, T5, PZ and P3 in sample 81-100 which involved in logical understanding, perception and visual processing.

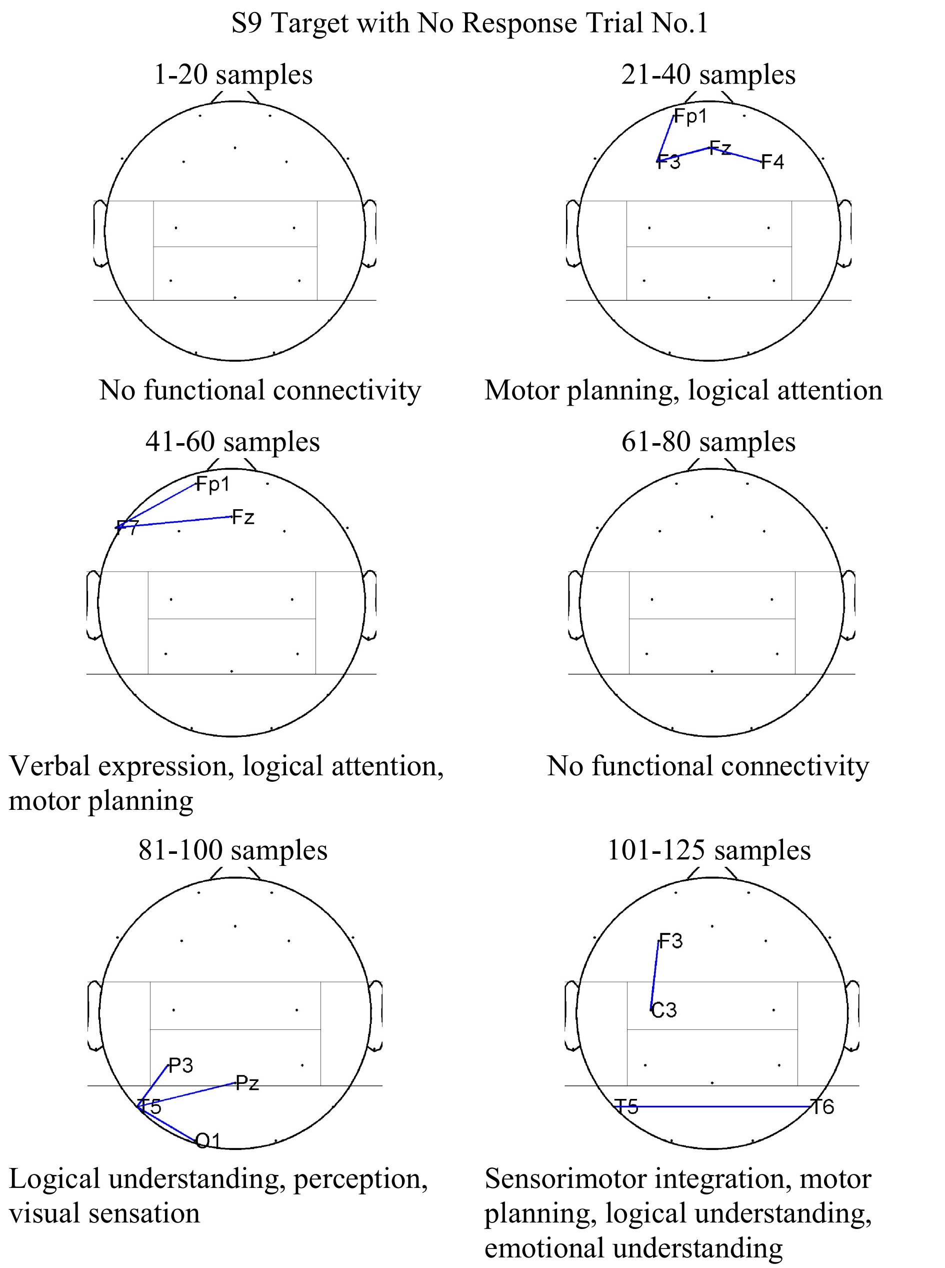

Fig. 4.28 Functional connectivity of 10-20 electrodes for target stimuli with no response for 9th subject

Fig. 4.29 shows the functional connectivity of 10-20 electrodes for non-target with no response for 9th subject. In the figure, here are only some connectivity in Fz, F4, F8 and Fp1 in sample 41-60. These involve in motor planning, logical attention and non-verbal expression. However, no connectivity involved in the last segment as subject does not need to respond to the non-target stimuli.

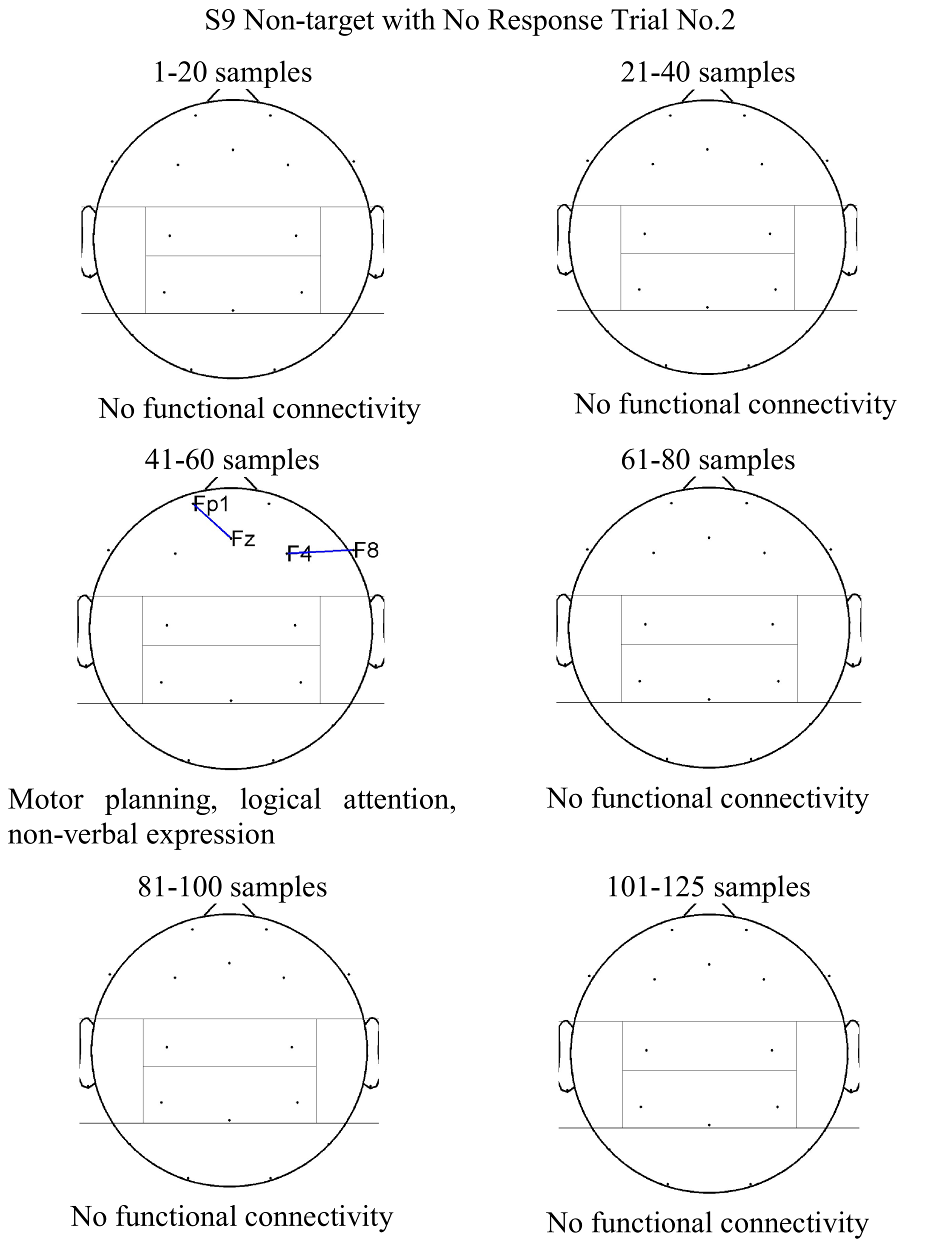

Fig. 4.29 Functional connectivity of 10-20 electrodes for non-target stimuli with no response for 9th subject

Fig. 4.30 shows the functional connectivity of all electrodes for target with response for 9th subject for three different trials (fastest, medium and slowest). For target with response, trial 10, 18 and 1 are the fastest, medium and slowest responses from the subject to the target stimuli. In the figure, high connectivity is observed for all cases in general for all segments compared with target with no response and non-target no response in Fig. 4.31 and 4.32. High connectivity can be observed in occipital lobe for every segment. In last segment, it shows high connectivity between occipital, temporal, parietal, frontal, and center region as response is given.

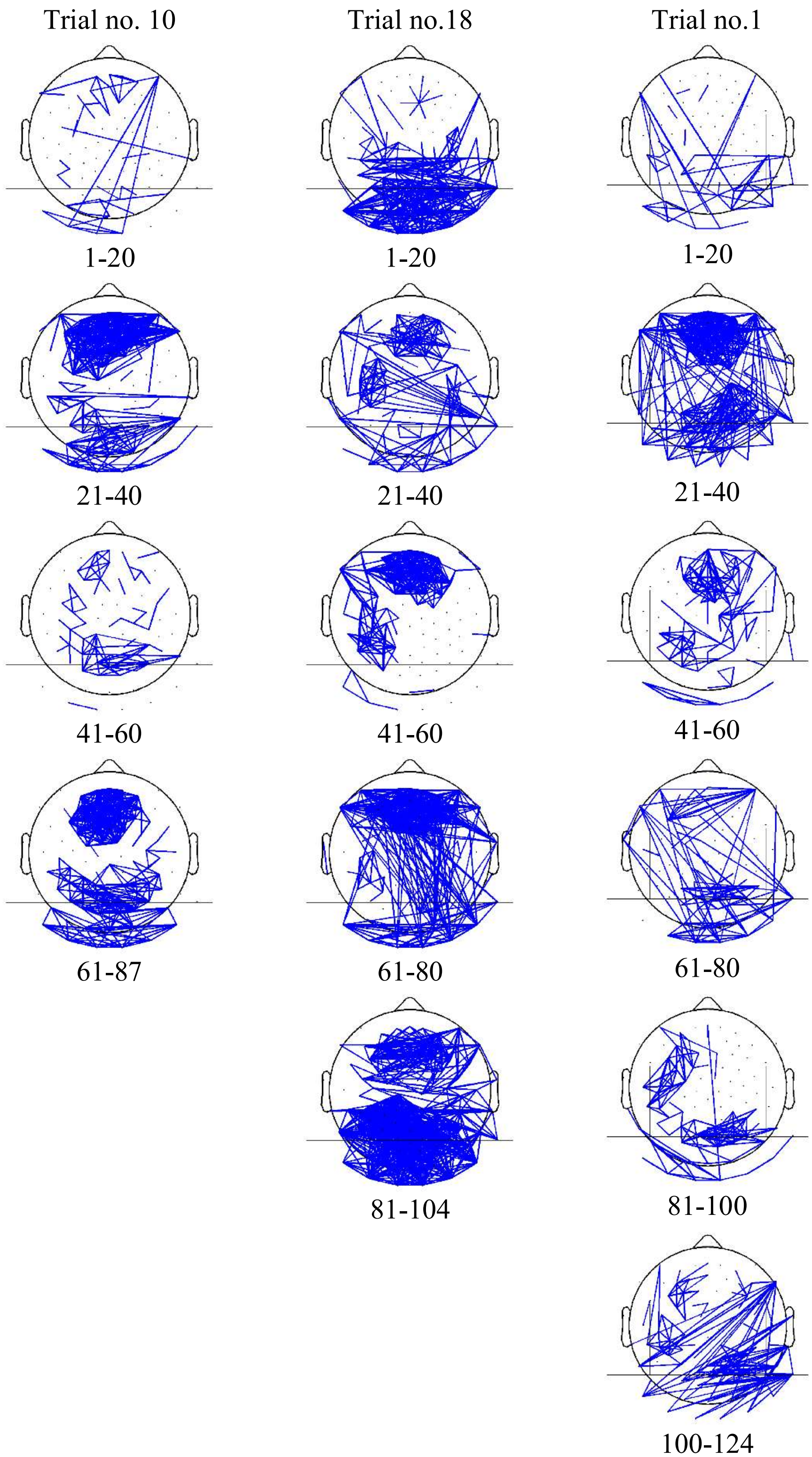

Fig. 4.30 Functional connectivity of all electrodes for target with response for 9th subject

Fig. 4.31 shows the functional connectivity of all electrodes for target with no response of 9th subject for three different trials. In the figure, target with no response shows less connectivity than target with response cases in Fig. 4.30. Since subject is not able to make response on the target stimuli. However, more connectivity been observed in the occipital lobe than the frontal lobes at the last segment as subject not able to respond on the target stimuli

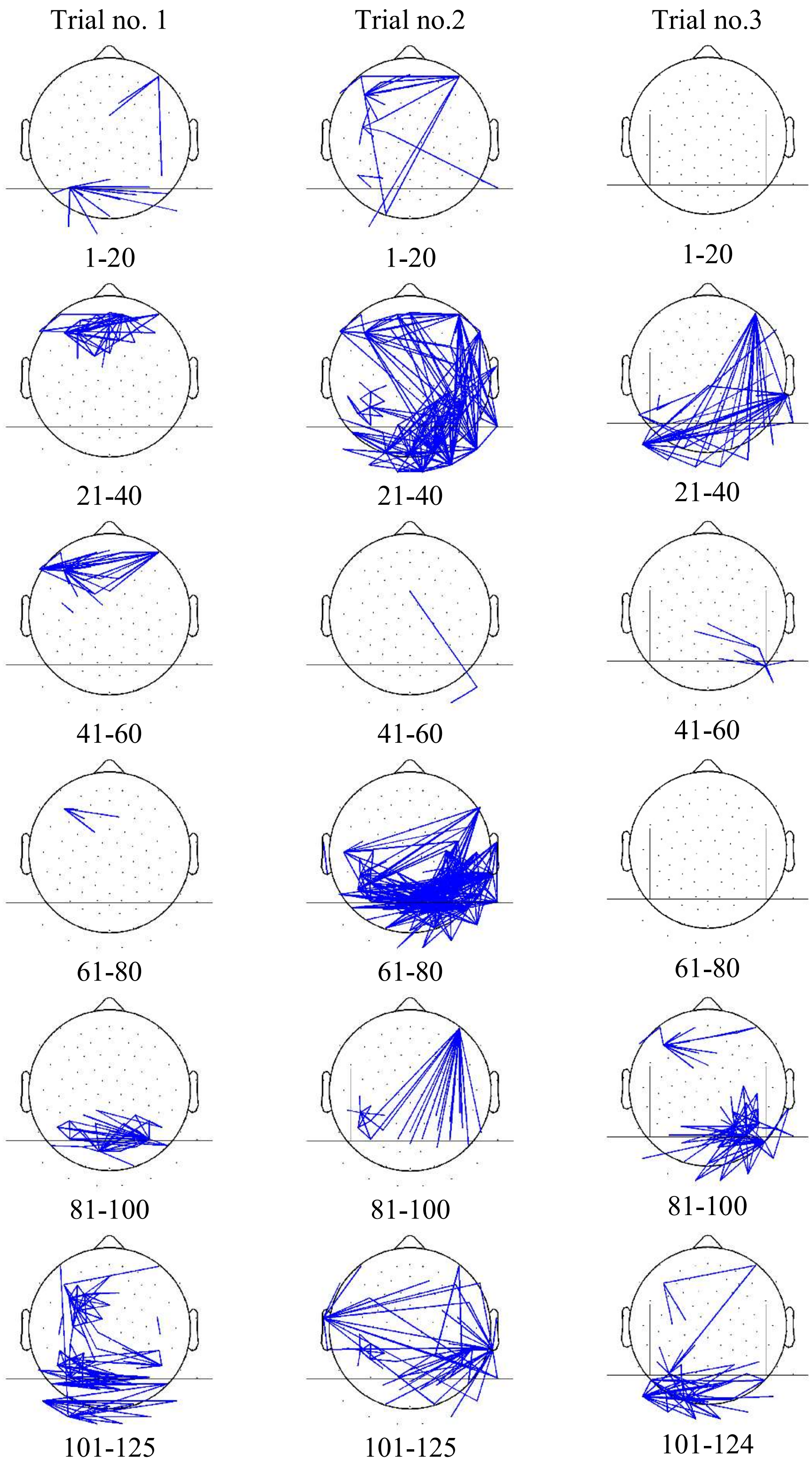

Fig. 4.31 Functional connectivity for target with no response for 9th subject

Fig. 4.32 shows the functional connectivity of all electrodes for non-target with no response for 9th subject for three different trials. For non-target with no response, three trials were selected from the subject which have consistent EEG data. In the figure, non-target with no response shows less connectivity than target with response cases in Fig. 4.30.

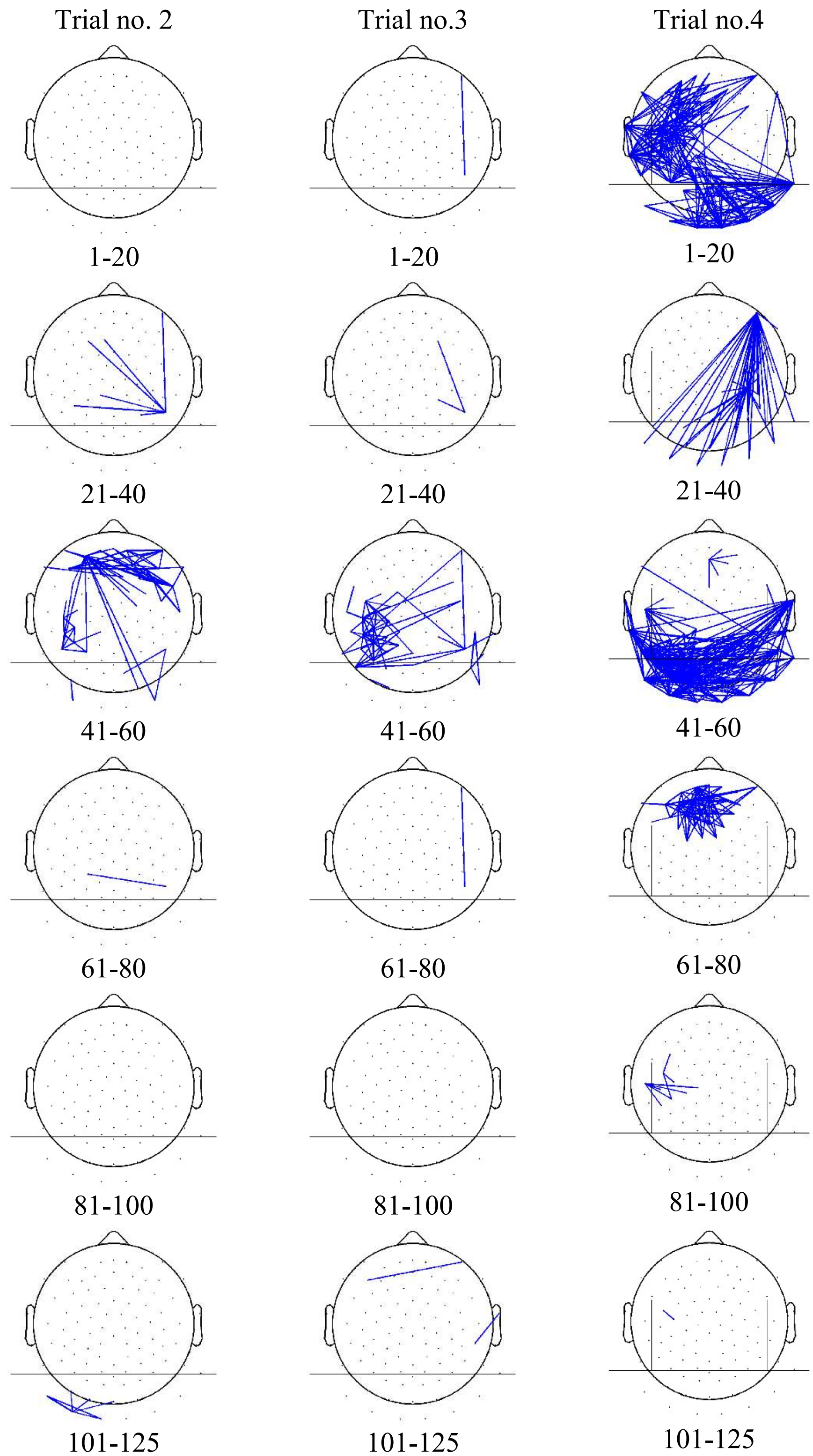

Fig. 4.32 Functional connectivity for non-target with no response for 9th subject

By summary, the target with response cases have high connectivity for every segment compared with target with no response and non-target with no response cases. Moreover, Target response has high connectivity in the last segment. Fig. 4.33 shows the comparison of the average activation graph and the functional connectivity for last segment of target with response cases for 9th subject. From the figure, we can observe the activation graph and the functional connectivity of last segment shows high average activation and high connectivity for frontal, occipital and parietal lobes, which shows that the average activation graph gives same result with the functional connectivity.

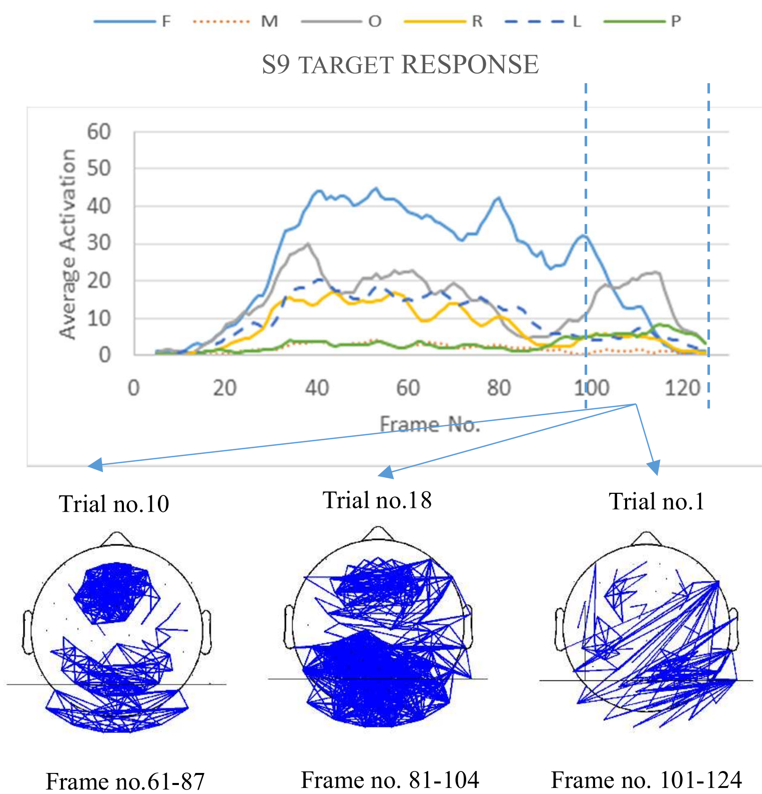

Fig. 4.33 Comparison of the average activation graph and functional connectivity for last segment of target with response cases for 9th subject

For non-target no response cases, high connectivity only observed from sample 1-60 and there is very less connectivity from sample 61-125 as subject has no need to respond to the stimuli. Fig 4.34 shows the comparison of the average activation graph and functional connectivity of the last segment of non-target with no response cases for 9th subject. From the figure, we are able to conclude that non-target with no response shows lower amplitude and lesser connectivity in last segment.

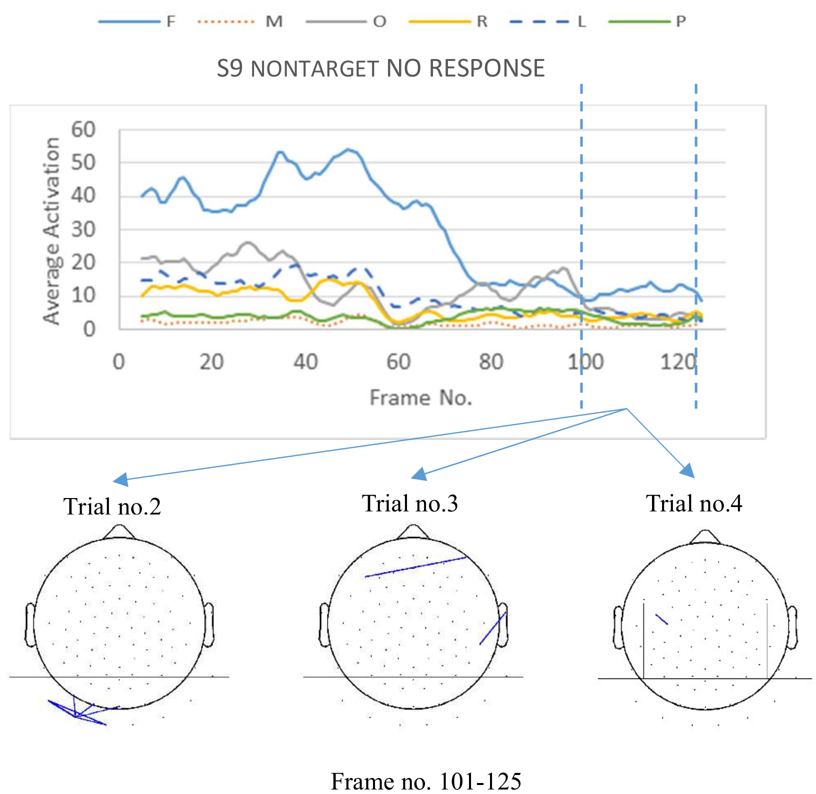

Fig. 4.34 Comparison of the average activation graph and functional connectivity for last segment of non-target with no response cases for 9th subject

Chapter 5

Conclusions and Future Recommendations

5.1 Conclusions

In this research, we have proposed novel algorithms to track brain activation using FS block matching and HS Optical flow motion estimation method for EEG topo-maps. MVs are tracked on EEG topo-maps with respect to time. We have also marked different brain lobes on the EEG topo-maps based on the electrode information for 10-20 and 10-10 international electrodes placement. After generating the motion vectors, low activation motion vectors are removed from the topo-maps based on intensity value. The connected motion vectors are grouped into a motion field or motion cluster. Finally, tracking is done by the overlapping of motion field between consecutive frames.

In experiment result, we have compared the parameters for HS and FS method. Both methods give same tracking pattern but HS gives higher PSNR and need less computation time. Its motion field is also more consistent than full search method. The behaviour of brain lobes for different cases has been observed. The graph is plotted based on the average activation flow for every frame of all subjects for all lobes. In the average activation graph, FS and HS method show almost similar pattern of graph. However, HS has higher activation amplitude compared with FS method. Furthermore, each lobe shows different patterns of graph for different oddball cases. This means that for different oddball cases the difference of the activation flow can be observed among different lobes. For frontal lobe, target response peak always come earlier or higher than target with no response at the end of the task. Besides, frontal lobes will have high amplitude of activation graph than other cases. For parietal lobe, the activation graph has very low amplitude. However, we are still able to observe a peak in the end of the task for target with response case. For occipital lobe, high peak occurs in the middle of the graph for all cases. However, the occipital lobe activation drop near the end of the task when the frontal lobe rises for target with response cases.

Average graph of individual subject for all lobes at different cases had been plotted. Seven different subjects were chosen based on poor (2^{nd}, 5^{th}, 13^{th}), average (7^{th} and 20^{th}) and good (9^{th} and 10^{th}) performance in the oddball experiment. Different performances show different patterns of the graph for different activities. For example, the occipital or frontal lobe shows inconsistent graph with many high peaks for poor performance. We can conclude that because of the inconsistent graph, subject is not able to concentrate or focus on the screen and his performance not very good. Hence subject is able to respond to the target stimuli for 12 or 13 times only.

We have measured the functional connectivity by using classical cross-correlation method. Here we have proposed a new algorithm to track functional connectivity. First, we extracted the EEG data from the stimuli that appears till the end of trial resulting in response or no response from the subjects. After that, we divided the data into 20 samples per segments and calculate their cross correlation. Lastly, we plot the connectivity between the electrodes that have highest correlation with zero lag for every segment in EEG topo-map. The pattern of connectivity for different cases has been observed. It has been seen that the pattern of connectivity between all different cases are different. For functional connectivity for 10-20 electrodes, we are able to observe the connectivity for Fz, F3, F4, C3 or C4 electrode in the last segment, which is used for motor planning or sensorimotor integrations; when subject responded on the target or non-target stimuli. In functional connectivity map, high connectivity can be observed in last segment when subject gives response to target on non-target stimuli which involves all lobes. For target with response, high connectivity is observed for all cases in general for all segments compared with other cases. Target with no response has less connectivity than target with response cases. For non-target with no response, high connectivity is present only in beginning, since subject does not need to respond to the non-target stimuli.

5.2 Future Recommendation

- First, tracking can be improve by increasing sampling rate of the EEG signal. EEG signal transfer very fast in the brain, so by increasing the sampling rate, the tracking result will be more accurate.

- Besides, the tracking can also be improved by reducing the block size for full search block matching or pixel range of motion vector for Horn-Schunck optical flow. Smaller block size or pixel range gives more information of the MVs in EEG topo-map. However, it will take longer computation time.
- Next, we can enhance the grouping method by acquiring more precise clusters on the EEG topo-map. We can use other grouping methods (e.g.: k-mean clustering) to separate the EEG activation into different clusters. Since EEG activation is produced from hundred billion of neurons in the brain, the more precise clusters will result in more accurate tracking.
- Lastly, we can track the EEG activity by extracting EEG signal at different frequency bands e.g.: delta (δ), theta (θ), alpha (α), beta (β), and gamma (γ). So, we will able to get more detailed and precise information in the result of tracking at different frequency bands.

REFERENCES

Amiri, S., Rabbi, A., Azinfar, L. & Fazel-Rezai, R., 2013. A review of P300, SSVEP, and hybrid P300/SSVEP brain-computer interface systems. *Brain-Computer Interface Systems – Recent Progress and Future Prospects.*

Baccalá, L. & Sameshima, K., 2001. Partial directed coherence: a new concept in neural structure determination. *Biological cybernetics,* 84(6), pp. 463-474.

Barjatya, A., 2004. Block matching algorithms for motion estimation. *IEEE Transactions Evolution Computation,* 8(3), pp. 225-239.

Barron, J., Fleet, D. & Beauchemin, S., 1994. Performance of optical flow techniques. *International journal of computer vision,* 12(1), pp. 43-77.

Bermudez, J. L., 2010. *Cognitive Science: An Introduction to the Science of the Mind.* s.l.:Cambridge University Press.

Blackwell, L., Trzesniewski, K. & Dweck, C., 2007. Implicit theories of intelligence predict achievement across an adolescent transition: A longitudinal study and an intervention. *Child development,* 78(1), pp. 246-263.

David, O., Cosmelli, D. & and Friston, K., 2004. Evaluation of different measures of functional connectivity using a neural mass model. *Neuroimage,* 21(2), pp. 659-673.

Delorme, A. & Makeig, S., 2004. EEGLAB: an open source toolbox for analysis of single-trial EEG dynamics including independent component analysis. *Journal of neuroscience methods,* 134(1), pp. 9-21.

Deshpande, G., Sathian, K. & Hu, X., 2009. Compensating for Zero-lag Correlation Effects in Time-lagged Granger Causality Analysis. *Neuroimage,* Volume 47, p. S147.

Fleet, D. & Weiss, Y., 2006. Optical flow estimation. *Handbook of mathematical models in computer vision,* Volume Springer US, pp. 237-257.

Herrmann, C. & Knight, R., 2001. Mechanisms of human attention: event-related potentials and oscillations. *Neuroscience & Biobehavioral Reviews,* 25(6), pp. 465-476.

Höller, Y. et al., 2013. EEG-response consistency across subjects in an active oddball task. *PloS one,* 8(9), p. e74572.

Horn, B. & Schunck, 1981. Determining optical flow. *Artificial intelligence,* 17(1-3), pp. 185-203.

Irimia, A. et al., 2012. Patient-tailored connectomics visualization for the assessment of white matter atrophy in traumatic brain injury. *Frontiers in neurology,* Volume 3, p. 10.

Jurcak, V., Tsuzuki, D. & Dan, I., 2007. 10/20, 10/10, and 10/5 systems revisited: their validity as relative head-surface-based positioning systems. *Neuroimage,* 34(4), pp. 1600-1611.

Kaminski, M. J. & Blinowska, K. J., 1991. A new method of the description of the information flow in the brain structures. *Biological cybernetics,* 65(3), pp. 203-210.

Korzeniewska, A. et al., 2003. Determination of information flow direction among brain structures by a modified directed transfer function (dDTF) method. *Journal of neuroscience methods,* 125(1), pp. 195-207.

Koslow, S. H. & Huerta, M. F., 1997. *Neuroinformatics: An Overview of the Human Brain Project (Progress in Neuroinformatics Research Series).* 1 edition ed. s.l.: Psychology Press.

Kus, R., Kaminski, M. & Blinowska, K., 2004. Determination of EEG activity propagation: pair-wise versus multichannel estimate. *IEEE transactions on Biomedical Engineering,* 51(9), pp. 1501-1510.

Liu, Y., 2013. Noise reduction by vector median filtering. *Geophysics,* 78(3), pp. V79-V87.

Lucas, B. & Kanade, T., 1981. An iterative image registration technique with an application to stereo vision. *IJCAI ,* 81(1), pp. 674-679.

Luu, P. & Ferree, T., 2005. *Determination of the HydroCel Geodesic Sensor Nets' Average Electrode Positions and Their 10–10 International Equivalents,* s.l.: Inc, Technical Note.

Metwally, Y., 2007. Basic concept of brainmapping. In: *Online Brain Mapping.* Ain Shams university, Cairo, Egypt: s.n., pp. 1-3.

Nisar, H. & Choi, T., 2000. *An advanced center biased three step search algorithm for motion estimation.* s.l., Multimedia and Expo, 2000. ICME 2000. 2000 IEEE International Conference on (Vol. 1, pp. 95-98). IEEE.

Nisar, H. & Choi, T., 2008. Fast block motion estimation algorithm based on motion classification and directional search patterns. *Optical Engineering,* 47(10), pp. 107001-107001.

Nisar, H. & Choi, T., 2009. *Fast and efficient fractional pixel motion estimation for H. 264/AVC video coding.* s.l., 16th IEEE International Conference on Image Processing (ICIP) (pp. 1561-1564). IEEE.

Nisar, H., Malik, A. & Choi, T., 2012. Content adaptive fast motion estimation based on spatio-temporal homogeneity analysis and motion classification. *Pattern Recognition Letters,* 33(1), pp. 52-61.

Nisar, H. et al., 2015. Tracking of EEG Activity Using Motion Estimation to Understand Brain Wiring. In: *Signal and Image Analysis for Biomedical and Life Sciences.* s.l.:Springer International Publishing, pp. 159-174.

Nisar, H. & Yeap, K. H., 2014. EEG/ERP Analysis: Methods and Applications. In: A. S. M. Kamel Nidal, ed. *Introduction to EEG/ERP.* s.l.:CRC Press, pp. 2-4.

Pechura, C. M. & Martin, J. B., 1991. *Mapping the Brain and Its Functions: Integrating Enabling Technologies Into Neuroscience Research.* Institute of Medicine (U.S.): Committee on a National Neural Circuitry Database.

Philip, J., Samuvel, B., Pradeesh, K. & Nimmi, N., 2014. *A comparative study of block matching and optical flow motion estimation algorithms.* Emerging Research Areas: Magnetics, Machines and Drives (AICERA/iCMMD), 2014 Annual International Conference , IEEE, pp. 1-6.

Picton, T., 1992. The P300 wave of the human event-related potential. *Journal of clinical neurophysiology,* 9(4), pp. 456-479.

Picton, T., 1992. The P300 wave of the human event-related potential. *Journal of clinical neurophysiology,* 9(4), pp. 456-479.

Polich, J., 2007. Updating P300: an integrative theory of P3a and P3b. *Clin Neurophysiol,* 118(10), pp. 2128-2148.

Qassim, Y., Cutmore, T., James, D. & Rowlands, D., 2013. Wavelet coherence of EEG signals for a visual oddball task. *Computers in biology and medicine,* 43(1), pp. 23-31.

Trans Cranial Technologies, 2012. *DIY tDCS.* [Online]
Available at: http://www.diytdcs.com/tag/1020-system-positioning/
[Accessed 11 November 2016].

Van Horn, J. et al., 2012. Mapping connectivity damage in the case of Phineas Gage. *PloS one,* 7(5), p. e37454.

Walker, J., Kozlowski, G. & Lawson, R., 2007. A modular activation/coherence approach to evaluating clinical/QEEG correlations and for guiding neurofeedback training: modular insufficiencies, modular excesses, disconnections, and hyperconnections. *Journal of Neurotherapy,* 11(1), pp. 25-44.

Weisstein, E. W., n.d. *L^2-Norm -- From Wolfram MathWorld.* [Online]
Available at: http://mathworld.wolfram.com/L2-Norm.html
[Accessed 22 November 2016].

Zhariy, M., 2005. *Introduction to Optical Flow.* [Online]
Available at: https://www.math.uni-bremen.de/zetem/cms/media.php/250/optical.pdf
[Accessed 17 November 2016].

List of Publications

Lim, S.H., Nisar, H., Yap, V.V. and Shim, S.O., 2015. *Tracking of electroencephalography signals across brain lobes using motion estimation and cross-correlation*. Journal of Electronic Imaging, 24(6), pp.061106-061106. doi:10.1117/1.JEI.24.6.061106

Lim, S.H., Nisar, H. and Yap,V.V., 2015, October. *Tracking of EEG activity using topographic maps*. In 2015 IEEE International Conference on Signal and Image Processing Applications (ICSIPA) (pp. 287-291). IEEE. doi: 10.1109/ICSIPA.2015.7412206.

Lim, S.H., Nisar, H. and Yap,V.V., 2016, October. *Comparison of Motion Field of EEG Topo-maps for Tracking Brain Activation paper*. In 2016 IEEE-EMBS Conference on Biomedical Engineering and Sciences

APPENDIX

APPENDIX A: Average Activation Graph for 2nd Subject

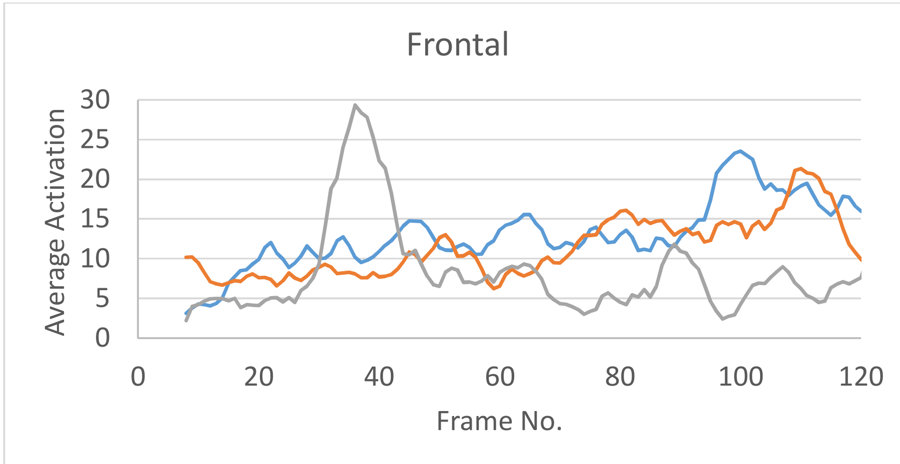

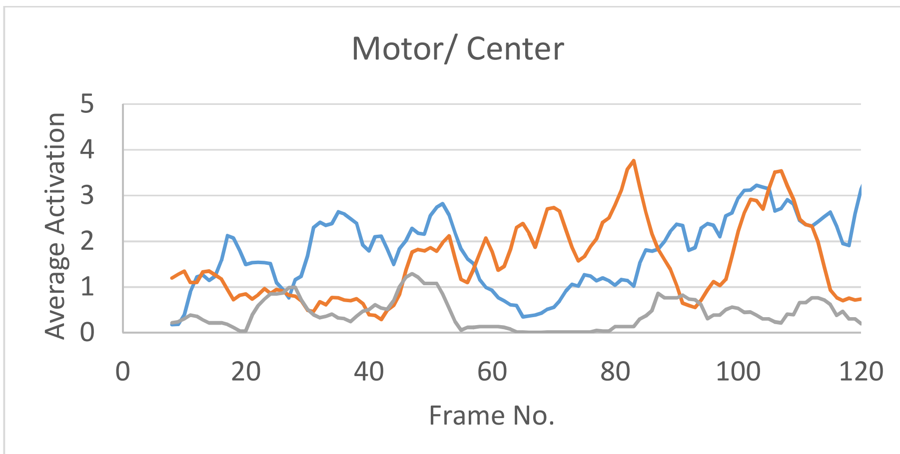

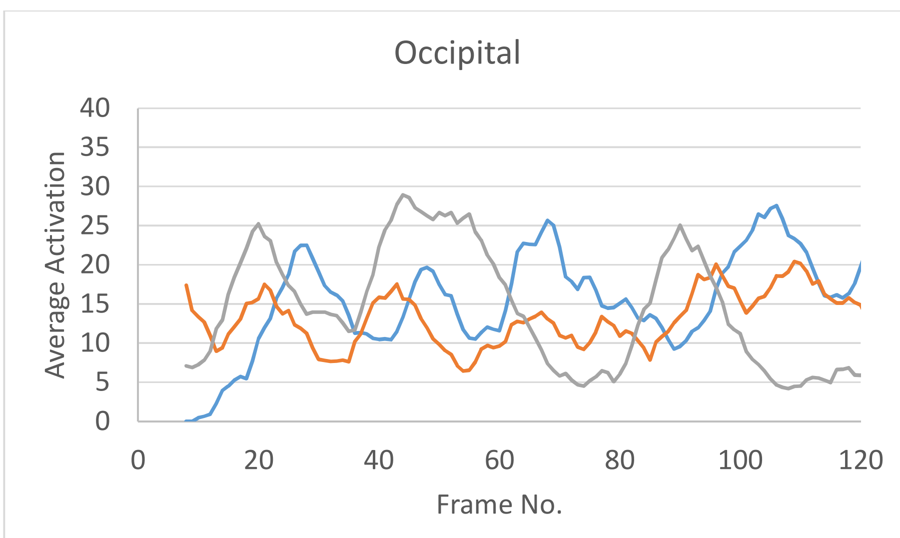

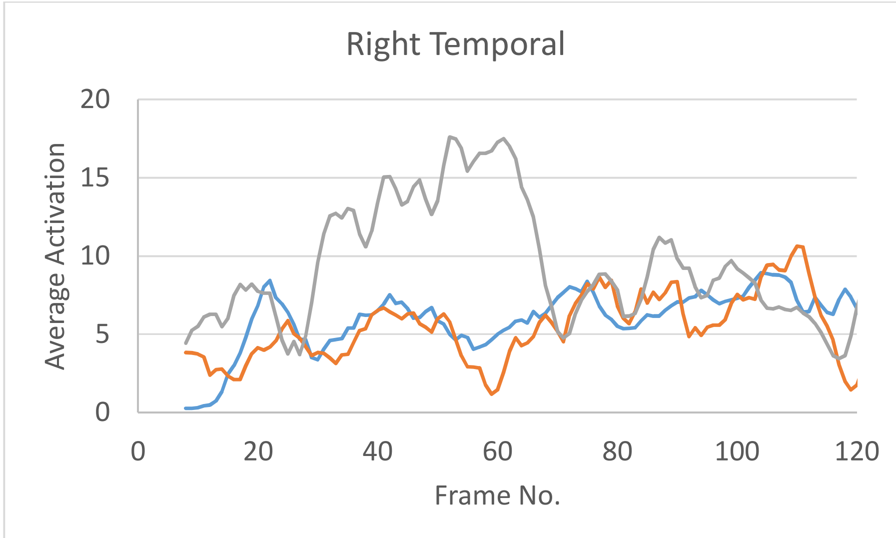
Right Temporal
20
15
10
5
0
Average Activation
0
20
40
60
80
100
120
Frame No.

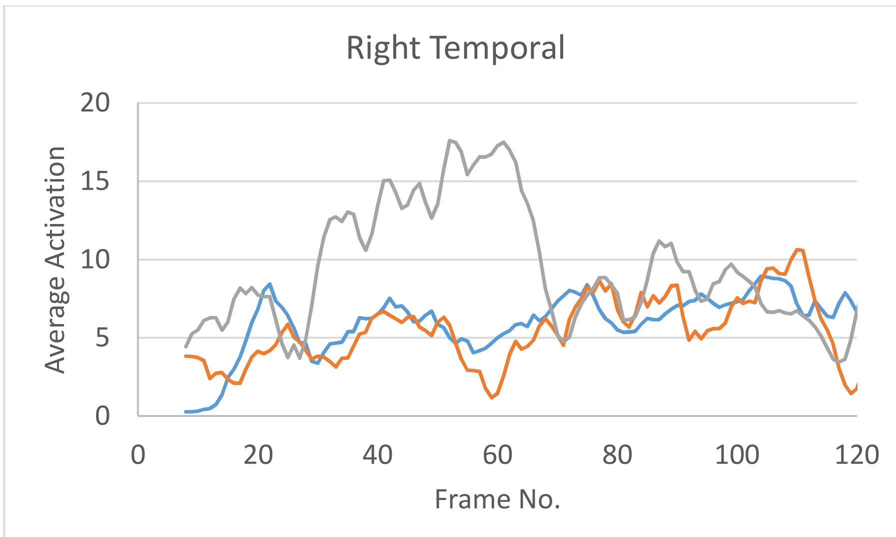
Right Temporal
20
15
10
5
0
Average Activation
0
20
40
60
80
100
120
Frame No.

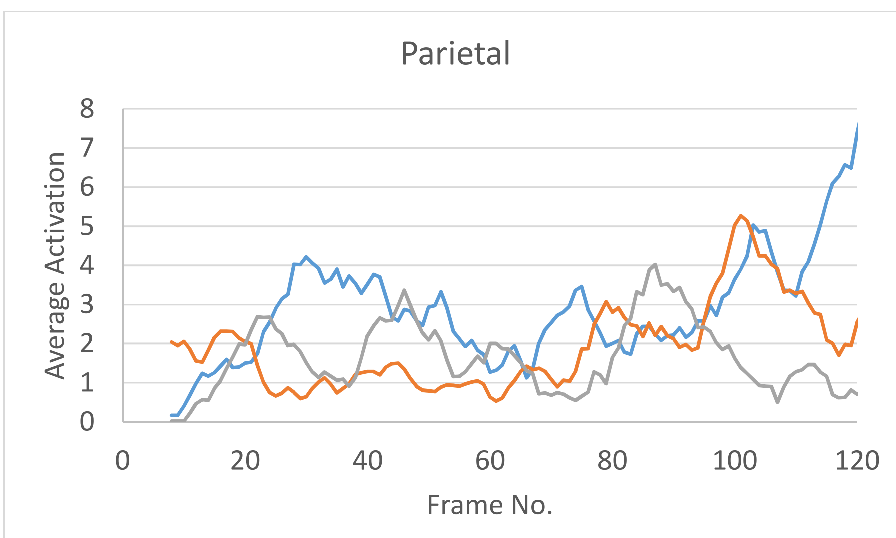
Parietal
8
7
6
5
4
3
2
1
0
Average Activation
0
20
40
60
80
100
120
Frame No.

APPENDIX B: Average Activation Graph for 5th Subject

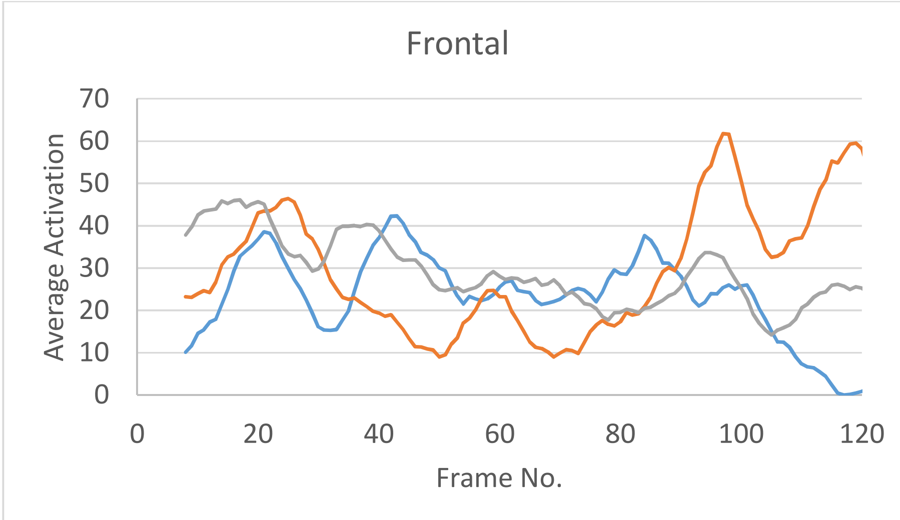

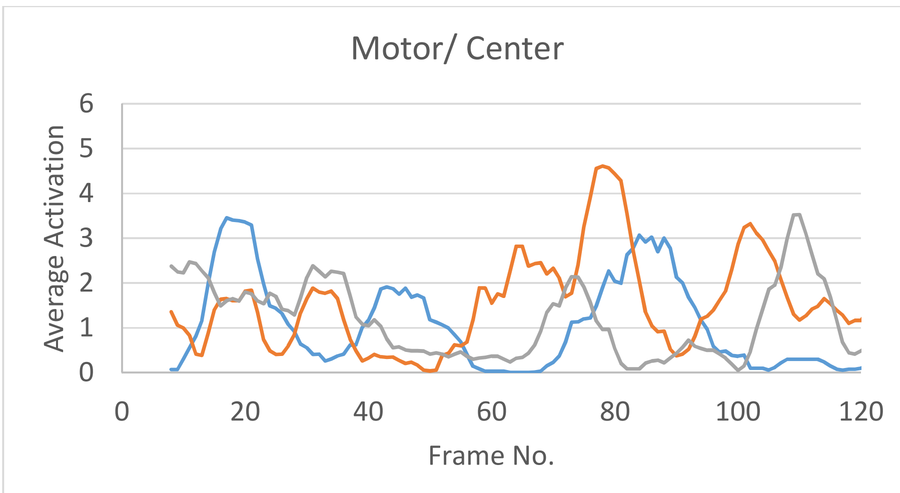

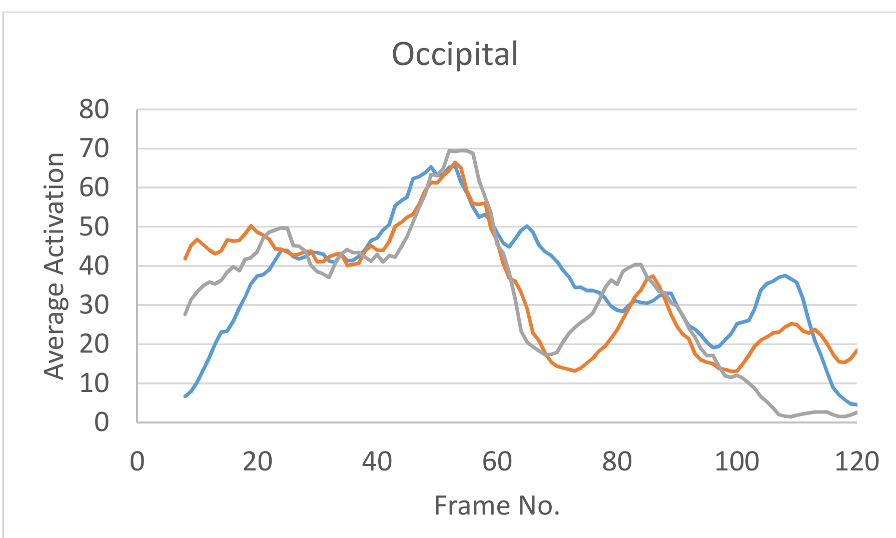

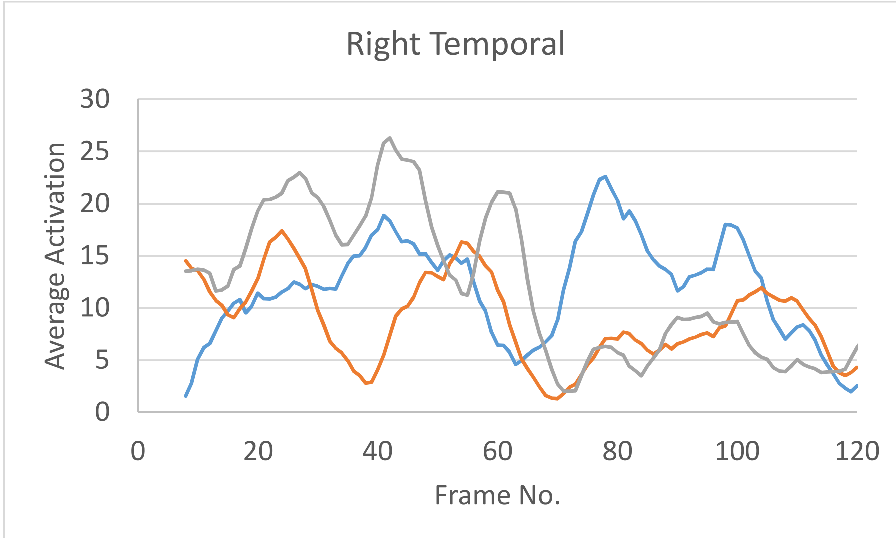
Right Temporal
30
25
20
15
10
5
0
Average Activation
0
20
40
60
80
100
120
Frame No.

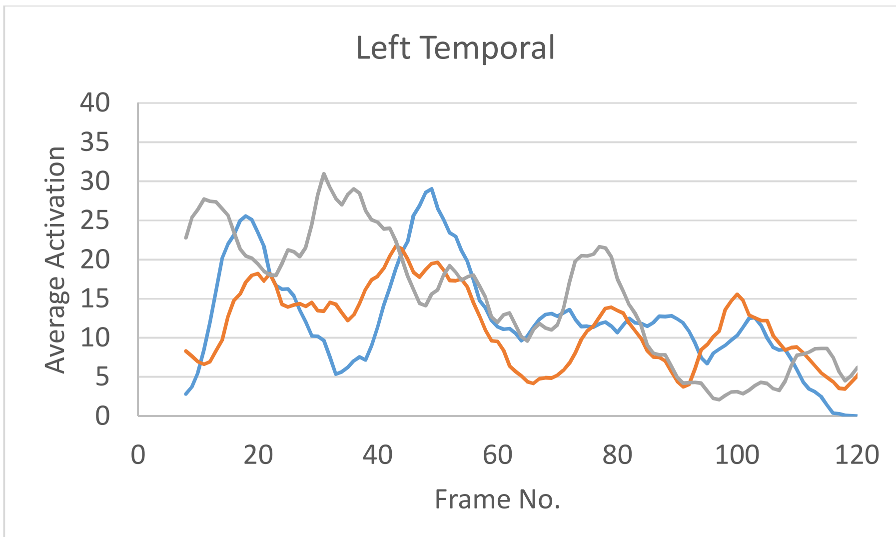
Left Temporal
40
35
30
25
20
15
10
5
0
Average Activation
0
20
40
60
80
100
120
Frame No.

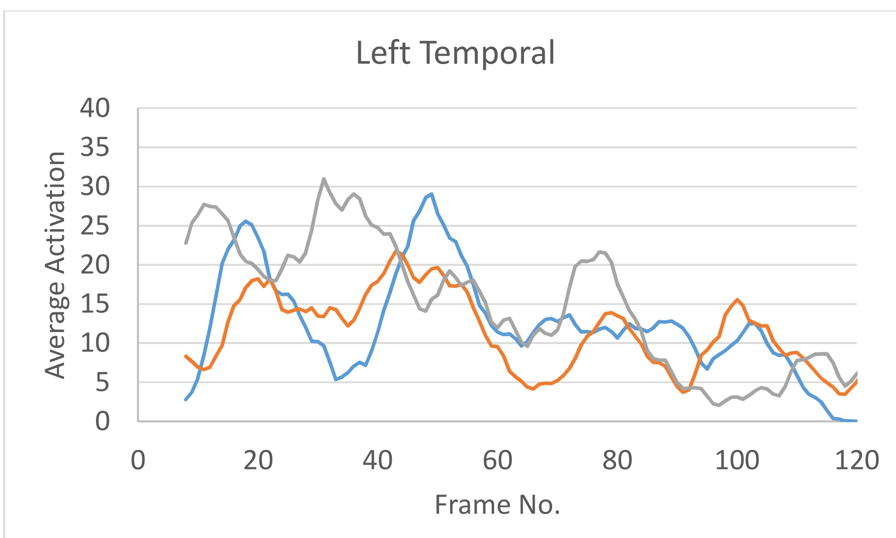
Left Temporal
40
35
30
25
20
15
10
5
0
Average Activation
0
20
40
60
80
100
120
Frame No.

APPENDIX C: Average Activation Graph for 13th Subject

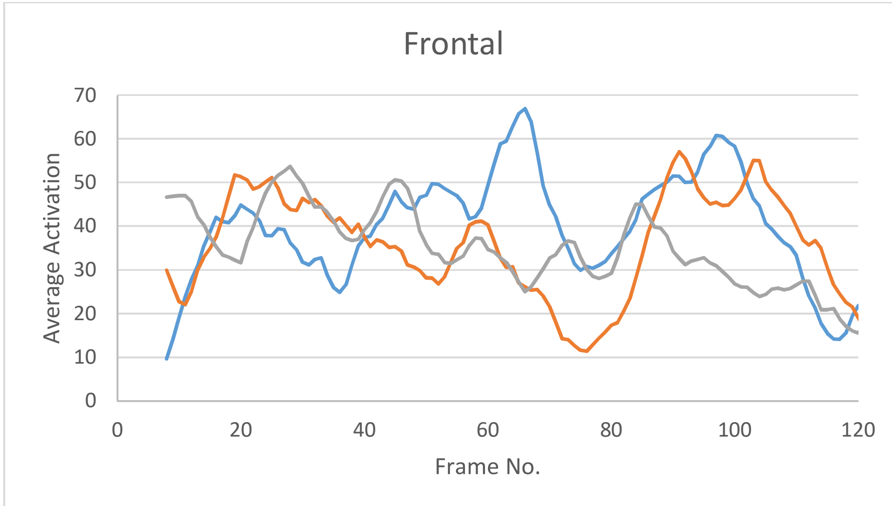

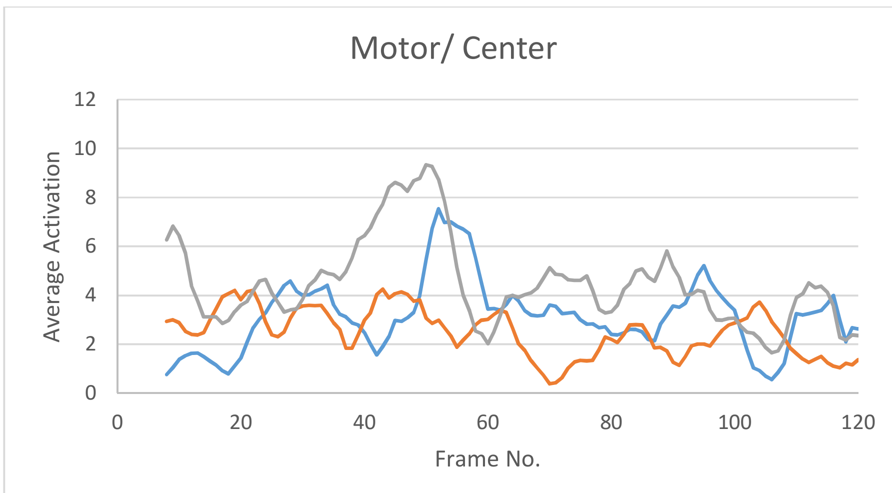

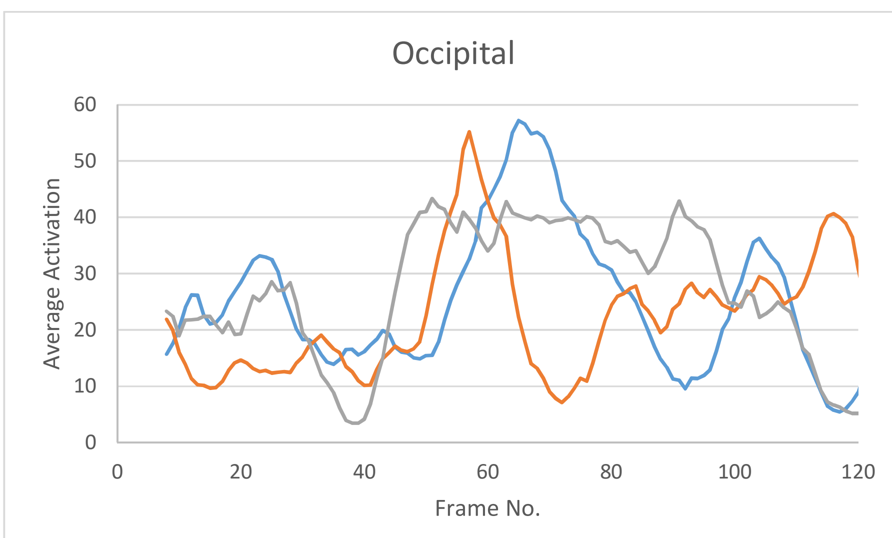

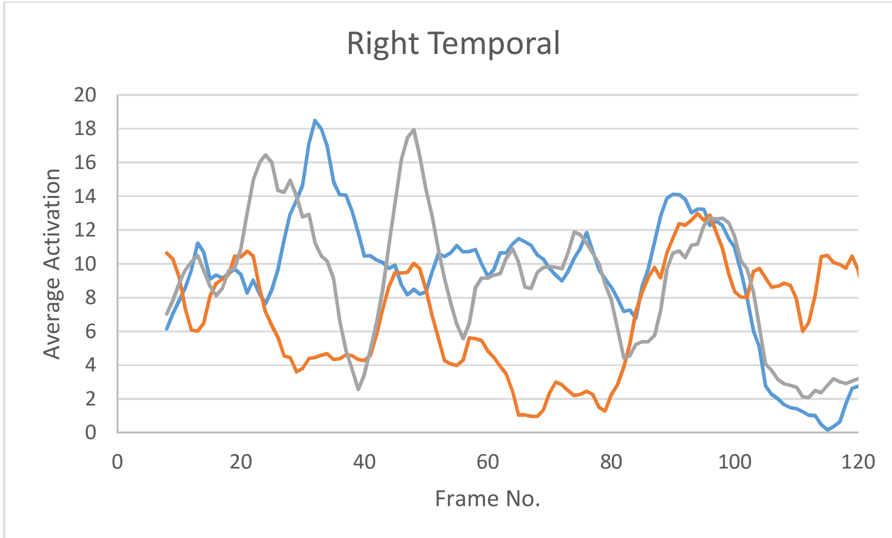
Right Temporal
Average Activation
0
2
4
6
8
10
12
14
16
18
20
0
20
40
60
80
100
120
Frame No.

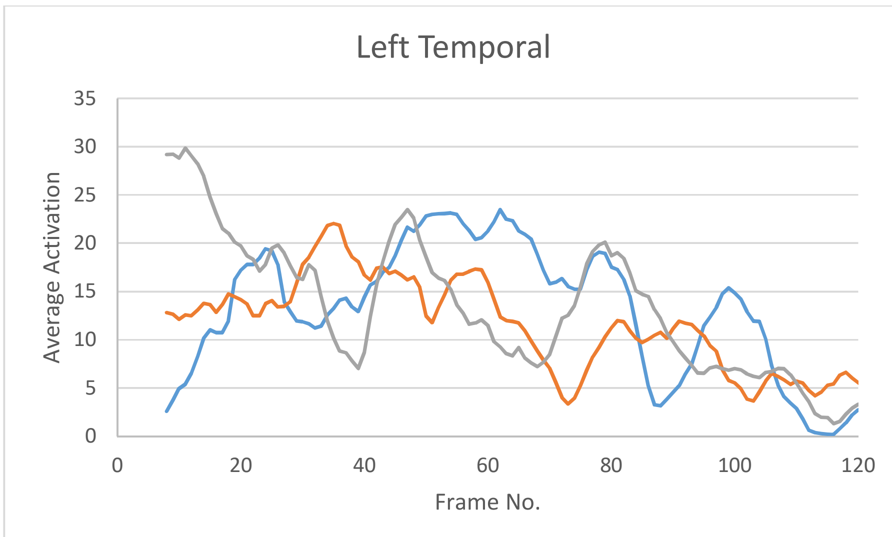
Left Temporal
Average Activation
0
5
10
15
20
25
30
35
0
20
40
60
80
100
120
Frame No.

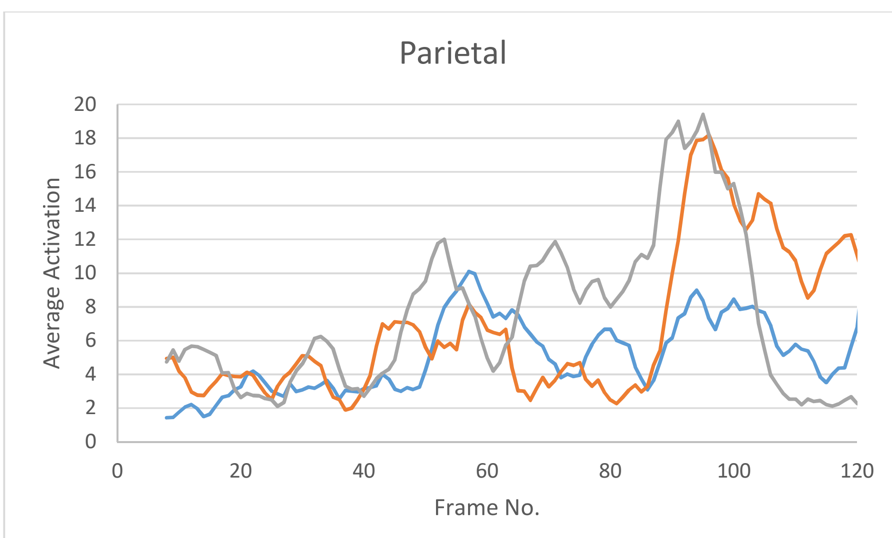
Parietal
Average Activation
0
2
4
6
8
10
12
14
16
18
20
0
20
40
60
80
100
120
Frame No.

APPENDIX D: Average Activation Graph for 7th Subject

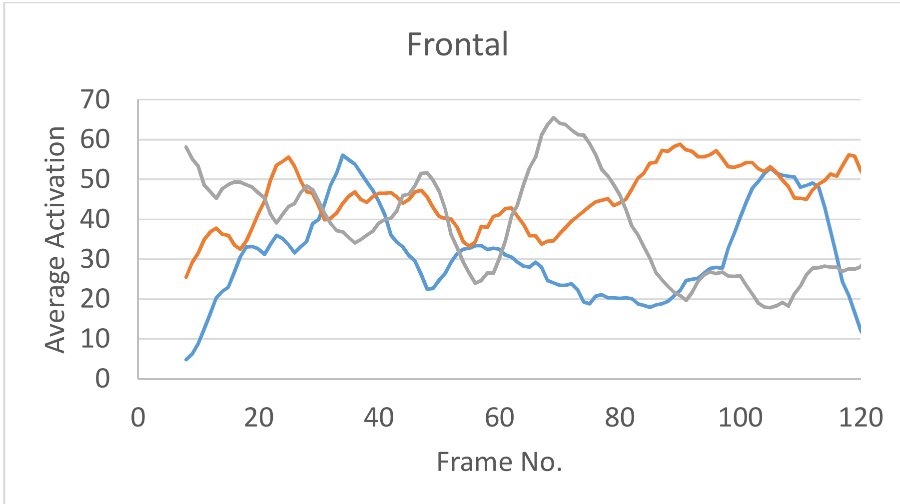

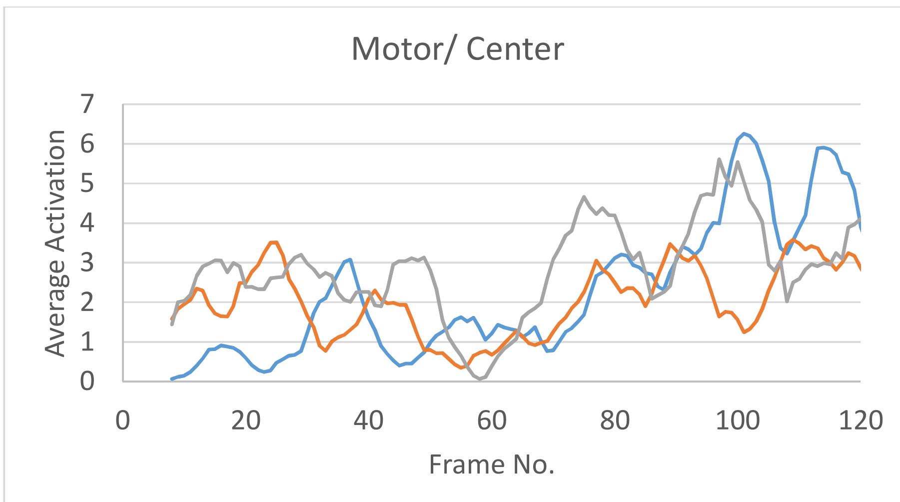

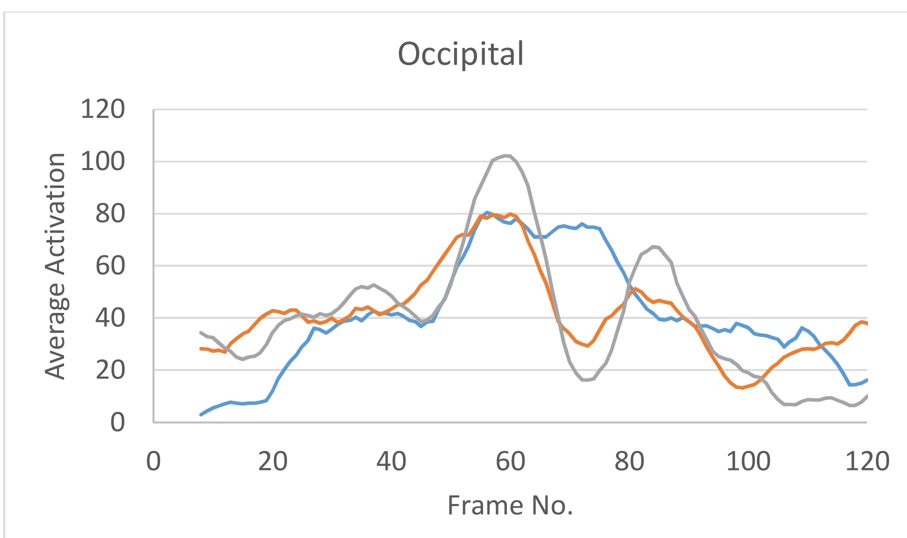

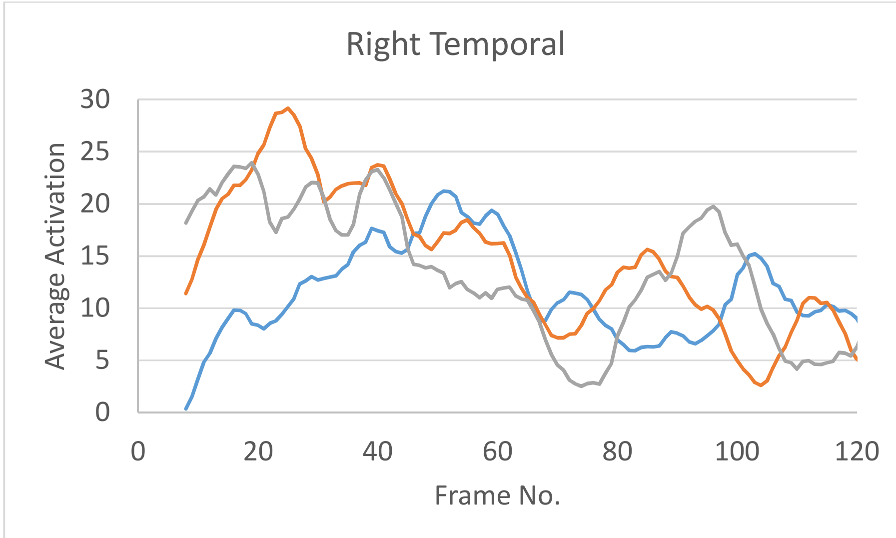
Right Temporal
30
25
20
15
10
5
0
0
20
40
60
80
100
120
Average Activation
Frame No.

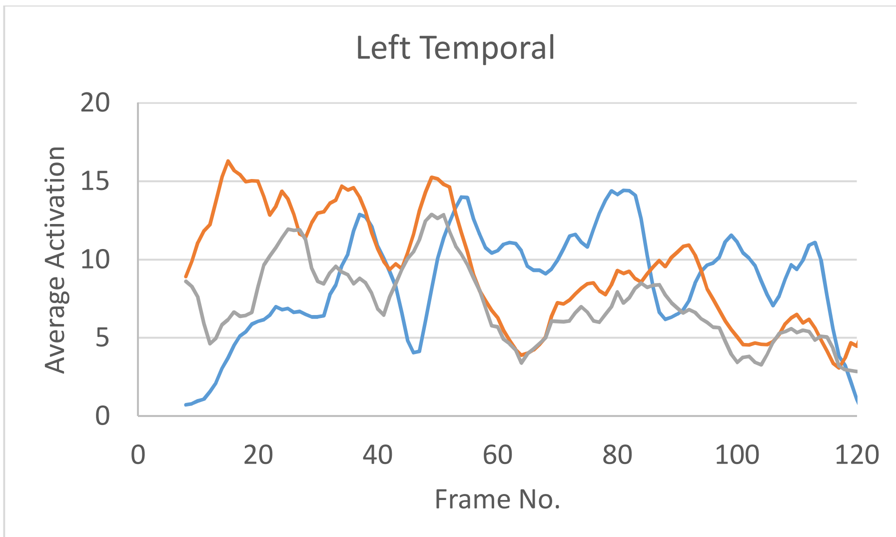
Left Temporal
20
15
10
5
0
0
20
40
60
80
100
120
Average Activation
Frame No.

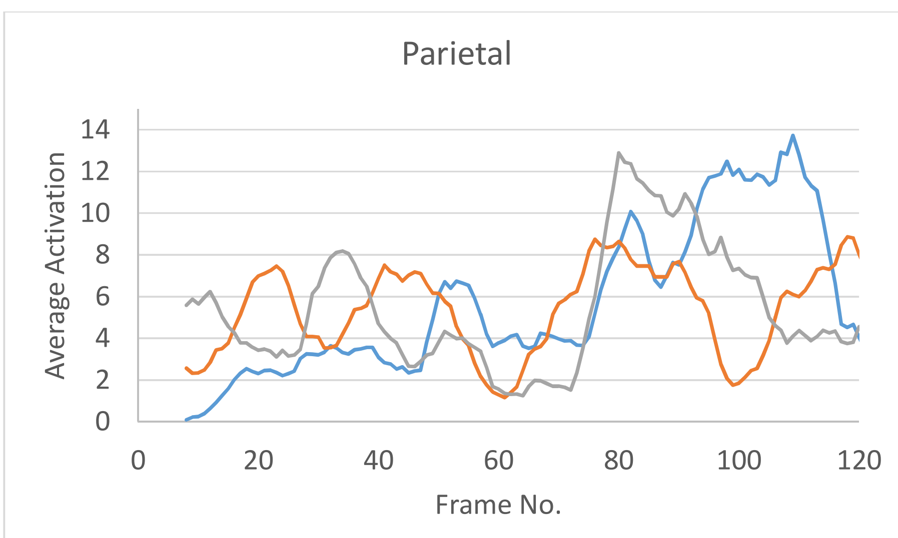
Parietal
14
12
10
8
6
4
2
0
0
20
40
60
80
100
120
Average Activation
Frame No.

APPENDIX E: Average Activation Graph for 20th Subject

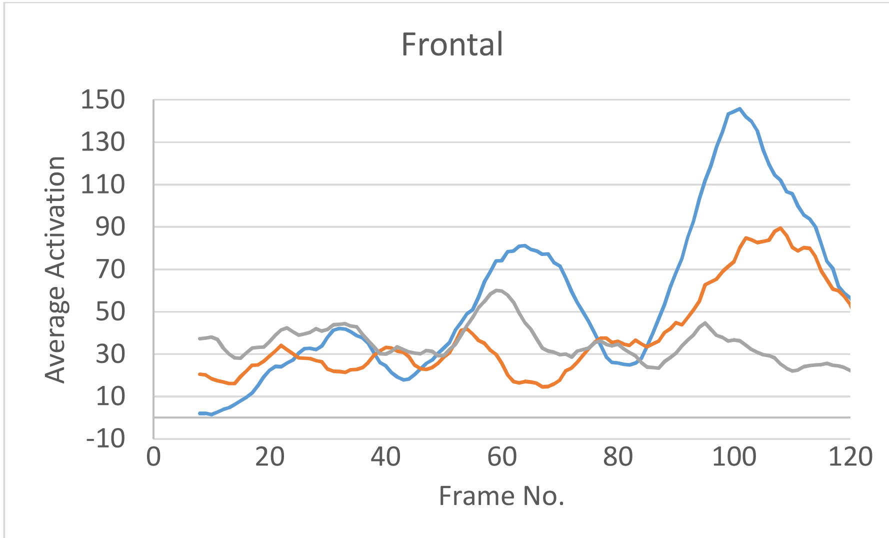

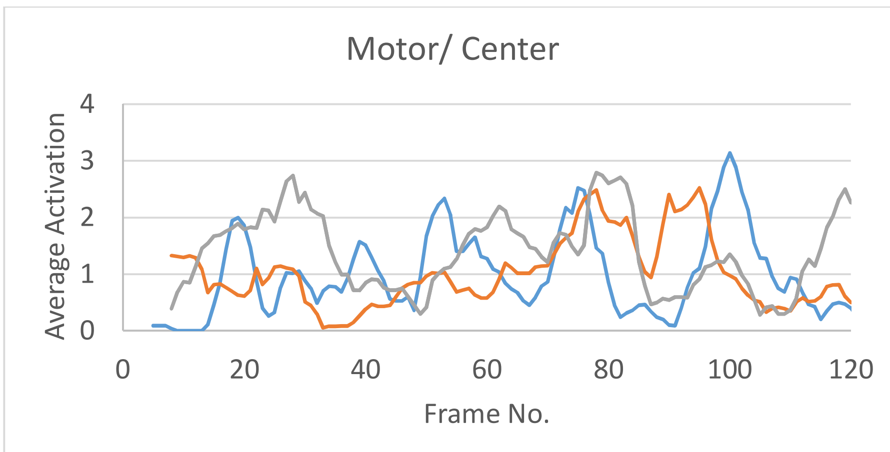

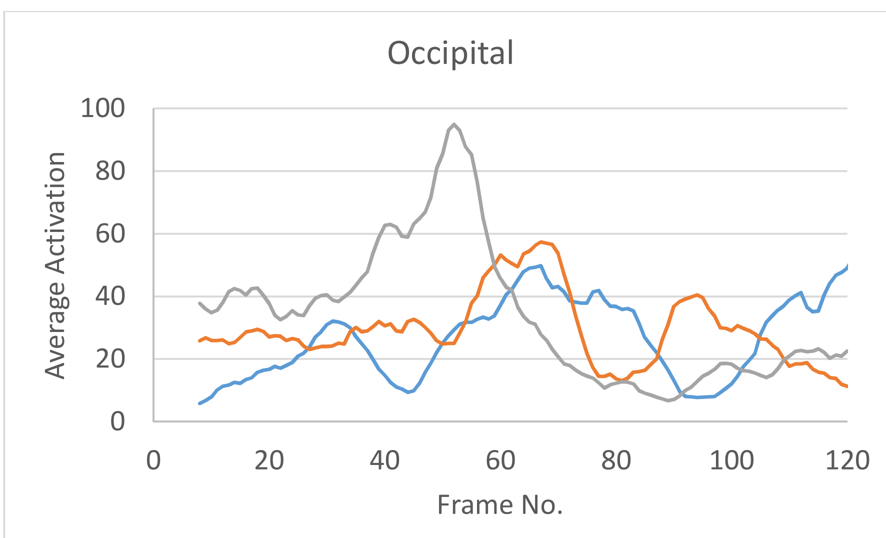

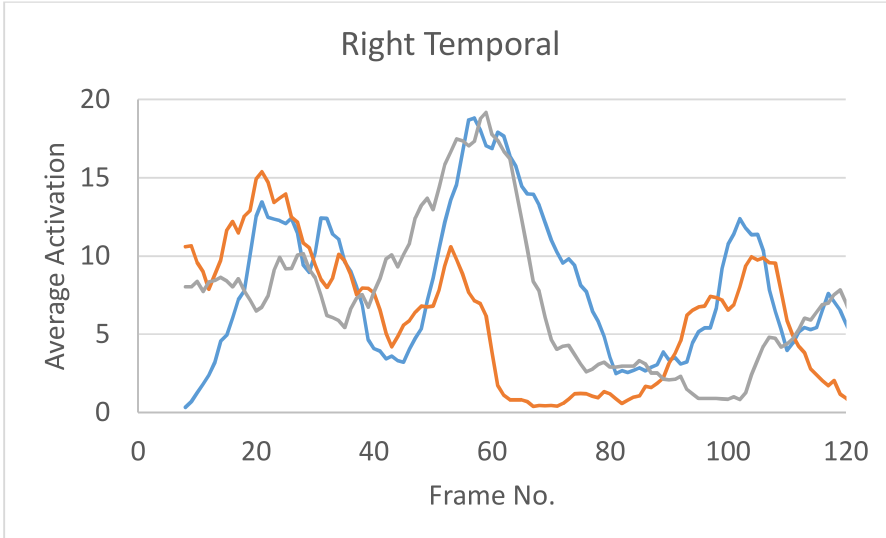
Right Temporal
Average Activation
20
15
10
5
0
0
20
40
60
80
100
120
Frame No.

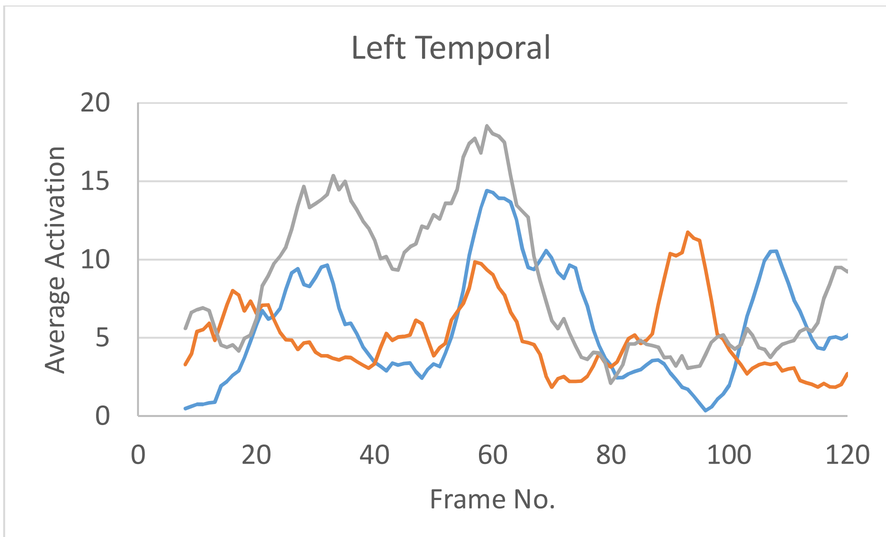
Left Temporal
Average Activation
20
15
10
5
0
0
20
40
60
80
100
120
Frame No.

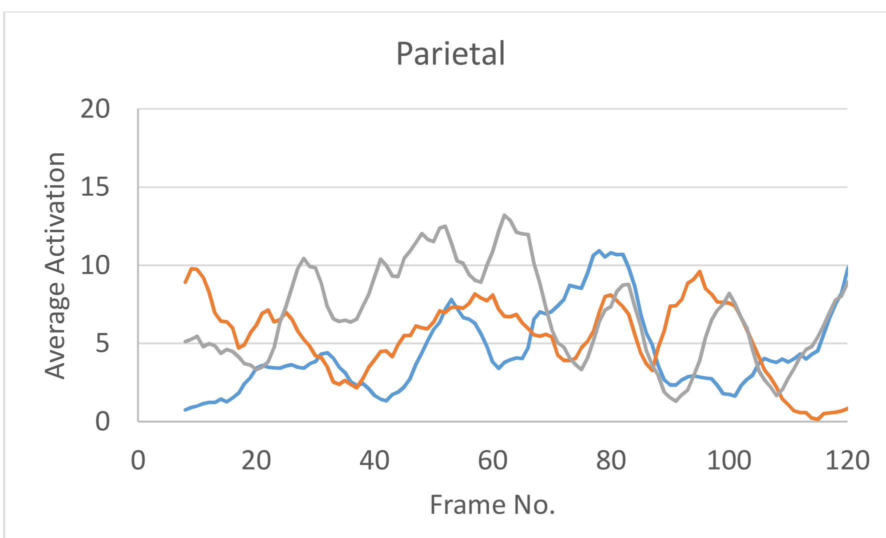
Parietal
Average Activation
20
15
10
5
0
0
20
40
60
80
100
120
Frame No.

APPENDIX F: Average Activation Graph for 9th Subject

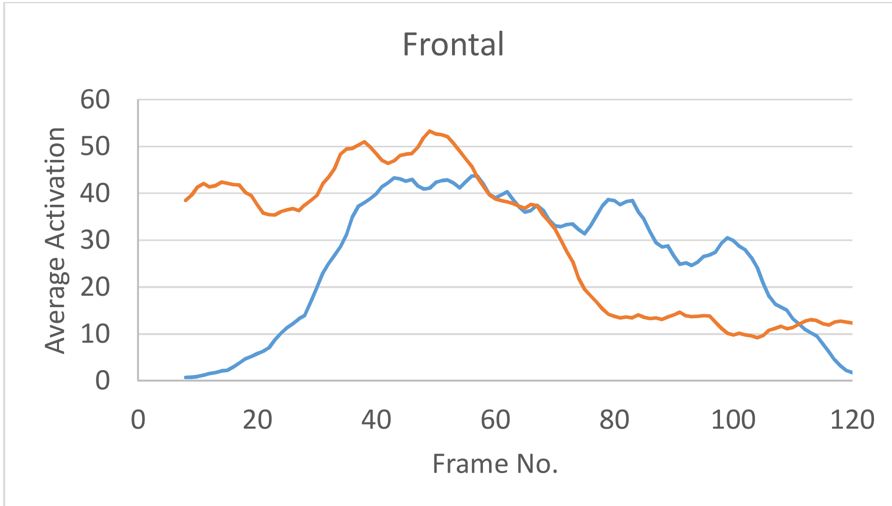

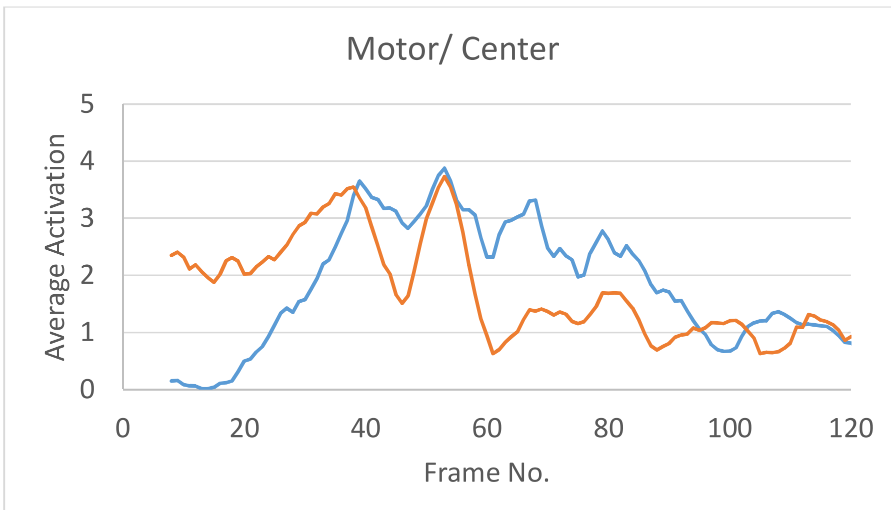

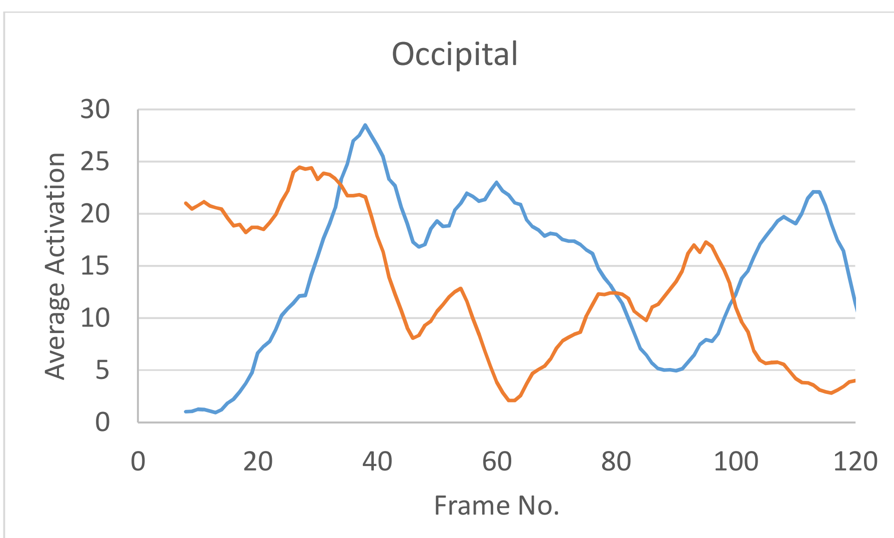

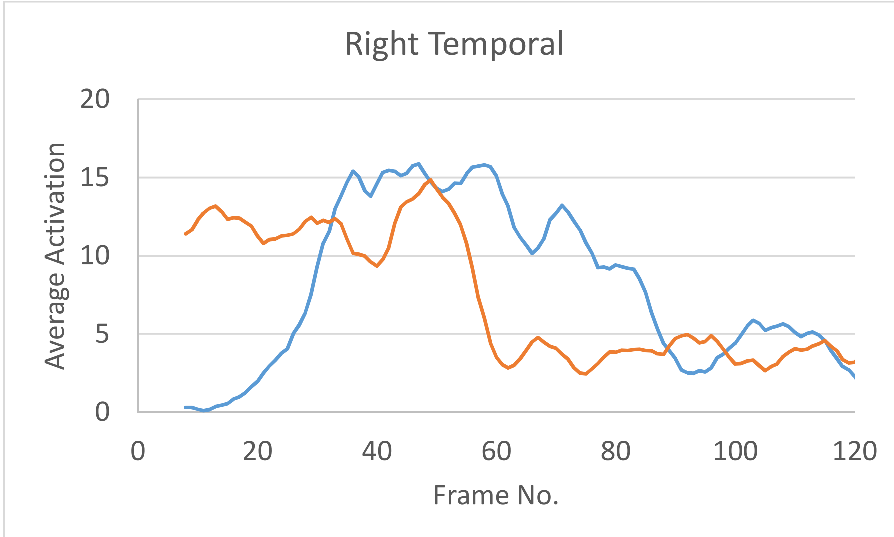
Right Temporal
Average Activation
0
5
10
15
20
0
20
40
60
80
100
120
Frame No.

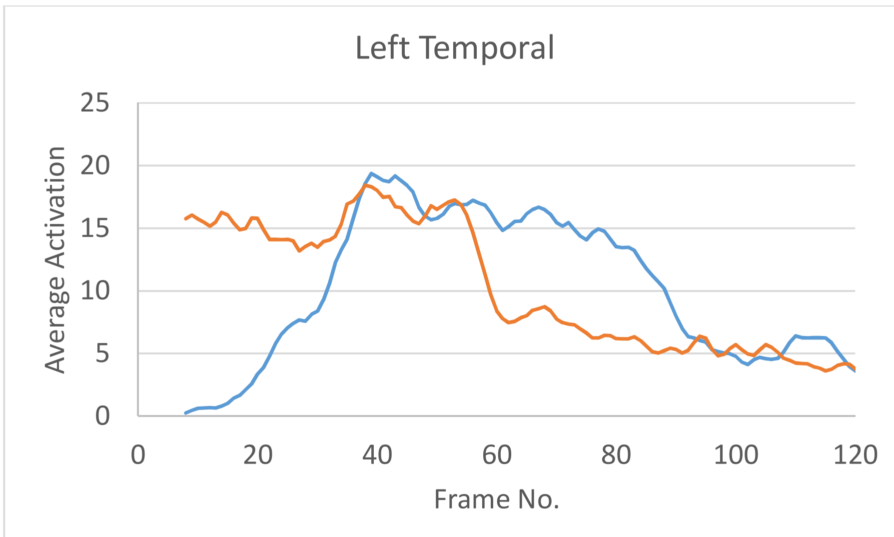
Left Temporal
Average Activation
0
5
10
15
20
25
0
20
40
60
80
100
120
Frame No.

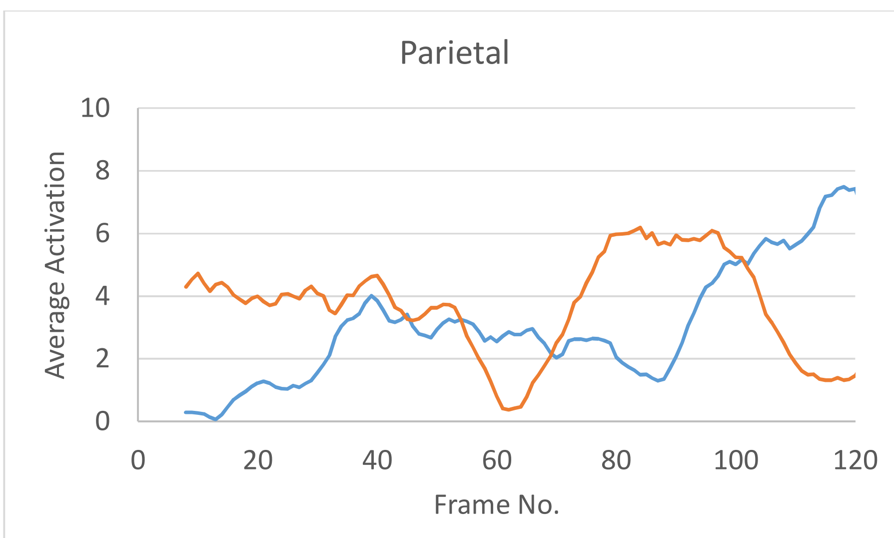
Parietal
Average Activation
0
2
4
6
8
10
0
20
40
60
80
100
120
Frame No.

APPENDIX G: Average Activation Graph for 10th Subject

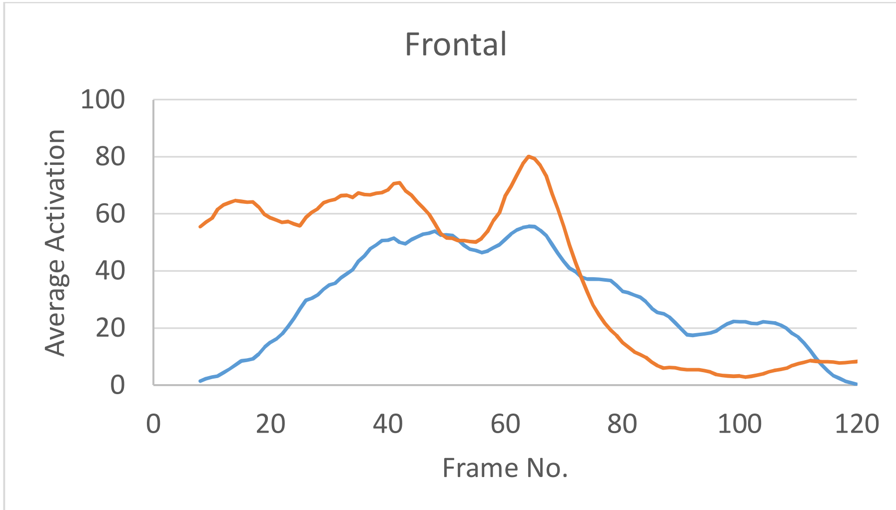

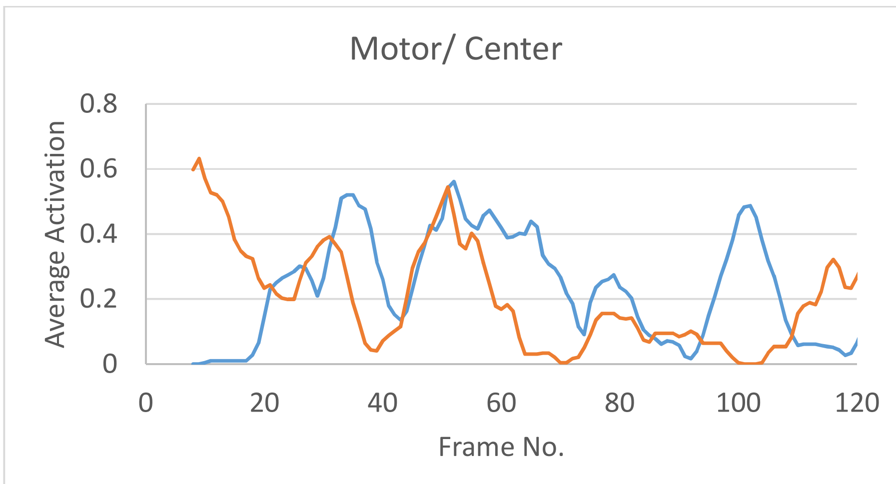

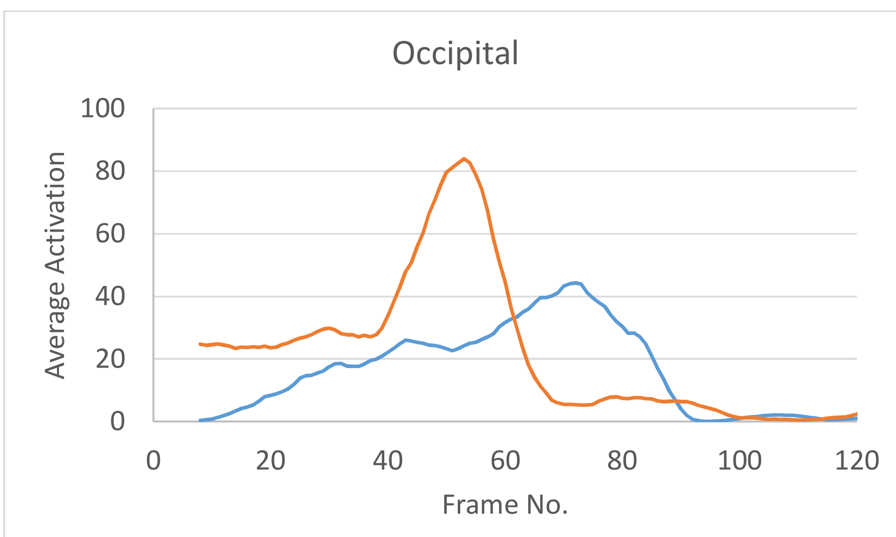

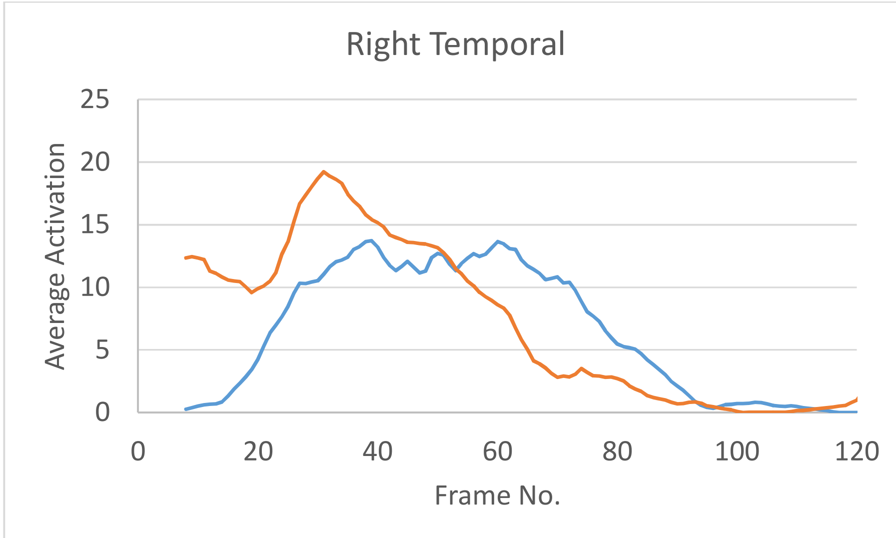
Right Temporal
Average Activation
25
20
15
10
5
0
0
20
40
60
80
100
120
Frame No.

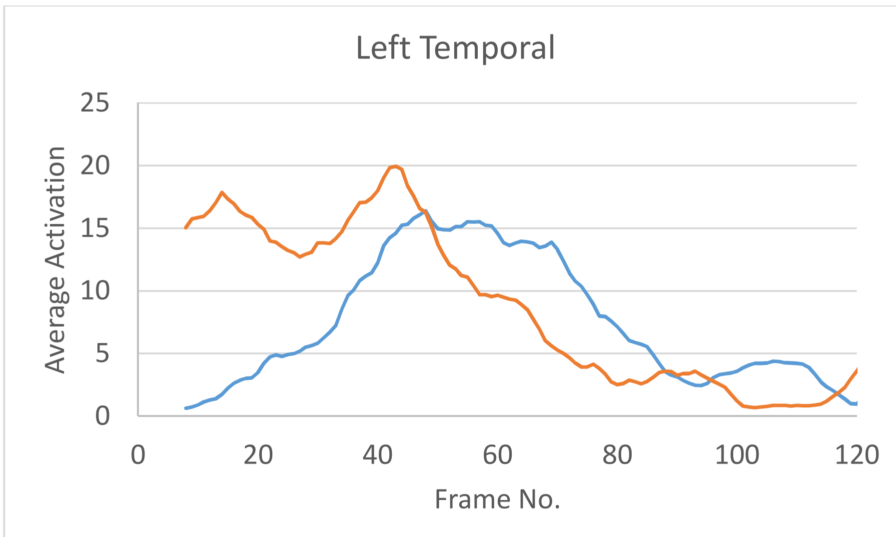
Left Temporal
Average Activation
25
20
15
10
5
0
0
20
40
60
80
100
120
Frame No.

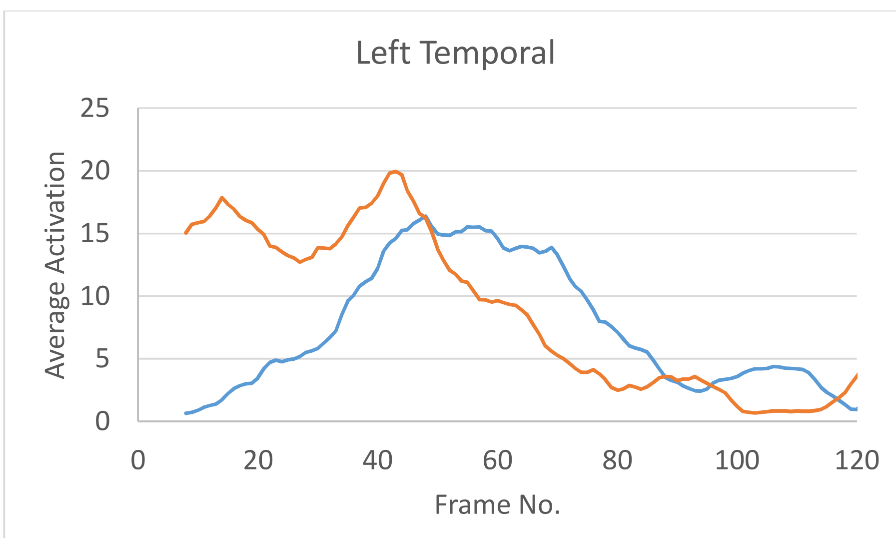
Left Temporal
Average Activation
25
20
15
10
5
0
0
20
40
60
80
100
120
Frame No.

APPENDIX H: Full Search Block Matching Algorithm

```
%   Motion vectors using full search method
%   imgP : The image for which we want to find motion vectors
%   imgI : The reference image
%   mbSize : Size of the macroblock
%   p : Search parameter

clear all;
close all;
clc;

fprintf('\tSystem Estimates Motion in Brain Topographic
Videos\n\n');
fprintf('\t\t\tKindly select video to be processed\n\n');

 % Require user input
inVideo = input('Input Video:', 's');

%Parameter selection
mbSize =8; p =4;
imgSize=0.5;

%% Read video and convert to sequence of Grayscale images
[readSeq readSeqColor] = readVideoGrayColor(inVideo);

%Crop and resize the video sequence to desired prosessing
dimension
cropSeq = imgCrop (readSeq);
frameSeq = imresize(cropSeq,imgSize);

% Obtain the size and sequences of the video
[row, col, seq] = size (frameSeq);


%Crop the color video sequence to desired prosessing dimension
for i =1:seq
    cropSeqColor{1,i}=imgCrop(readSeqColor{1,i});
    frameSeqColor{1,i}=imresize(cropSeqColor{1,i},imgSize);
end

%Template to store vectors
vectors = zeros(2,row*col/mbSize^2,seq);

%Template to store min MAD in each search
costs = ones(2*p + 1, 2*p +1) * 65537;

Ver = row/mbSize;
Hor = col/mbSize;

blockCost = zeros(Hor,Ver,seq);
blockCostBlue = zeros(Hor,Ver,seq);


minVals = zeros(2500,49);
computations = 0;
increment =0;
```

```
% we start off from the top left of the image
% we will walk in steps of mbSize
% for every marcoblock that we look at we will look for
% a close match p pixels on the left, right, top and bottom of
it

for s = 1:1:seq % calculate the motion vector frame by frame

    c = s+1;
    if(c <=seq)
    increment = increment +1;
    imgI = frameSeq(:,:,c); % ref frame
    imgP = frameSeq(:,:,s); % current frame
    imgIColor=frameSeqColor{1,c};
    imgPColor=frameSeqColor{1,s};

    a = 0;
    mbCount = 1;
    for i = 1 : mbSize : row-mbSize+1
        if(i >=340)
            0;
        end
        b = 0;
        a = a + 1;
        for j = 1 : mbSize : col-mbSize+1

        % the exhaustive search starts here
        % we will evaluate cost for  (2p + 1) blocks vertically
        % and (2p + 1) blocks horizontaly
        % m is row(vertical) index
        % n is col(horizontal) index
        % this means we are scanning in raster order
        b = b + 1;
        for m = -p : p
            for n = -p : p
                refBlkVer = i + m;   % row/Vert co-ordinate for
ref block
                refBlkHor = j + n;   % col/Horizontal co-
ordinate
                if (refBlkVer <1 || refBlkVer+mbSize-1> row
                        || refBlkHor < 1 || refBlkHor+mbSize
                        -1 > col)
                    continue;
                end

% calculate the cost (SAD) for in the search window
                costs(m+p+1,n+p+1) = imgMAD(imgP(i:i+mbSize-
                  1,j:j+mbSize-1),
                  imgI(refBlkVer:refBlkVer+mbSize-1,
                  refBlkHor:refBlkHor+mbSize-1), mbSize);

% extract the grey and blue intensity for in the search
                blockCost(a,b,increment) =
                  sum(sum(abs(imgP(i:i+mbSize-1,j:j+mbSize-
                  1))))/(mbSize*mbSize);
                blockCostBlue(a,b,increment)=
                  sum(sum(abs(imgPColor(i:i+mbSize-
                  1,j:j+mbSize-1,3))))/(mbSize*mbSize);
                if(c ==seq)
                    blockCost(a,b,increment+1) =
```

```
                    sum(sum(abs(imgI(i:i+mbSize-
                    1,j:j+mbSize- 1))))/(mbSize*mbSize);
                blockCostBlue(a,b,increment+1)=
                    sum(sum(abs(imgIColor(i:i+mbSize-
                    1,j:j+mbSize-1,3))))/(mbSize*mbSize);
            end
        end
    end

    % Now we find the vector where the cost is minimum
    % and store it ... this is what will be passed back.
    [dx, dy] = minCost4(costs);

    % finds which macroblock in imgI gave us min Cost
    vectors(1,mbCount,increment) = dy-p-1;    % row co-
ordinate for the vector
    vectors(2,mbCount,increment) = dx-p-1;    % col co-
ordinate for the vector
    mbCount = mbCount + 1;
    costs = ones(2*p + 1, 2*p +1) * 65537;
    end
end
end
end
motionVect = vectors;
```

APPENDIX I: Horn-Schunck Optical Flow Algorithm

```
function HS(im1, im2, alpha, ite, uInitial, vInitial,
displayFlow, displayImg)
% Horn-Schunck optical flow method
% Horn, B.K.P., and Schunck, B.G., Determining Optical Flow,
AI(17), No.
% 1-3, August 1981, pp. 185-203
http://dspace.mit.edu/handle/1721.1/6337
%
% Usage:
% [u, v] = HS(im1, im2, alpha, ite, uInitial, vInitial,
displayFlow)
% For an example, run this file from the menu Debug->Run or
press (F5)
%
% -im1,im2 : two subsequent frames or images.
% -alpha : a parameter that reflects the influence of the
smoothness term.
% -ite : number of iterations.
% -uInitial, vInitial : initial values for the flow. If
available, the
% flow would converge faster and hence would need less
iterations ; default is zero.
% -displayFlow : 1 for display, 0 for no display ; default is
1.
% -displayImg : specify the image on which the flow would
appear ( use an
% empty matrix "[]" for no image. )
%
% Author: Mohd Kharbat at Cranfield Defence and Security
% mkharbat(at)ieee(dot)org , http://mohd.kharbat.com
% Published under a Creative Commons Attribution-Non-
Commercial-Share Alike
% 3.0 Unported Licence http://creativecommons.org/licenses/by-
nc-sa/3.0/
%
% October 2008
% Rev: Jan 2009

% Read video and convert to sequence of Grayscale images
inVideo = input('Input Video:', 's');
readSeq = readVideo (inVideo);

% Obtain the sequences of the video
[~, seq] = size (readSeq);

%% obtain vector in between range of pixel
rSize=8;
%%image size
imgSize=0.5;

%Crop the color video sequence to desired prosessing dimension
for i =1:seq
    cropSeq{1,i}=imgCrop(readSeq{1,i});
    frameSeq{1,i}=imresize(cropSeq{1,i},imgSize);
end

% Obtain the size and sequences of the video
[row, col, ~] = size (frameSeq{1,1});
```

```
increment = 0;

for s = 1:1:seq
    c = s+1;
    if(c <=seq)
    increment = increment +1;

    %% Default parameters
    if nargin<1 || nargin<2

        im1=frameSeq{:,s};
        im2=frameSeq{:,c};
        img{1,increment}=frameSeq{:,s};
        img1=frameSeq{:,s};
        img2=frameSeq{:,c};

%Obtain the color value of the image
        R1=im1(:,:,1);
        G1=im1(:,:,2);
        B1=im1(:,:,3);
        R2=im2(:,:,1);
        G2=im2(:,:,2);
        B2=im2(:,:,3);
        gray1 = rgb2gray(im1);
        gray2 = rgb2gray(im2);

    end
    if nargin<3
        alpha=1;
    end
    if nargin<4
        ite=1;
    end
    if nargin<5 || nargin<6
        uInitial = zeros(size(im1(:,:,1)));
        vInitial = zeros(size(im2(:,:,1)));
    elseif size(uInitial,1) ==0 || size(vInitial,1)==0
        uInitial = zeros(size(im1(:,:,1)));
        vInitial = zeros(size(im2(:,:,1)));
    end
    if nargin<7
        displayFlow=1;
    end
    if nargin<8
        displayImg=im1;
    end

    %% Convert images to grayscale
    if size(size(im1),2)==3
        im1=rgb2gray(im1);
    end
    if size(size(im2),2)==3
        im2=rgb2gray(im2);
    end
    im1=double(im1);
    im2=double(im2);

    im1=smoothImg(im1,1);
    im2=smoothImg(im2,1);
```

```
    % Set initial value for the flow vectors
    u = uInitial;
    v = vInitial;

    % Estimate spatiotemporal derivatives
    [fx, fy, ft] = computeDerivatives(im1, im2);

    % Averaging kernel
    kernel_1=[1/12 1/6 1/12;1/6 0 1/6;1/12 1/6 1/12];

    % Iterations
    for i=1:ite
        % Compute local averages of the flow vectors
        uAvg=conv2(u,kernel_1,'same');
        vAvg=conv2(v,kernel_1,'same');
        % Compute flow vectors constrained by its local average
and the optical flow constraints
        u= uAvg - ( fx .* ( ( fx .* uAvg ) + ( fy .* vAvg ) +
            ft ) ) ./ ( alpha^2 + fx.^2 + fy.^2);
        v= vAvg - ( fy .* ( ( fx .* uAvg ) + ( fy .* vAvg ) +
            ft ) ) ./ ( alpha^2 + fx.^2 + fy.^2);
    end

    u(isnan(u))=0;
    v(isnan(v))=0;

% extract the motion vector and color intensity for every pixel
range
    m=0;
    for i=1:row
        if floor(i/rSize)==i/rSize
           m=m+1;
        end
        n=0;
        for j=1:col
            if floor(i/rSize)==i/rSize &&
              floor(j/rSize)==j/rSize
                n=n+1;
                r1(m,n,increment)=R1(i,j);
                g1(m,n,increment)=G1(i,j);
                b1(m,n,increment)=B1(i,j);
                r2(m,n,increment)=R2(i,j);
                g2(m,n,increment)=G2(i,j);
                b2(m,n,increment)=B2(i,j);
                GRAY1(m,n,increment)=gray1(i,j);
                GRAY2(m,n,increment)=gray2(i,j);

                vx(m,n)=u(i,j);
                vy(m,n)=v(i,j);
            end
        end
    end

    [Nx, Ny] = size(vx);
    vxx(:,:,increment)=vx;
    vyy(:,:,increment)=vy;
    end
end
```

```
Ver = row/mbSize;
Hor = col/mbSize;
Vvx = zeros(Hor,Ver,increment);
Vvy = zeros(Hor,Ver,increment);
marks=zeros(Hor,Ver,increment);
marks_temp=zeros(Hor,Ver,increment);
motionVect1 = zeros(2,(Hor)*(Ver),increment);
motionVect2 = zeros(2,(Hor)*(Ver),increment);
distrix = zeros(9,1);
sub=cell(9,1);
Vyy = zeros(Hor,Ver,increment);
Vxx = Vyy;
Vyy2 = zeros(Hor+1,Ver+1,increment);
Vxx2 = Vyy;
Vy = zeros(Ver,Hor,increment);
Vx = Vy;
ss=1;
J=0;
K=0;
L=0;
PSNR=zeros(increment,2);

for i = 1:increment
    Vyy (:,:,i) = reshape (motionVect(1,:,i),Hor,Ver);
    Vxx (:,:,i) = reshape (motionVect(2,:,i),Hor,Ver);
    Vy  (:,:,i) = Vyy (:,:,i).'; % y movement
    Vx  (:,:,i) = Vxx (:,:,i).'; % x movement
    Vx2(:,:,i)=Vx(:,:,i);
    Vy2(:,:,i)=Vy(:,:,i);
end

%Vector median filter
Vx_pad = padarray(Vx,[1 1]);
Vy_pad = padarray(Vy,[1 1]);
Vx_pad_temp = zeros(Ver,Hor);
Vy_pad_temp = zeros(Ver,Hor);
for i = 1:increment
    for j = 2:Hor
        for k = 2:Ver
            u=0;
            p=1;
            for m = -1:1
                for n = -1 : 1
                    sub{p,1}=[Vy_pad(j+m,k+n,i)
                        Vx_pad(j+m,k+n,i)];
                    p=p+1;
                end
            end

% calculate the cost (SAD) for in the search
            for q =1 : 9
                sigmad  = 0;
                for r =1 : 9
                    d = norm(sub{q,:}-sub{r,:});
                    sigmad  = sigmad  + d;
                end
                distrix (q,1) =sigmad ;
            end
```

```
% find the lowest L2-norm distance
            [u,v] = find(distrix <= min(min(distrix)));
            med=sub{u,1};
            Vy_pad_temp(j,k)=med(1);
            Vx_pad_temp(j,k)=med(2);
            Vy2(j,k,i)=Vy_pad_temp(j,k);
            Vx2(j,k,i)=Vx_pad_temp(j,k);
        end
    end
end
```

APPENDIX K: Grouping and Labelling of Motion Vectors

```
%% Group and label the motion vector base on the color of
topomp
grayscale=0:5:150;
[~,ss]=size(grayscale);
vx1=Vx2;
vy1=Vy2;
for i=1:increment %vector 1
    for j=1:Hor
        for k=1:Ver
% extract high activation motion vector
            if(vx1(j,k,i) ~= 0 || vy1(j,k,i) ~= 0)
                  if(blockCostBlue(j,k,i)>=10||
                   blockCost(j,k,i)>grayscale(1,1))
                     vx1(j,k,i) = 0;
                     vy1(j,k,i) = 0;
                 end
            end
        end
    end
end
[marks1 vx1  vy1]=vecLabel(vx1,vy1,Hor,Ver,increment); % Group
and label motion vector 1
% compare vector 2 with vector 1 with different color threshold
on topomap
for pp=1:ss-1
    vx2=Vx2;
    vy2=Vy2;
    for i=1:increment% vector 2
        for j=1:Hor
            for k=1:Ver
                if(vx2(j,k,i) ~= 0 || vy2(j,k,i) ~= 0)
                     if(blockCostBlue(j,k,i)>=10||
                       blockCost(j,k,i)>grayscale(1,pp+1) )
                        vx2(j,k,i) = 0;
                        vy2(j,k,i) = 0;
                     end
                end
            end
        end
    end
    [marks2 vx2  vy2]=vecLabel(vx2,vy2,Hor,Ver,increment); %
Group and label motion vector 2

    marks_new=zeros(Hor,Ver,increment);
    vx_new=zeros(Hor,Ver,increment);
    vy_new=zeros(Hor,Ver,increment);
    label=1;
    for i=1:increment
        MARKS1=marks1(:,:,i);
        MARKS2=marks2(:,:,i);
        minlabel2=min(min(MARKS2(MARKS2>0)));
        maxlabel2=max(max(marks2(:,:,i)));
        for l = minlabel2:maxlabel2
            [j,k]=find(marks2(:,:,i)==l);
            m=[];
            for jj=1:size(j,1)
                m(jj,1)=marks1(j(jj,1),k(jj,1),i);
            end
```

```
            L=unique(m(m>0));
            [s,~]=size(L);
            if(s>1)
                for n=1:s
                    marks_new(marks1==L(n,1))=label;
                    vx_new(marks1==L(n,1))=
                        vx1(marks1==L(n,1));
                    vy_new(marks1==L(n,1))=
                        vy1(marks1==L(n,1));
                    label=label+1;
                end
            elseif(s<=1 || isempty(s))
                    marks_new(marks2==l)=label;
                    vx_new(marks2==l)= vx2(marks2==l);
                    vy_new(marks2==l)= vy2(marks2==l);
                    label=label+1;
            end
        end

    end
    vx1=vx_new;
    vy1=vy_new;
    marks1=marks_new;
    MaxLabel1=max(marks1(:));
end
```

APPENDIX L: Tracking of MVs Clusters

```
Function vecTracking
(Vx2,Vy2,Nx,Ny,increment,VideoFile,marks,MaxLabel,rSize,img,Lab
elRegion,p,imgSize)

BR=imread('empty_topo.png');
cropBR=imgCrop(BR);
BrainRegion=imresize(cropBR,imgSize);
[sx,sy,~]=size(BrainRegion);

% set the brain region
BrainRegion(round(276*imgSize),round(1):round(sx),:)=150;%front
al
BrainRegion(round(524*imgSize),round(1):round(sx),:)=150;%occip
ital
BrainRegion(round(390*imgSize),round(150*imgSize):round(557*img
Size),:)=150;%center/motor
BrainRegion(round(276*imgSize):round(524*imgSize),round(150*img
Size),:)=150;%left
BrainRegion(round(276*imgSize):round(524*imgSize),round(557*img
Size),:)=150;%right
t=1;
PASS=[];
list=[];
lobe=[];
VXXmap=[];
VYYmap=[];
nn=0;
location=[];

% track the path for every label group of motion field
for label=1:MaxLabel
nextLabel=0;
marks_temp=zeros(Nx,Ny);
for i =1:increment
    marks_temp=marks(:,:,i);
    [J,~]=find(marks_temp==label);
    [JJ,~]=find(PASS==label);
    if (~isempty(J) && isempty(JJ))
        nn=nn+1;
        list(nn,1)=label;
        I=i;
        break;
    elseif((~isempty(JJ))||(i==increment && isempty(J)))
        nextLabel=1;
    end
end
if(nextLabel==1)
    continue;
end
Vx_path=zeros(Nx,Ny,increment);
Vy_path=zeros(Nx,Ny,increment);
track=zeros(Nx,Ny,increment);
track2=zeros(Nx,Ny);
VXX=zeros(increment,1);
VYY=zeros(increment,1);
Vlabel=zeros(Nx,Ny,increment);

%%check for overlapping
```

```
for i=I:increment
    nxt=0;
    NT=0;
    for j=2:Nx
        for k=2:Ny
            xmin=Nx;
            xmax=0;
            ymin=Ny;
            ymax=0;

%%find median value by using l2-norm method when i = I (I =
current frame I=initial frame
            if(i==I && marks(j,k,i)==label)
               track(marks==label)=label;
               y = 1:Nx;
               x = 1:Ny;
               [X,Y] = meshgrid(x,y);
               distrix=[];
               U=[];
               [XX,YY] = find(track(:,:,i)==label);
               for P=1:size(XX,1)
                   sigmad=0;
                   for Q=1:size(XX,1)
                       d = norm([XX(P,1) YY(P,1)]-[XX(Q,1)
                         YY(Q,1)]);
                       sigmad=sigmad+d;
                   end
                   distrix (P,1) =sigmad ;
               end
               [U,~] = find(distrix <= min(min(distrix)));
               cX=XX(U(1,1),1);
               cY=YY(U(1,1),1);
               Vlabel(cX,cY,i)=label;
               cX_initial=cX;
               cY_initial=cY;
               track2=zeros(Nx,Ny);
               i2=i;
               a=1;

% find the median value using L2 norm method when i >1
               if(i>1)
                   if(marks(j,k,i-1)~=0 && NT==0)
                        marks2=marks(:,:,i-1);
                        distrix=[];
                        U=[];
                        [XX,YY] = find(marks2==marks(j,k,i-1));
                        for P=1:size(XX,1)
                            sigmad=0;
                            for Q=1:size(XX,1)
                                d = norm([XX(P,1) YY(P,1)]-
                                     [XX(Q,1) YY(Q,1)]);
                                sigmad=sigmad+d;
                            end
                            distrix (P,1) =sigmad ;
                        end
                        [U,~] = find(distrix <=
                            min(min(distrix)));
                        cX=XX(U(1,1),1);
                        cY=YY(U(1,1),1);
                        VXX(i-1,1)=cX;
                        VYY(i-1,1)=cY;
```

```
                    NT=1;

                end
            end

%% find the median value using L2 norm method when i~=I
            elseif(i>=I+1)
                if(marks(j,k,i)~=0 && track(j,k,i)==0 &&
                  track(j,k,i2)~=0)
                    for m=2:Nx
                        for n=2:Ny
                            if(marks(m,n,i)==marks(j,k,i))
                                track2(m,n)=label;;
                            end
                        end
                    end
                    if(1)
                        t=t+1;
                        track(:,:,i)=track(:,:,i)+track2(:,:);
                        y = 1:Nx;
                        x = 1:Ny;
                        [X,Y] = meshgrid(x,y);
                        distrix=[];
                        U=[];
                        [XX,YY] = find(track2==label);
                        for P=1:size(XX,1)
                            sigmad=0;
                            for Q=1:size(XX,1)
                                d = norm([XX(P,1) YY(P,1)]-
                                    [XX(Q,1) YY(Q,1)]);
                                sigmad=sigmad+d;
                            end
                            distrix (P,1) =sigmad ;
                        end
                        [U,~] = find(distrix <=
                           min(min(distrix)));
                        cX=XX(U(1,1),1);
                        cY=YY(U(1,1),1);
                        if(cX~=0 &&cY~=0)
                            Vlabel(cX,cY,i)=label;
                        end
                        nxt=1;
                        PASS(t,1)=marks(j,k,i);
                    end
                    track2=zeros(Nx,Ny);

                end
            end
           if(nxt==1)
               break;
           end
        end
        if(nxt==1)
            break;
        end
    end

    [xx,yy]=find(Vlabel(:,:,i)==label);
    [r,~]=size(yy);
    if(r~=0)
        VXX(i,1)=xx;
```

```
            VYY(i,1)=yy;
            for j=2:Nx
                for k=2:Ny
                    if(track(j,k,i)==label)
                        Vx_path(j,k,i)=Vx2(j,k,i);
                        Vy_path(j,k,i)=Vy2(j,k,i);
                    end
                end
            end

        end
        if(i>=I+1)
            [xx,yy]=find(Vlabel(:,:,i)==label);
            [r,~]=size(yy);
            if(isempty(xx) && isempty(xx))
                xx=0;yy=0;
            end
            VXX(i,1)=xx;
            VYY(i,1)=yy;
        end
        if(I>1)
            if(VYY(I-1,1)~=0 && VXX(I-1,1)~=0)
                VXXmap{nn,I-1}=VXX(I-1,1);
                VYYmap{nn,I-1}=VYY(I-1,1);
            end
        end
        if(VYY(i,1)~=0 && VXX(i,1)~=0)
            VXXmap{nn,i}=VXX(i,1);
            VYYmap{nn,i}=VYY(i,1);

        elseif(VYY(i,1)==0 && VXX(i,1)==0)
            VXXmap{nn,i}=[];
            VYYmap{nn,i}=[];
            lobe{nn,i}=[];
        end
        track_tf=track(:,:,i);
        if(sum(track_tf(:))==0)
            i2=i-a;
            a=a+1;
        else
            i2=i;
            a=1;
        end
    end

    end

    %% check for the tracked path
    xidx = rSize:rSize:Nx*rSize;
    yidx = rSize:rSize:Ny*rSize;
    [X,Y] = meshgrid(xidx,yidx);
    X_a=[];
    Y_a=[];
    for l=1:nn
        a=1;
        for i=1:increment
            X_a{l,a}= VXXmap{l,i}*rSize;
            Y_a{l,a}= VYYmap{l,i}*rSize;
            a=a+1;
        end
```

```
end
X_a( all(cellfun(@isempty,X_a),2), : ) = [];
Y_a( all(cellfun(@isempty,Y_a),2), : ) = [];
[mm,~]=size(X_a);
dd=1;

% Plot the tracking line
for ii=1:increment
    imshow(BrainRegion,[]);
    hold on;
    quiver(X,Y,Vx2(:,:,ii),Vy2(:,:,ii),'blue');
    grid on;
    for i=1:dd
        for l=1:mm
            if(i<dd)
                  if(~isempty(X_a{l,i})&&~isempty(X_a{l,i+1}))
                        plot([Y_a{l,i},Y_a{l,i+1}],[X_a{l,i},X_
                        a{l,i+1}],'-
                        ','Color','b','LineWidth',2);
                  end
            end
        end
    end
    hold off
    dd=dd+1;
end
```